Connexin expression in CNS: Pathological significance and Lithium-mediated neuroprotection

Doctorate thesis

Valentina Cicirata

UNIVERSITY OF CATANIA

UNIVERSITY BORDEAUX II

International Ph.D program in Neuropharmacology

XXV cycle

Connexin expression in CNS: Pathological significance and Lithium-mediated neuroprotection

Doctorate thesis

Valentina Cicirata

UNIVERSITY OF CATANIA

UNIVERSITY BORDEAUX II

International Ph.D program in Neuropharmacology

XXV cycle

Coordinator: Prof. Filippo Drago

Tutor: Prof. Filippo Drago

Table of contents

Aknowledgement…….5

Abstract…….6

List of abbreviations……8

Introduction……..9

1.Gap junction……..9

1.1.Connexins…….11

1.1.1 Gap Junnctions function……15

1.1.2.Functionl control of gap junction conductance……..16

1.2. Pannexins……..19

1.2.1. Pannexins in CNS…….22

1.3. Anatomical distribution of Gap Junction in the mammalian brain…….23

Neurons……..*23*

Astrocytes……*25*

Oligodendrocytes……*26*

Schwann cells……*26*

1.4. Gap Junction in Neuropathological conditions…….27

1.4.1. Brain Ischemia……..28

1.4.2. Epilepsy……..28

1.4.3. Demyelinating syndromes……..29

1.4.4. Neurodegenerative diseases……....30

2. Lithium and neuroprotection……31

Chapter I……34

Dynamic expression of Cx47 in mouse brain development and in the cuprizone model of myelin plasticity

Chapter II……77

Expression of connexin57 in mouse development and in harmaline-tremor model

Chapter III……..113

Expression pattern of Connexins and Pannexins in primary human astroglial cell cultures exposed to Glutamate or Lipopolysaccharide

Chapter IV……139

Effects of lithium treatment in the expression of Cx43, Cx30 and Cx26 by using both *in vitro* and *in vivo* models of Alzheimer's pathological conditions

3. General Discussion and Conclusion.....153

References list……156

AKNOWLEDGEMENT

ABSTRACT

The communication between cells in physiological and pathological conditions is mediated by clusters of intercellular channels called Gap Junctions which are composed by transmembrane proteins family called connexin (Cx). The expression and function of connexins in several pathological conditions is a topic of great interest and with unknown aspects to be investigated further. This is the theme of my thesis, which investigates the expression of connexins in different models of pathology of the CNS and also the possibility to modulate the response by neuroprotective agents like Lithium Chloride.

Three different studies were performed:

i) Dynamic Expression of Cx47 in Mouse Brain Development and in the Cuprizone Model of Myelin Plasticity: the study shows the dynamic expression of connexin47 (Cx47) in oligodendrocytes and myelin of mice, either in myelinogenesis occurring in early development or in an ex- perimental model of new-myelinogenesis of adult mice.

ii) Expression of Connexin57 in mouse development and harmaline-tremor model: the up-regulation of the Cx57 transcripts reported in this model suggested a possible involvement of Cx57 in the electrotonic coupling of the cerebellar system.

iii) Expression oattern of connexins and pannexins in primary human astroglial cell cultures exposed to glutamate or lipolysaccharide: the effects of the administration of LPS (1,10, 100 μg/ml) or glutamate (10, 50, 100 μM) for different time intervals (12, 24 and 48 h) were tested in human astrocytes. Four parameters were compared: cytological modification, cell viability, level of ROS and GSH, the level of mRNA of connexins (Cxs): Cx26, Cx30, Cx43 and pannexins (Panx): Panx 1 and Panx2. Main findings were:1) the stressors (LPS and glutamate) increased the mRNA level of Cx26 and Cx30, while Cx43, Panx1 and Panx2 were not significantly modified; 2) the level of Cx26 and Cx30 increased strongly at lower doses of stressors while increasing the doses of the stressors, the increment of Cx26 and Cx30 progressively lowered. Conversely, the level of the ROS increased with the doses of the stressors; 3) an inversed relation occurred between level of Cxs (Cx26 and Cx30) and grade of injury of the cells (as proved by astrocytosis and by MTT test).

Since there will be a close correlation between neurodegenerative disease and expression of connexin, the last step of the work concerns the possibility to control

the expression of connexins by the administration of a neuroprotective agent such as lithium.

LIST OF ABBREVIATIONS

CNS: central nervous system

Cx: connexin

GJ: gap junction

GJC: gap junction communication

HCs: hemichannels

Panx: pannexin

GJIC: gap junctional intercellular communication

Cx43: connexin 43

Cx26: connexin 26

Cx30: connexin 30

Panx1: pannexin 1

Panx2:pannexin 2

qRT-PCR: Quantitative real-time Polimerase Chain Reaction

Vm: membrane voltage

Vj: transjunctional voltage

CaM: calmodulin

MAPK: mitogen-activated protein kinase

CBX: carbenoxolone

FRIL: freeze-fracture replica immunolabeling

AD: Alzheimer's disease

PD: Parkinson's disease

INTRODUCTION

1. Gap Junctions

Cells in tissues share ions, second messengers, and small metabolites through clusters of intercellular channels called Gap Junctions. The intercellular communication coordinated cellular activity and is a key condition for the existence of pluricellular organisms. Gap junctions are clusters of intercellular channels that allow direct diffusion of ions and small molecules between adjacent cells. Without this type of direct transmission, the exchange of information would not be possible. Indeed GJs regulate cellular synchronization, cells growth and metabolic coordination in tissues. Gap Junctions are intercellular channels composed by transmembrane proteins family called connexin (Cx) and recently, a new important class of GJ proteins has been recognized in vertebrates, the pannexins (Panxs), which are considered homologous to the innexins of the invertebrates. Phylogenetic analysis revealed that Panxs are highly conserved in *Nematoda, Mollusca, Arthropoda* and also in mammals [1]. The high maintenance of the Panxs in classes which are so distant in terms of phylogenesis suggests the importance of their functions [2]. They are present in all Metazoan kingdom. The first proteins identified have been the connexins, found only in Chordates. Indeed, in invertebrates are present the innexins, similar in the structure and membrane topology to connexins but not in the amino acidic sequence. In recent years, by sequencing of mammalian genomes, pannexins have been identified as genes homologues to innexins [3,4]. Three Panxs and more than 20 Cxs were cloned in mammals. Each cell type express a specific set of these proteins. The set of Cxs and Panxs expressed in single cells is functionally important because their combination in GJ channels is critical for permeability to specific signaling molecules or ions [5]. Each cell type expresses a given set of GJ proteins, but their expression pattern is not stable in time. In fact, the pattern expressed in resting condition usually changed after injury both in vitro [6] or in vivo models [7], suggesting altered permeability to signaling molecules in suffering conditions. These proteins are characterized by a similar characteristic structure,

comprising four alpha helix transmembrane domains (TM1-TM4), N- and C-terminal intracellular regions, two extracellular loops (E1-E2) and one cytoplasmatic loop (I1) [8, 9]. This structure is essential for the formation of a hemichannel, indeed six Cxs, Panxs or Inxs oligomerize to form a hexameric pore complex, respectively called connexon, pannexon or innexon. Two opposing hemichannels, each arising out from a cell, give rise to a gap junction, most commonly assembled as GJs plaque, characterized by a reduced space between the cells (about 2-4 nm) and composed by clusters of few or hundreds of gap junction channels. The association of the two hemichannels is mediated by H-bonds occurring between the extracellular loops of the proteins (Figure 1).

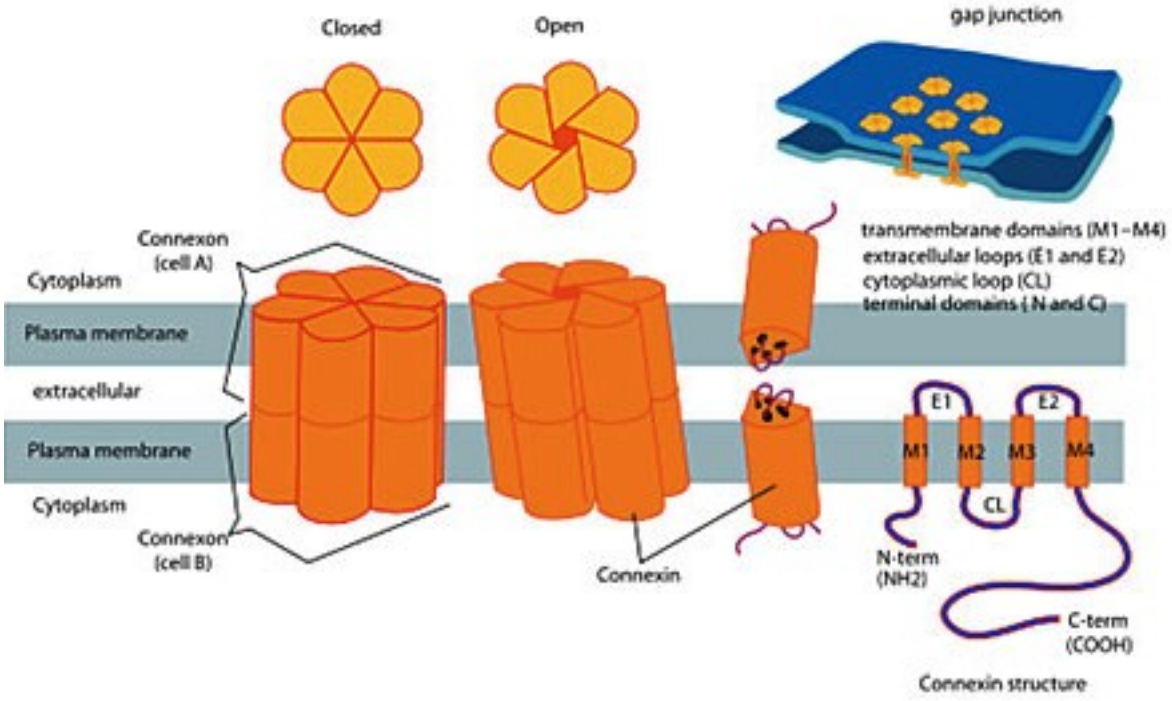

Figure.1 Schematic representation of gap junctions and their components. Two cells are interconnected by a plaque of gap junction channel, every formed by the opposition of two hemichannels. (On the right) Structure of a protein forming GJs characterized by: four transmembrane domains (M1-M4); N- and C-terminal intracellular regions; two extracellular loops (E1-E2) and one intracellular loop.

1.1 Connexins

Connexins are the molecular constituents of Gjs, which are clusters of intercellular channels that allow the direct intercellular exchanges of ions and small molecules (e.g., IP3, ATP, glutamate, and energy metabolites). The connexins proteins are encoded by a family of genes divided in five subfamilies α, β, γ, δ and ε. The five groups show differences in the structure and sequence due to a different phylogenetic origin.

Up to now, the family of connexins genes comprises 21 members in human and 20 in mouse genome, of these 19 are orthologous. The nomenclature of connexins includes the indication of the species of origin, "h" for human and "m" for mouse (the species in which they have been first studied), the family name "Cx" and the number corresponding to the predicted molecular mass deduced on the basis of cDNA sequence (range of 23-62 kDa) [12, 13]. There is also another nomenclature, based on the use of the abbreviation ''Gj'', for gap junction, the group they belong (A, B, C, D, E for α, β, γ, δ and ε respectively) and by a number in according to the order of discovery. For example, mCx43, the first discovered connexin, belonging to the α-group, is also called Gja1.

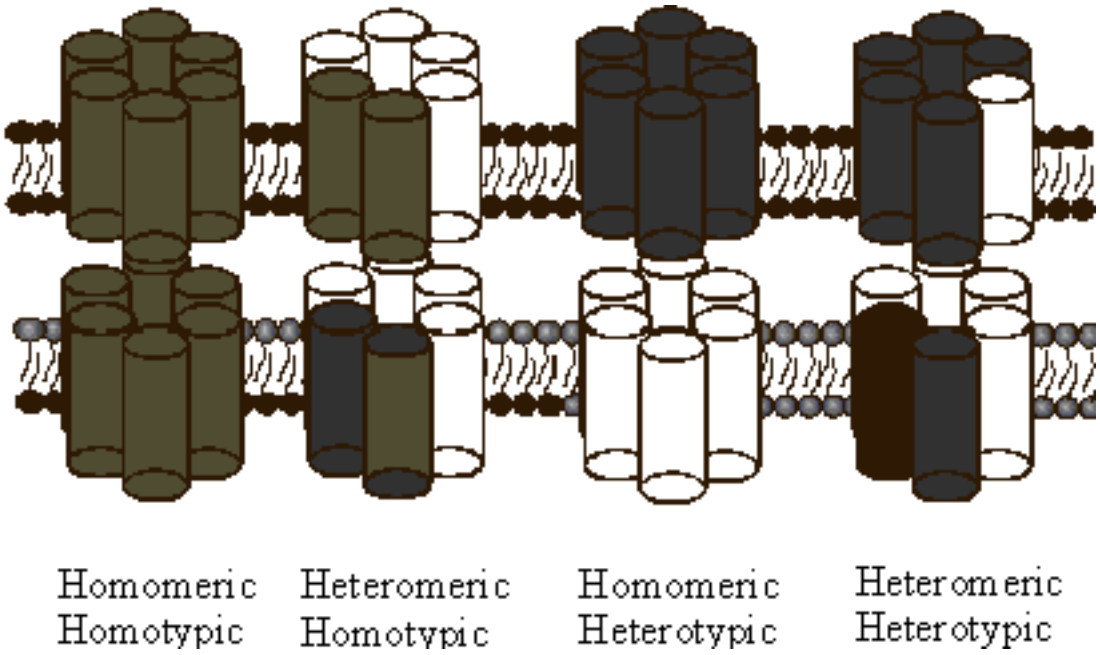

Figure 2. Gap junction channels formed from two identical hemichannels are called *homotypic*, while those with differing hemichannels are heterotypic. In turn, hemichannels of uniform connexin composition are called homomeric, while those with differing connexins are heteromeric. Channel composition is thought to influence the function of gap junction channels.

Various tissues and cell type can express more than one type of connexins. Connexins can form a large variety of channels; consequently, the connexons can be homomeric, if composed by the same type of connexins, or heteromeric in the case of two or more type of Cxs. Furthermore, a gap junction can be homotypic, if constituted of two identical hemichannels made from one type of connexin, or heterotypic, i.e. formed by two different hemichannels, each of which is made of a different type of connexin. Not all the connexins are able to form a heterotypic GJ. The different composition dictates different physiological properties as gating, single-channel conductance and the permeability to biological molecules [14-16] (Fig.2). The oligomerization of the connexins into a hemichannel (HC) occurs in the endoplasmic reticulum (ER), where the neoformed connexons pass in the Golgi apparatus and then in trans-Golgi network. They interact with chaperone proteins and inside to vesicles are transported along microtubules and actin filaments to the membrane cell, through which they freely

diffuse and are integrated in the outer edges of existing plaque. The connexon arrived at the membrane cell, is aided by E- and N-cadherins, to bind with another connexon arising from adjacent cells and to form the gap junction channel [16, 17-19]. Gap junction plaques are highly dynamic regions, in which new connexons are added at the periphery and old connexons are removed from the centre of the plaques. The removal occurs with invagination of a vesicle containing a portion of membrane with all or a part of GJ. This structure, named "annular junction", is released in cytosol and its components are degraded through the lysosomal and proteosomal pathway [20-22]. Gap junctions biosynthesis and assembly are tightly regulated, indeed these structure have a half-life of only few hours. This rapid process is probably fundamental for a quick adaptation of the cells to mutated physiological or environmental conditions (Figure 3).

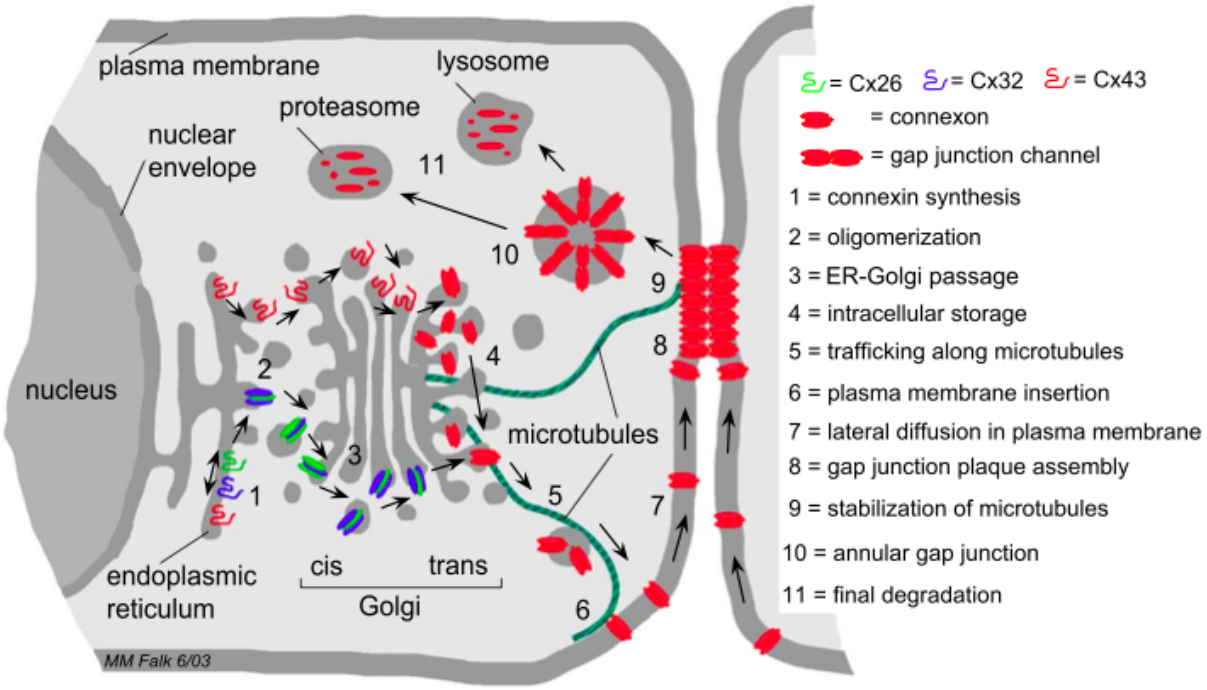

Figure 3. Schematic representation of the steps that lead to synthesis, assembly, and degradation of gap junction membrane channels based on the current literature. Gap junction biosynthesis and degradation involves (1) synthesis of connexin polypeptides at endoplasmic reticulum membranes, (2) oligomerization into homo- and heteromeric gap junction connexons (hemi-channels), (3) passage through the Golgi stacks, (4) intracellular storage within trans Golgi membranes, (5) trafficking along microtubules, (6) insertion of connexons into the plasma membrane, (7) lateral diffusion of connexons in the plasma membrane, (8) aggregation of individual gap junction channels into plaques, (9) stabilization of peripheral microtubule plus-ends by binding to Cx43-based gap junctions, (10) internalization of the channel plaque leading to cytoplasmic annular junctions, and (11) complete degradation via lysosomal and proteasomal pathways. (Image from Segretain and Falk, 2004)

1.1.1Gap junctions functions

Gap junctions are implicated in a large variety of functions as embryonic development, morphogenesis, cell differentiation, cell proliferation and migration, electrical and mechanical synchronization (cardiac, muscle and brain cells), transmission of trophic or death molecules. All these functions have been discovered using targeted mutated connexins or through the over expression of some connexins isoforms. The importance of these proteins and, hence, of gap junctional communication is evident by the large number of human genetic diseases associated with connexins mutations or with pathogenic single nucleotide polymorphisms. Among this for example the X-linked Charcot-Marie-Tooth syndrome, a peripheral neuropathy with atrophy of distal muscles and low number of myelinating fibers, has been linked to mutations in Cx32 gene, suggesting its participation in myelination of peripheral nerves. Mutations in Cx43 can cause oculodentodigital dysplasia characterized by craniofacial, neurologic, limb and ocular abnormalities. Still mutations of Cx46 and Cx50 result in cataracts [23-27]. Connexins proteins are expressed in all tissue except in differentiated skeletal muscle, erythrocytes and sperm cells. This almost ubiquitary presence is a further confirmation of their importance for the correct functioning of the organisms. Recent studies show that connexons are also active in single plasma membranes and that they might be essential in intercellular signalling beyond their incorporation into gap junctions, so they may act as hemichannels (HCs) in different physiological and pathological process. In contrast to GJs, HCs show low open probability and low permeability to small molecules under resting conditions. HCs have been implicated in autocrine/paracrine signalling to provide a pathway for release of ATP, glutamate, NAD+ and prostaglandins. The role of hemichannels seems to be very important, because they act in the cells of various organs in response to extracellular signaling, injury, ischemic preconditioning and mechanical stimulation [28 - 30].

1.1.2 Functional control of Gap Junction conductance

A gap junction forms a hydrophilic channel pore of about 100-150 Å in length and 12.5 Å in width. It allows the passage of small molecules under 1kDa like ions, water, nucleotides, small peptides, metabolites. In this way, GJs provide to ionic and metabolic coupling among the cells. For some substances, this coupling is bidirectional and is driven by an electrochemical gradient, for others GJs there is a high degree of selectivity. Indeed the channels composed by different connexins show different permeability; for example some channels are specific for the cations or the anions, while others are able to discriminate between similar molecules as cAMP and cGMP. The junctional conductance, i.e. the passage of molecules or ions through GJ channel, is subjected to regulation by a number of physiological factors, such as voltage, intracellular pH and calcium, second messengers, or phosphorylation. Conductance of a single homo-connexins channel ranges from ~10 picoSiemens (pS) to ~300 pS [31-34]. The most important factor for the permeability is the structure of channel pore. Indeed the pore width, the electrical field and the electrical charge on the pore surface affect the permeability of ions and molecules passing through the channel. The permeation pathway of a gap junction channel consists of an intracellular channel entrance, a pore funnel and an extracellular cavity. The pore funnel surface is formed by the six N-terminal regions of connexins. Because the funnel forms a constriction site at the cytoplasmic entrance of the pore, the size and electrical character of the side-chains in this region should have a strong effect on both the molecular cut-off size and the charge selectivity of the channel. Indeed the substitutions or deletions of residues in N-terminal regions can affect single channel conductance, molecular permeability and charge selectivity [34].

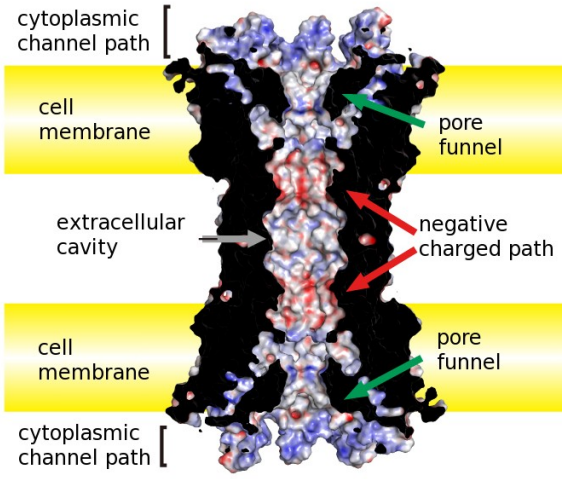

Figure 4 Pore structure of the Cx26 GJ channel. The permeation pathway of Cx26 GJ consists of an intracellular entrance (the pore funnel formed by N-terminal regions), a negative charged path and an extracellular cavity. (Image adapted from Maeda et al., Cell. Mol. Life Sci, 2011)

The gap junctional communication is regulated at multiple levels. The regulation can be at short or long-term; the more rapid mechanism involves changing in the conductance or in the probability of opening of a single channel while in the slow mechanism occur an alteration of number of channels for changes in synthesis and degradation. Gap junction channels have different gating mechanisms are voltage sensitive. Indeed, they are under the influence of two types of electrical field, the membrane voltage (Vm), i.e. the voltage difference between intra and extracellular space, and the transjunctional voltage (Vj), that is established when the membrane voltages are not equal in the two coupled cells. Some connexins are sensitive to both Vj and Vm, others only to Vj. As regard the dependence by Vm, different connexins show different sensitivity; for example Cx43, Cx30 and Cx26 channels close with depolarization, whereas Cx45 upon hyperpolarization. The dependence of junctional conductance by Vj regards all GJs analyzed; so this mechanism is specific for GJs channels and is characterized by two forms of gating, fast or low, depending by the time reaction of opening and closing. Different studies revealed that N-terminal domain, forming the pore funnel, determine the magnitude and polarity of Vj. A cytoplasmic movement of the N-terminal portion,

where the voltage sensor is believed to reside, has been suggested to initiate voltage-dependent gating (Figure 4). Therefore, the substitution of the residues on N-terminal, changes the conductance or sensitivity. Indeed there are hemichannels that are close at positive voltage, as Cx26, Cx30, while others at negative voltage, Cx32, Cx43, Cx45 [36 - 40].

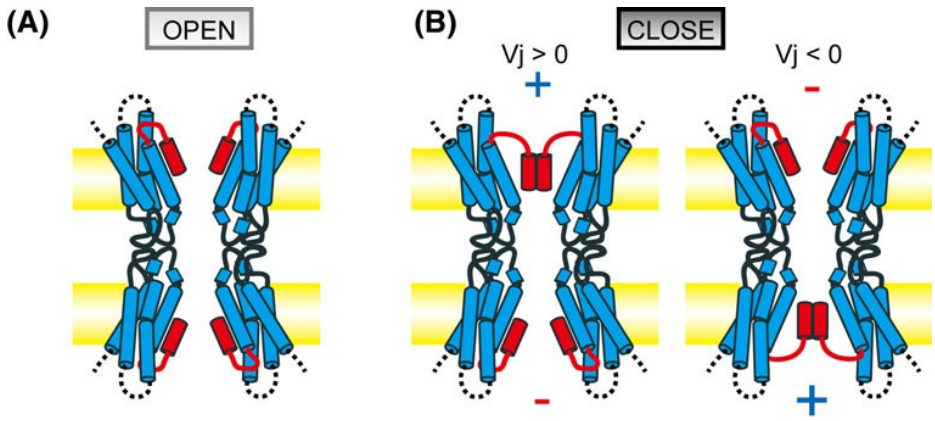

Figure 5 Plug gating model for transjunctional voltage-dependent gating of the Cx26 gap junction channel. (A): When there is no difference in membrane voltages between two neighbouring cells N-term region (in red) form the pore funnel and attach to TM1 by hydrophobic interactions. (B): When there is a difference in membrane voltages between two cells, the positive electric field causes the releasing of N-term from TM1. Once released, N-term region will assemble on the top of the pore with the others N-term region. (Image adapted from Maeda et al., Cell. Mol. Life Sci, 2011).

Others factors modulating gap junction conductivity are the Ca2+ and pH. An increase in intracellular calcium concentration reduces GJ communication. Indeed it is a signal to protect the other cells by the damaged cells, even if the sensitivity depend on connexin

and cell types, in a range from 500-600 nM to μM concentration of Ca2+. There are also experimental evidences that the gating of GJs, Ca2+-dependent, could be mediated by calmodulin (CaM), an intermediate messenger protein that transduces calcium signals by binding calcium ions and then modifying its interactions with various target proteins, among which there are connexins [41, 42]. Also an increase in intracellular pH decreases junctional conductance of gap junction channels and some connexins are markedly more sensitive to acidification than others, although it's not still clear whether H+ acts directly on GJ channel [43- 45]. An extensive way with which connexins are regulated regards several post-translational modifications. The C-terminal region of Cxs contains serine, tyrosine and threonine, residues that may be phosphorylated by different protein kinases. At least eight kinases, including protein kinase A, protein kinase C, mitogen-activated protein kinase (MAPK) and so many phosphatases control the phosphorylation/dephosphorylation of various connexins. Except for the not phosphorylable Cx26, these modifications in Cxs are associated with changes in gating, conductance, permeability, but this depends on specific connexin isoforms or cell type. However, other modifications have been identified such as hydroxylation, methylation, and acetylation. Other effects regard the assembly into GJ plaque, their biosynthesis or their proteolytic degradation, regulating in this way their half-life [46-49]. In addition, ubiquitination would seem an important mechanism which connexins are regulated; the most studied Cx43 for example, can be ubiquitinated at plasma membrane or at ER level. Recently it has been implicated also a stimolation for Cx43 [50-52]. There are chemical agents able to block the GJ communication, they belong to multiple class and structures. Some are lipophilic such as heptanol, octanol and halothane, glycyrrhetinic acid derivatives such as carbenoxolone (CBX), quinine derivatives and some others different for structure and action mechanism. These molecules have been used to study the functions of GJs in vitro and in vivo, but although many of these are used to treat common diseases, as quinine for malaria, they give a plethora of side effects, due sometimes by blocking other channels. The development of selective blockers will allow better understanding of GJs communication [53].

1.2. Pannexins

Pannexins belong to a new family of proteins, also able to form GJs. They have more similar homology with innexins than with connexins, so that initially it was thought

they belonged to the innexins family. Many later studies showed that Panxs are a distinct family of proteins; they do not share the strongly conserved residues of Inxs even if as these last possess two cysteine residues in extracellular loops, and in contrast to connexins have a larger intracellular loops (~68 aa vs. ~30 aa).In the genomes of human and rodent species, are coded three proteins, Panx1, Panx2 and Panx3. Their calculated molecular mass is respectively 48, 73 and 45 kDa. In human genome Panx1 and Panx3 gene are located on chromosome 11 and Panx2 on chromosome 22, while in rat genome the first two are located in chromosome 8 and Panx2 on chromosome 7 [54, 55]. Panx1 and Panx2 transcripts are found in many rodents tissue, as brain and spinal cord, eye, thyroid, prostate, kidney; in humans are found also in hearth, gonads and skeletal muscle (in which there is no presence in rodents). Panx1 protein is expressed in numerous tissues in both human and rodents. Instead Panx2 is present in many tissues in rodents, but in humans is expressed only in the central nervous system (CNS). The expression of Panx3 seems confined to skin and cartilage cells, even if real-time PCR screening indicate that Panx3 mRNA is present also in kidney, spleen and brain [56, 57]. Pannexins have been found in large accumulation in ER and Golgi apparatus, suggesting that post-translational modifications and assembly in pannexons occur in the same way as demonstrated for connexins. The first studies on this protein were made by Bruzzone et al. using an expression system in Xenopus oocytes, in which they discovered that the channel formed by pannexins, if activated by voltage, had given rise to passage of molecules. But they concluded that Panx1 alone was able to form homomeric channels, while Panx2 could form only heteromeric channels with Panx1 [58]. To date, increasing evidences show that also Panx2 alone is capable to form a functional homomeric channel. Indeed the heteromeric channels Panx1/Panx2 are unstable and disaggregate in few hours, this could explain because the heteromeric is present in systems as Xenopus oocytes or in HEK 293, but in mammalian cells and brain tissue the two proteins exist separately [59]. Another controversy regards the ability of Panxs to form or not gap junction channels, but recent studies revealed evidence that they may form GJs in vitro cells, but to date it hasn't been demonstrated in vertebrate. As connexons, after activation pannexons open into large non-selective pores permeable to ions and small molecules up to 1 kDa and under a wide range of membrane depolarization. Panxs hemichannels differ from connexins HCs because they exhibit larger currents, faster kinetics of pore opening and a conductance of over 500 pS [58]. Different stimuli are able to open pannexons, among these mechanical stress, positive membrane potential, extracellular ATP, elevation in intracellular calcium, ischemic insult and inflammation, while acidification of cytoplasm cause the closing of

the channels. The presence of mechanisms distinct from those of connexins, makes possible the co-expression of the two proteins types in the same cells [60]. The pannexons may play a role in generation of oscillatory and synchronization activity in brain. They can be involved in the propagation of calcium waves, to which normally have been implicated the GJs connexins-formed [61]. Panxs would use a mechanism based on release of adenosintriphosphate (ATP). This has been demonstrated in blood endothelium, where mechanical stress or ischemia open pannexons in endothelial cells and cause the extracellular release of ATP. The released ATP acts on purinergic receptors P2Y, whose activation has effect on phospholipase C, increasing the IP3 and causing the release of calcium from intercellular stores; this at the end cause a consequent release of other ATP that can propagate using classical way of GJs or via pannexons. In this way, the propagation is ensured also without direct cell contact. This action probably is essential for the cells in normal tissue because Panxs channels, contrary to Cxs channels gated by cations as Ca2+ or Mg2+, are able to open when external concentration of calcium is at physiological level. So pannexons may propagate calcium waves and to have a role in vasodilatation, inflammatory response and ischemic death of neurons [62- 64]. Other evidences of calcium waves propagation are in erythrocytes, where there is expression only of Panx1 and not of Cx43 (the main Cx involved in calcium waves). In these the release of ATP occurs in response to ischemia and mechanical stress and after exhibit the same pathway observed in endothelium [65]. The Pannexins are the only ones, between the three families, to be extensively glycosylated. There is the presence of consensus sequence on the second extracellular loop and this modification seems important for intracellular trafficking and insertion in the cell membrane. Moreover, the glycosylation could prevent docking with other pannexons in adjacent cells [11, 66]. By analysis of amino acids sequence there are one phosphorylation site for Panx1 and multiple site for Panx2 and, as in connexins, these allow the activation/deactivation of the channels [67]. Another possible regulator of Panxs is the β-subunit of voltage-dependent potassium channel (Kvβ3), a protein belonging to the family of regulatory beta-subunits of the voltage-dependent potassium channels. The co-expression of Panx1 and Kvb3 has been showed in principal neurons of the hippocampus and in Purkinje cells of the cerebellum. The mechanism would involve the binding of Kvβ3 to the carboxy-terminus of Panx1 and maybe in response to changes of the intracellular redox potential, it would control the inactivation mechanisms of Panx1 hemichannels [68].

1.2.1. Pannexins in CNS

Pannexin 1 and Panx2 transcripts are detected in many regions in rodents CNS, retina, cortex, hippocampus, cerebellum, olfactory bulb, spinal cord. Panx1 is expressed primarily in neurons and maybe in oligodendrocytes. Panx2 seems to be brain-specific, but the two proteins are inversely regulated during the development of the rodents brain. Panx1 show high levels of expression in the embryonic and young postnatal brain and decline considerably in the adult, whereas Panx2 mRNA expression is low in the prenatal brain but increase substantially during subsequent postnatal development with peaking at postnatal day 15 [69, 70]. Pannexins transcripts are particularly abundant in the adult cortex, in hippocampal and neocortical pyramidal cells but also in GABAergic interneurons, (to note the presence in both excitatory and inhibitory neurons, while Cx36 is present only into inhibitory interneurons), reticular thalamus, the inferior olive, magnocellular hypothalamic neurons, midbrain and brain stem motoneurons, Purkinje and Golgi cells in the cerebellum [6]. Panx1 protein is widely expressed in mammalian tissues; as regard brain is found in several regions including cortex, striatum, olfactory bulb, hippocampus, thalamus, inferior olive, inferior colliculus, amygdala, spinal cord, retina, and cerebellum. At the cellular level, Panx1 has been localized in different neuronal types, including olfactory bulb mitral cells, Purkinje cells, dopaminergic, cholinergic and glutamatergic neurons. In the cerebral cortex and hippocampus is localized in the postsynaptic cell membranes.

Panx1 is also detected in cultured astrocytes, immature oligodendrocytes and neurons, using immunofluorescence and Western blot analysis, but it has not been found in the cell surface of astrocytes [6, 69- 73]. Panx2 protein is expressed exclusively in the brain including the olfactory bulb, hippocampus, amygdala, superior colliculus, substantia nigra, cerebellum, hypothalamus and spinal cord. Its presence it has been confirmed in the majority of pyramidal cells and in GABAergic interneurons but as regard the expression in glial cells there are still contrasting opinions; under resting conditions, hippocampal astrocytes do not express Panx2 even if it appears in hippocampal astrocytes several hours after ischemia/reperfusion [6, 71-74]. The presence in brain becomes important because pannexins are present in all regions in which lack connexins but are alike coupled both metabolically and electrically. For example, the abundance of Panxs in Purkinje cells or in hippocampal pyramidal cells, that do not express Cx36 or Cx45, suggests that these are responsible for electric coupling and generation of high-frequency oscillations. Experiments in mice KO for Cx36 show a reduction in gamma frequency, while ultrafast oscillations are not modified. These data are consistent with

the absence of Cx36, present only in hippocampal interneurons, while other channels may determine fast oscillations occurring in pyramidal cells [75-77]. However, the impact of Panxs channels on neuronal network synchronization remains to demonstrate. It remains also unknown whether pannexins form functional GJCs and/or hemichannels. There are many controversial works regard the formation of GJs; in some systems as Xenopus oocytes or C6 glioma cells an over-expression of Panx1, but not Panx2, mediate intercellular coupling, while in other systems and other groups report no communication. In contrast, functional hemichannels formed by both Panx1 and 2 are demonstrated in different cellular system and in hippocampal neurons [70, 71, 78].

1.3. Anatomical distribution of Gap Junctions in the mammalian brain

Electrical synapses are prevalent during the early phase of neurogenesis. Studies both in vitro and in vivo showed that gap junctions coupled all progenitor cells, neuroblasts and proliferating cells, in order to coordinate the neuronal communication. After about two weeks of postnatal development this communication is replaced by chemical synapses, but in mature neurons the expression of connexins is maintained and has a role in the coordination of neuronal activity and in mediation of synchrony and network oscillations [79- 81]. The expression of different connexins depends by developmental stage, cell type and brain region. With electrophysiology, transgenic animals, cell imaging and freeze-fracture replica immunolabeling (FRIL) it has been possible examine the presence of these proteins in CNS vertebrates. Several different connexins were detected in different nervous cells type.

Neurons

Electrotonic coupling between mammalian neurons has been shown in many areas of the CNS and has been implicated in neuronal synchronization [82-85]. During development, there is a high degree of intercellular coupling between neurons. Studies in the rat indicate that neuroblasts are coupled with approximately 30–60 others in columns within the ventricular zone of the developing cerebral cortex [86-89]. The zone is comprised of mitotically active epithelial cells lining the ventricles. These cells have been shown to express Cx43 and Cx26 [90], and the coupling appears to involve both neural precursors and radial glia [91]. Thus gap junctional intercellular communication (GJIC) may establish cortical domains in the developing neocortex that underlie the

adult pattern of functional archi- tecture [88,89,92]. Although Cx43 has been reported in neurons of the cortical plate, the expression of Cx32 in mature neurons [93] is controversial [94, 95]. The expression pattern of Cx26 [96] and Cx36 [97,98] in the developing brain is more consistent with the transient gap junctional coupling observed in the neocortex. In addition, Cx47 is also observed in the CNS [99], but its expression seems to be different from that of Cx36 in neurons of developing CNS, but there is some co-localization with Cx36 in cerebellum [99]. Cx37 is observed in motor neurons and Cx40 is expressed in developing neurons of spinal cord [100]. In the adult CNS, neurons are coupled via gap junctions mainly composed of Cx36 [95] and Cx45 [101] in the cortex and hippocampus. These neuronal gap junctions play an important role in forming electrical synapses [102,103]. Cx45 is expressed widely in the developing brain and in the adult brain localized in cerebral cortex, hippocampus and thalamus [101]. Cx45 is also observed in olfactory nerves [104]. In the retina, Cx26 is expressed in horizontal cells [105] and Cx36 in AII amacrine cells [105], although Cx26 is not shown in the neurons in the adult cortex and hippocampus [106]. Recently, it has been reported that hemichannels of horizontal cells in the retina are mainly composed of Cx26 and regulate the activity of the Ca2 + channels and subsequent glutamate release [105]. The availability of various antibodies has made it possible to detect connexins which compose gap junctions [95,107] as well as hemichannels [108, 109], allowing characterization of the functional state, distribution and colocalization of connexins. In order to understand the role of specific connexins in the CNS, a knockout strategy has been employed by several investigators. Initial examination suggested some subtle neural changes may be apparent in the Cx43 knockout mice at birth [110]. However, the neural phenotype of the Cx43 knockout mice is confounded by cardiac malformation and neonatal death [111]. In these mice, the abnormal migration of neural crest was observed [112,113]. More recently, we have reported a disturbance in the migra- tion of neurons in the neocortex of the Cx43 null mice [114]. Cx32 knockout mice are viable and fertile, and display demylenation in the PNS [115,116]. Moreover, neuronal hyperexcitability and myelin defects in the neocortex were observed [117], and the accumulation of oligodendrocyte progenitor cells and amplified apoptosis has been reported in the CNS of Cx32 knockout mice [118]. Cx36 knockout mice are viable and display no obvious anatomical abnor- malities [119], however detailed neurodevelopmental and anatomical studies have not been reported. Studies using Cx36 knockout mice in vitro suggest that the neuronal gap junctions are critical in the formation of gamma frequency oscillations in the hippocampus [103] and in generating synchronous activity in the cortex [102]. These mice show selective impairment of

hippocampal gamma oscillations [120]. Knockout of the other neuronal candidate, Cx26, is lethal at E9 – 10[121], and thus additional strategies must be followed to investigate its function in neuronal development [122]. Cx45 knockout mice die at E8-9 due to abnormal vascular development. Therefore, it is impossible to study the gap junctional function using adult Cx45 knockout mice. The expression of Cx45 has also been reported in the embryonic cortex and hippocampus [123], but its role in the development of the CNS remains to be determined. In vitro studies have suggested a role for gap junctional coupling in neuronal differentiation. When NT2 human embryonal carcinoma cells differentiate into neurons in response to retinoic acid (RA), the expression of Cx43, and the level of gap junctional coupling, progressively disappear [124]. Blocking of gap junctions disrupts RA-induced neuro- nal differentiation of both human NT2 [125] and mouse P19 cells [126]. Moreover, the differentiation of NT2/D1 progen- itor cells are reduced by blocking of gap junctions and hemichannels, suggesting hemichannels also play a role in the neuronal differentiation [127]. It therefore appears that the temporal pattern of connexin expression and gap junctional coupling during neuronal differentiation is critical.

Astrocytes

The main cell type in the brain coupled by gap junctions is the astrocyte. Astrocytes have traditionally been viewed to have a role in the metabolic and trophic support of neurons [128]. Intimate interactions have been shown to be involved in the role of radial glia in directing migration of neurons in the cortex [129]. Indeed, gap junctional coupling between radial glia and neural precursors may be critical for this process [30]. Gap junctions in astrocytes are primarily composed of Cx43 [130,131], in addition to other connexins, including Cx30 [132,133], Cx47 [134], Cx40, Cx45, Cx46 and Cx26 [134]. Moreover, gap junctions provide a substrate for formation of a functional astrocytic syncytium [130,131,136,137], implicated in the spatial buffering capacity of astrocytes, particularly in dealing with extracellular K+ arising from neuronal activity [138,139]. The propagation of intercellular Ca2 + waves is an important feature of astro- cytes in response to activation [140]. Studies from several laboratories have shown that gap junctions are involved in mediating intercellular Ca2 + signaling throughout the glial syncytium [141-143]. Astrocytic hemichannels also play a role in the release of adenosine triphosphate (ATP) associ- ated with Ca2 + signaling

[144,145]. Moreover, the inhibition of glycolytic and oxidative metabolism resulted in an increase of astrocytic hemichannels [146], suggesting in- volvement of hemichannels in this pathological condition. Astrocytes cultured from Cx43 knockout mice exhibit reduced gap junctional coupling and Ca2 + wave propagation [147, 148]. Meanwhile, Cx43 knockout astrocytes express other connexin subtypes (Cx30, 40, 45, 26, 46) [135], suggesting that connexins other than Cx43 could not compensate for the reduction of GJIC in astrocytes. Even astrocytes derived from heterozygote Cx43 knockout mice showed a significant reduction in gap junctional coupling [147, 149]. These hetero- zygote mice have been used for in vivo studies (see below). Recently, mice lacking Cx43 specifically in astrocytes have been generated by using the cre-recombinase system [150]. These mice can survive to adulthood, unlike Cx43 knockout mice, and exhibit amplified motor activity with increased hippocampal spreading depression, providing a valuable model for in vivo studies. Although Cx30 has been shown only in astrocytic gap junctions in the CNS, no major abnormality was observed in the brains of Cx30-deficient mice, although they exhibit severe hearing loss [151].

Microglia

Microglia are important cells in the CNS, participating in the reactive gliosis. Although resting microglia do not show phagocytosis, activated microglia behave like phagocytes [152]. Under normal conditions, microglia show little expres- sion of Cx43, however, this increases following stimulation by inflammatory cytokines [6] or Ca2 + ionophores [153], allowing for enhancement of gap junctional coupling. Cx36 has been also found to form gap junctions in microglia [155], suggesting the direct communication between microglia. Moreover, brain macrophages/microglia decrease Cx43 expression and gap junctional coupling in co-cultured astro- cytes [155, 156]. It is important not only to understand the phagocytic function of microglia but also to understand the role of microglial gap junctions in the inflammatory response of the CNS.

Oligodendrocytes

Several reports have indicated that oligodendrocyte gap junctions are composed of Cx32 [157-162], Cx36 [154], Cx29 [163] and Cx47 [164]. We have shown that

expression of Cx32 coincides with maturation of oligodendrocytes temporally and spatially [159,165]. The function of gap junctions in oligodendrocytes is thought to be primarily metabolic to allow ions and nutrients to pass from the somata to all the layers of the myelin [166,167]. The importance of this channel has recently been realized by the reported mutations of Cx32 associated with X-linked Charcot – Marie – Tooth disease, a peripheral demyelinating disorder [168 – 172]. It was initially thought that human and rodent Schwann cells are susceptible to pathology, leading to peripheral nerve demyelination, while oligodendrocytes appeared not to be affected. Cx32 knockout mice showed a reduced myelin volume and an enhanced excitability in the CNS [117], and a progressive peripheral neuropathy has been observed after 3 months of age [115,116]. Cx29 has also been specifically observed in oligodendrocytes and Schwann cells [163]. The expression of Cx29 exists mainly at the paranodes and juxtaparanodes [163], whereas Cx32 is not observed in the paranodes [176], indicating a difference in the distribution of these two connexins. In the pathogenesis of demyelination associated with the Cx32 deficiency, the compensatory role of Cx29 may have to be explored. Recently, Cx47 was observed to be expressed mainly in oligodendrocytes [164]. Cx47 null mice exhibit degeneration of nerve fibers, particularly in the optic tract [164]. Moreover, Cx47 and Cx32 double knockout mice exhibited a more severe demyelination in the CNS [164,177], indicating that both connexins play a critical role in myelination.

Schwann cell

The Schwann cells of peripheral nervous system. These cells proliferate after nerve development or after injury to promote the myelination; maybe GJs play a role in this process, distributing and synchronizing important signals to proliferation. Cx32 and Cx29, identified in Schwann cells, show the same distribution pattern at paranodal regions and in Schmidt-Lanterman incisures (small canals that interrupt the myelin sheath present in nerve cells; these incisions allow the nourishment of the cells isolated from the myelin). Cx32 is required for normal functions in peripheral nerve, as demonstrated with Cx32 knocked out (KO) animals or in Charcot-Marie Tooth disease. The role of Cx29 is not clear for controversial effects described in KO animal models [178-181].

1.4. Gap Junction in neuropathological condition

1.4.1. Brain ischemia

Cerebrovascular diseases rank are the third leading cause of death in the USA and fourth in Canada, most commonly manifesting as ischemic brain stroke [182,183]. In the context of experimental brain ischemia models, the neuro- protective role of astrocytic gap junctions is still controversial. Blocking astrocytic gap junctions enhances neuronal vulnerability to glutamate cytotoxicity in culture [184]. Moreover, blocking gap junctions in a hippocampal slice culture enhanced neuronal damage under experimental ischemia using oxygen and glucose depletion [185]. In vivo, heterozygote Cx43 knockout mice showed a significantly increased stroke volume compared to wild-type mice following middle cerebral artery occlusion (MCAO) and exhibited enhanced apoptosis in the penumbra [186]. These results suggest that astrocytic gap junctions play a neuroprotective role in oxidative and metabolic stress. On the other hand, neuronal death caused by oxygen and glucose depletion was decreased when Cx43 was blocked by specific antisense oligodeoxynucleotide in the hippocampal slice culture [187]. Similarly, the stroke volume following MCAO in the rat model was reduced by blocking gap junctions using octanol [188]. Therefore, it has been suggested that the spreading depression caused by ischemic insult goes through astrocytic gap junctions which remain open during the ischemic condition, resulting in the expansion of the stroke volume [189]. However, there are problems in interpreting the results obtained with gap junction blockers such as octanol because of the lack of specificity, particularly when administered systemically. In addition, there is no selectivity with regard to astrocytic gap junctions since all gap junctions in the tissue are affected. The use of more specific approaches to target gap junctions is desirable, for example using Cx43 antisense and interfering RNA. More recent use of targeted deletion of connexins, specifically in astrocytes, is providing evidence that astrocytic gap junctions play a neuroprotective role in ischemic insults through reduction of apoptosis and inflammation [190]. The role of astrocytic hemichannels in ischemic insult is still unknown. Recently, it has been reported that astrocytic hemichannels, which are closed under normal conditions, remained open under experimental ischemia induced by glucose and oxygen depletion. It is possible that open hemichannels allow for the release of glutamate causing loss of membrane potential [191], or hemichannels may contribute to the distribution of anti-apoptotic factors in the lesion area [192]. Cx32 knockout mice have been reported to exhibit an enhanced vulnerability of hippocampal neurons against brief global brain ischemia compared to wild-type mice [193],

suggesting that gap junctions of hippocampal interneurons play a neuroprotective role in ischemic insults. Moreover, expression of astrocytic gap junctions can be affected by macrophages and microglia express Cx43 following activation. In this context, the regulation of connexin expression can be mediated by various types of cells other than neurons and astrocytes following ischemic stress.

1.4.2. Epilepsy

There are two major clinical symptoms of epilepsy: the partial seizure where excessive electrical discharge is re- stricted to a given area in the brain, and the general seizure involving the entire brain [194]. The pathogenesis of seiz- ures may be associated with abnormal stimulation occurring in a certain region of the brain causing depolarization of the membrane, expanding to the surrounding cells. Gliosis at the lesion is usually observed in epileptic brain tissue. However, the participation of Cx43 which composes mainly astrocytic gap junctions is controversial (reviewed in Ref. [195]).In models of experimental epilepsy, strong recurrent excitatory activity, such as that produced by GABA receptor blocking, K+ pump blocking, and repetitive stimulation is used as the epileptic trigger [196]. Electrical coupling through neuronal gap junctions is reported to play an important role in the expansion of the epileptic wave [197]. Blocking of astrocytic gap junctions decreases Ca2 + oscillations in co-cultured neurons [197]. An increase of Cx32 expression was observed in the hippocampus in a model of bicuculline-induced epileptiform activity [198], although a decrease in the level of Cx36 mRNA has been reported in the hippocampus of the kainate-treated rat [199]. Meanwhile, neuronal gap junctions are required for the appearance of very fast oscillations associated with seizure activity [200]. Cx43 mRNA levels were increased in the temporal cortex of epilepsy patients [201]. Therefore, the role of gap junctions in epilepsy is still controversial. In the future, the gap junctional coupling between various types of cells in vivo should be evaluated under epileptic stimulation.

1.4.3. Demyelinating Syndromes

Alterations in connexins present in the myelynating glial cells (forming intercellular junctions in oligodendrocytes and autaptic, within themselves, in Schwann cells) all promote demyelination diseases. Interestingly, connexins present in the astrocytes, the major macroglial cell type in the nervous ystem and not traditionally associated with the

myelination process, also contribute to some myelin pathologies. Oligodendrocytes and Schwann cells express three different connexins: Cx47, Cx32 and Cx29, although only the first two are believed to form gap junction channels [202]. Whereas, Cx47 forms extensive gap junctions with astrocytes in soma and outer myelinated fibers, Cx32 is the most abundant within the layers of myelin itself (‘‘reflexive’’ or ‘‘autologous’’ gap junctions), between loops of the myelin sheath in individual oligodendrocytes and Schwann cells [203], although it can also form gap junctions with other astrocytic connexins. These more direct pathways between the myelin layers allow a much shorter route for metabolite exchange. The precise mechanism by which deficient gap junction communication alters myelin formation and maintenance, and why some axonal fibers are more affected than others are questions that remain to be answered. Myelin gap junctions seem to be in an unique position not only to regulate metabolite trafficking to and from the myelin sheath but also to guarantee myelin structure and proper compaction by regulating ionic and water fluxes. Further studies on the interdependence between connex- ins, aquaporins, ion channels, the gliovascular interface, and cell–cell junctions and on how astrocytic proteins interact, in turn, with the myelinating cells, oligodendrocytes and Schwann cells, will lead us into a new exciting time to understand the role of glial cells in myelination[204].

1.4.4. Neurodegenerative Disease

One of the major neurodegenerative diseases is Alzheimer’s disease (AD). Clinically, cerebral atrophy is observed mainly in the frontal cortex of AD patients and pathologically, neurofibrillary degeneration and senile plaques are shown in the lesions [205]. The senile plaque is a round deposit composed of amyloid protein surrounded by astrocytic processes. An increase in the expression of Cx43 was observed at the site of these amyloid plaques. Pathological evaluations have revealed the importance of astrocytic participation in the lesion using presenilin mutant knockin mice [206,207]and apoE null mice [208 – 210]. However, there is no report clarifying the relation between gap junctions and AD. AD is a progressive disease and the lesion exhibits a successive expansion, suggesting that the glial network may play a critical role in the pathogenesis of AD. Parkinson’s disease (PD) is a common neurodegenerative disease. Clinical symptoms are progressive tremor, muscle rigidity and gait disturbance [205]. In the brain of PD patients, the loss of dopaminergic neurons is observed in the substantia nigra-striatum [205]. The 1-methyl-4-phenyl- 1,2,3,6-tetrahydropyridine (MPTP)-model

of PD exhibited an increase of Cx43 expression in the striatum, although the coupling of astrocytes was not increased [211]. The alteration of gap junctions in the brains of PD patients has not yet been reported. Therefore, the pathological role of gap junctions in PD is still ambiguous. Although most of the mechanisms of tremors and dyskinesias which are commonly observed in PD patients are still obscure, the inferior olive has been focused on as the pathological generator of tremors [212, 213]. Neurons of the inferior olive are electrically coupled through gap junctions which plays a role in creating oscillatory activity [140]. Some studies have reported that the GJIC of inferior olive neurons is responsible for tremors [213,214], however, no difference of the severity of tremor induced by harmaline was observed between Cx36 knock- out mice and wild-type mice [215]. More experiments will be required to clarify the mechanism of tremors. In neurodegenerative diseases, it is also important to evaluate the inflammatory response because both AD and PD exhibit inflammation in the lesion [216]. Indeed, anti- inflammatory drugs may reduce the incidence of AD and delay the progression of the disease [217, 218]. As mentioned previously, activated microglia express gap junctions composed of Cx43 [6]. Moreover, activated macrophages decreased the expression of astrocytic gap junctions [7]. Therefore, further investigation of the possible gap junctional neuroprotective role of glial cells and inflammatory cells in neurodegenerative diseases is warranted.

2. Lithium and neuroprotection

Literatures data show the protective effects of lithium at the neuronal level. These include lithium modulation of autophagy, growth factors, excitotoxicity, and a variety of mechanisms underlying cell death, neurogenesis, and neuronal differentiation. All these effects represent the result of a multifaceted pharmacology, which is becoming more and more complex. Nonetheless, when trying to dissect the various mechanisms of action of lithium, two primary targets emerge: *glycogen synthase kinase 3beta* and *phosphatidylinositol phosphatase*. The numerous lithium effects on biochemical systems are placed downstream of these two main mechanisms. At several steps, these mechanisms interconnect to each other, thus making it difficult to keep distinct the biochemical cascades promoted by lithium. In this way, it is not surprising that, despite being described as different phenomena at the behavioral level, molecular mechanisms underlying the effects of lithium on mood, motor activity, and sensitization overlap with those responsible for neuroprotection and neurorestoration. It is likely that the ancestral

role of this ion as a modulator of cell survival, cell growth, movement, and mood is the consequence of a few molecular mechanisms operating in different neuronal networks, where a variety of cascade events take place. A variety of experimental models show neuroprotective effects of Li +, ranging froM acute neurological insults (ischemic, [219]; epileptic, [220]; traumatic, [221]., and brain damage) to neurodegeneration [Huntington's disease, [222]; Parkinson's disease (PD), [223]; Prion diseases, [224]; ALS, [225]; cerebellar ataxia, [226]; inclusion- body myositis, [227]; dementia, [228]; [229]; [230]]. Interestingly, the neuronal basis of neuroprotection might share the same mechanisms as the psychotropic effects of the drug. In fact, there is converging evidence that mood disorders and neuronal damage are often associated while both conditions seem to benefit from the modulation of the same intracellular pathways. Altogether these pre- clinical studies provide a strong background for the trans- lation of the neuroprotective effects of Li+ into modern neurological, and psychiatric practice.

In switching from intracellular mechanisms to diseases, the powerful effects of Li+ administration on the expression of specific growth factors seem to be a key effect for the therapeutic role of Li+ both in neuronal degeneration and psychopathology. However, Li + induced neurotrophin changes in the brain are not always conclusive, and the mechanism of action remains partly unknown, calling for further studies aimed at elucidating this critical feature of Li + . A few experimental conditions in which Li+ provides neuroprotection involve glutamateneurotoxicity. Infact, Li+ pretreatmentisable to protect different cell types against excitotoxicity caused by glutamate, a-amino-3-hydroxy-5-methyl-4-iso- xazolepropionic acid, and kainate ([231]; [232]; [225]). Consistent with excitotoxicity, the protective effects of Li+ are likely to extend beyond VEGF or BDNF expression. In fact, Li + dose-dependently decreases the levels of p53 and Bax, and causes a time-dependent and dose-dependent increase in Bcl-2 [233]. The p53 protein is a nuclear protein that binds to specific DNA sequences and functions as a transcription activator: it promotes the expression of Bax proapoptotic gene, but suppresses the expression of Bcl-2, an antiapoptotic gene [234]. Lithium- induced changes in the levels of Bax and Bcl-2 are likely to be because of inhibition of p53 expression. Lithium may also reduce directly the expression of Bax/Bcl-2; in fact, Li+ activates other transcription factors, such as cyclic AMP response element binding proteins ([235]; [236]) and activating protein-1 ([235] ;[237]). All these Li + -induced changes in transcription factors depend on a direct inhibition of GSK-3b or PI3K/Akt/ GSK-3b. Finally, the powerful autophagy-inducing effect of Li+ was recently claimed as a pivot for the neuronal mechanisms underlying

the clearance of altered proteins and mitochondria, which provide a powerful defense for several subsets of neurons. Given the multiple steps affected by Li+ in the biology of the neuron and the presence of different targets contributing to its nonconventional pharmacology, it remains hypothetical to firmly propose a single mechanism of action for Li +-induced neuroprotection. Even focusing on excitotoxicity does not help very much as there are several potential mechanisms contributing to Li + -induced protection against glutamate overactivity. Moreover, it is very likely that protective effects of Li+ extend far beyond excitotoxicity. In fact, as reported at the beginning of the review, Li+ prevents detrimental processes within neurons, but also promotes neuronal sprouting and produces a neurogenetic effect. The ancestral role of this ion in mediating the basic functions of the cell seems to be bound to innumerable metabolic pathways, which call for extensive investigation to cover the complex pharmacology of such a small ion [238]. Among a plethora of intracellular transduction mechanisms affected by Li, two main effects emerge: the inhibition of GSK-3b and PI phosphatase. Several biochemical pathways located downstream to these enzymes are modulated by Li . A number of these pathways are interconnected, making it difficult to distinguish which effect derives from the sole modulation of a specific biochemical event. Consequently, when trying to translate such a complex biochemical pharmacology into clinical outcomes, it is puzzling to decipher which intracellular pathway plays a major role. For the same reason it is often arbitrary to distinguish between the mechanisms responsible for desired therapeutic effects and detrimental side effects. Lithium pharmacology remains under debate; nonetheless a growing body of evidence indicates novel biochem- ical targets of Li+ action. These include Li+ modulation of autophagy, growth factors, excitotoxicity, apoptotic cell death, neurogenesis, and neuronal differentiation. Remarkably, all these effects may well apply to the novel experimental therapeutics promoted by Li, and the classic effect of the ion as a mood stabilizer. In fact, the molecular mechanisms underlying the effects of Li on mood overlap with those responsible for neuroprotection and neurorestoration. It is likely that the ancestral role of this ion as a modulator of cell biology extends to a variety of neuronal networks producing several behavioral effects. In this way the novel pharmacology of Li is a sort of template that recapitulates the novel insights into the biology of neuropsychiatric diseases.

Chapter 1

GLIA 58:1594–1609 (2010)

Dynamic expression of Cx47 in mouse brain development and in the cuprizone model of myelin plasticity

Rosalba Parenti1*, Federico Cicirata1, Agata Zappalà1, Angela Catania1, Francesco La Delia1, Valentina Cicirata1, Oliver Tress2, Klaus Willecke2.

1 Department of Physiological Science, University of Catania, V.le A. Doria, 6 95125 Catania, Italy

2 Institut fuer Genetik Rheinische Friedrichs-Wilhelm-Universitaet Bonn, Germany

Running title: Cx47 in development and plasticity process.

Number of words: 9135 ; figures: 9

*Correspondence to: Dr. Rosalba Parenti, Department of Physiological Science, University of Catania, V.le A. Doria, 6 95125 Catania, Italy.

E-Mail: parenti@unict.it

Keywords: Gap Junction; connexin; oligodendrocyte; development; plasticity

ABSTRACT

The study shows the dynamic expression of connexin47 (Cx47) in oligodendrocytes and myelin of mice, either in myelinogenesis occurring in early development or in an experimental model of new-myelinogenesis of adult mice. Cx47 first appeared in the embryonic mouse brain at E10.5; successively the expression increased, principally in regions populated by developing oligodendrocytes. The expression declined postnatally towards adulthood and was restricted to a few specific areas, such as the corpus callosum, the striatum, the cerebellum and the spinal cord. Since the expression of Cx47 in developing oligodendrocytes preceded those of Cx32 and Cx29, a role of Cx47 in myelinogenesis was postulated.

This hypothesis was tested in a model of re-myelination, which principally involved the corpus callosum, occurring in adult mice by treatment with cuprizone. Cx47 was up-regulated during demyelination and recovered during the remyelination phase. During demyelination, Cx47 was first over-expressed in the corpus callosum and later, when the myelin virtually disappeared in the injured areas, Cx47 was expressed in astrocytes located inside and closely around the demyelinated areas. The remyelination of injured areas occurred after stopping the administration of cuprizone and continued to complete recovery. In this period the expression of Cx47 shifted from astrocytes to new-formed myelin. So, Cx47 exhibits in this model a transient and de novo expression in astrocytes with a topographic segregation in the injured areas, only when oligodendrocytes and the myelin were most severely affected.

Taken as a whole the evidence would suggest that Cx47 play a key role in myelination.

INTRODUCTION

Intercellular communication through gap junctions (GJ) allows metabolic and electrical coupling of cellular networks. GJs are extensively distributed in the nervous system throughout life (Bruzzone et al., 1996). GJ channels are formed by oligomerized proteins called connexins (Cxs). Many Cxs have been identified in the central nervous system (Dermietzel, 1998). Evidence would suggest that each cell type usually expresses a specific set of Cxs which influences the permeability of channels formed, according to the metabolic or functional necessity (Bruzzone et al., 1994; Veenstra, 1996; Bevans et al., 1998; Cottrell and Burt, 2005; Johnstone et al., 2009).

Much experimental evidence has shown that Cxs are expressed during the whole life time, showing an evident expression during development. This is likely due to the role played by GJs in the establishment of regulatory compartments, and the formation of morphogenic gradients. Dynamic changes of Cxs expression may result in divergent cellular differentiation patterns by influencing the spread of intercellular signaling molecules, (Nadarajah et al., 1998; Rozental et al., 1998, 2000; Bittman and LoTurco, 1999; Prime et al., 2000; Mercier and Hatton, 2001; Parenti & Cicirata, 2004).

Oligodendrocytes, which myelinate nervous axons in the CNS, are extensively coupled via GJs (Dermietzel et al., 1997; Nagy et al., 2003; Nagy and Rash, 2003; Kamasawa et al., 2005). Oligodendrocytes are not coupled together; rather, together with astrocytes, they form a "glial syncytium." (Ahn et al., 2008; Orthmann-Murphy JL et al., 2008; Scherer et al., 1995). GJs may connect different parts of single cells surrounding nervous axons or different cells; so they provide essential pathways for intra- and intercellular ionic homeostasis (Nagy and Rash, 2003). Connexins expressed in oligodendrocytes are principally Cx32, Cx29 and Cx47 (Nagy et al., 2004). Cx32 is mostly expressed in perikarya of oligodendrocytes (Nagy et al., 2003; Kleopa et al., 2004). Cx29 is mostly expressed on sheets of mature myelin (Nagy et al., 2003; Kleopa et al., 2004). Cx47 is co-localized with Cx32 in oligodendrocyte somata (Menichella et al., 2003; Nagy et al., 2004; Li X et al., 2004; Kamasawa et al., 2005; Kleopa et al., 2004).

During development, Cx32 and Cx29 are temporally regulated. In fact, both Cx32 and Cx29 expression levels increase during the first few postnatal week concomitant with

the process of myelination in the brain and are highest in the adult brain (Dermietzel et al, 1989; Scherer et al., 1995; Nadarajah, 1997; Melanson-Drapeau et al., 2003; Nagy et al., 2003).

The expression of Cx47 was studied by Menichella (et al., 2003), who reported the temporal profile of Cx47 mRNA in extracts of brain regions during postnatal development. No information is yet available regarding Cx47 expression in prenatal life.

This study was planned to analyze in detail the expression of Cx47 protein from early stage oligodendrocyte development to adult life. Firstly we generated, purified and tested polyclonal antibodies against Cx47 in chicken. Our material showed that Cx47 was expressed in early embryonic life and that this expression was topographically and temporally organized. When compared to Cx32 and Cx29, Cx47 showed a temporal pioneering expression, suggesting a key role of Cx47 in the differentiation of oligodendrocyte progenitors and in myelinogenesis.

We tested this hypothesis in a model of experimental remyelination occurring in adult mice. Consequently, the expression of Cx47 was studied in oligodendrocytes following administration of cuprizone, a toxic copper chelator, which induces a transient demyelination process, followed by remyelination leading to complete normal recovery. In this model olidendrocytes degenerated during demyelination and re-generated during recovery. The expression pattern of Cx47 dynamically changed in the demyelination - remyelination process and thereafter progressively reduced to resting levels in coincidence with full morphological restoration. When the injury of both oligodendrocytes and myelin was more severe (resulting in substantial absence of both them in inured areas), Cx47 was de novo and transiently expressed by astrocytes principally located inside demyelinated areas. The shifted expression of Cx47 from oligodendrocytes/myelin to astrocytes and thereafter from astrocytes to oligodendrocytes/myelin, inside demyelination areas, would suggest that Cx47 plays a role in myelin remodelling.

MATERIALS AND METHODS

Animals and tissue preparation

CD1 mice were used for the developmental study. Embryonic days E 9.5, E10.5, E11.5, E13.5, E17.5, postnatal days P0, P7, P12, and adult (P21-28) were used. Presence of the vaginal plug indicated the first day of conception (E0.5). Embryos were obtained from pregnant CO2-anesthetized mice. Unfixed whole embryos (E9.5-11.5) and dissected brains (all other ages) were used for Western blotting analysis as described below. For immunohistochemistry, embryonic brains were fixed by immersion in 4% paraformaldehyde while the postnatal animals were perfused transcardially with 50-150 ml PBS and 50-250 ml 4% paraformaldehyde, followed by a 1-4 h submersion in the fixative. Thirty percent sucrose was used for cryoprotection. The brains were stored in the same sucrose solution, at 4 °C, for 24-48 hours. Brains were rinsed in PBS, embedded in albumin-gelatin and rapidly frozen in isopentane cooled in liquid nitrogen and stored at –80°C. Brain coronal and sagittal sections were cut at 10-20 μm with a cryostat (Leica), collected on gelatin coated slides and processed for immunohistochemistry as described below.

C57BL/6 female mice (8 weeks old, 20–25 g) were used for de- and remyelination study. Animals (Charles River Laboratories, Italy) were housed in specific pathogen-free conditions. Mice were continuously fed a powdered diet containing 0.2% bis-cyclohexanone oxaldihydrazone (cuprizone, Sigma, Aldrich Milan, Italy) w/w mixed into their regular chow as previously described (Matsushima and Morell, 2001). The following groups (6 animals/group) were included in the study: groups 1 and 2, fed for 3 or 5 weeks on a cuprizone-containing diet (i.e., Cup3w and Cup5w, respectively); groups 3, 4 and 5, fed for 5 weeks on a cuprizone-containing diet, followed by a 1, 3, or 6 weeks of recovery period on a regular diet (i.e., Cup1wR, Cup3wR, and Cup6wR, respectively). In parallel, each group of control mice of same age were fed with regular chow and sacrificed (C3w, C5w and C1wR, C3wR, and C6wR). At the end of their treatment period, the mice were euthanized by either decapitation to obtain fresh frozen brain tissue for total protein extraction or by transcardiac perfusion for immunohistochemistry. Brain tissue was harvested and frozen on dry ice and stored at -80°C until used. For transcardiac perfusion, animals were deeply anaesthetized with ketamine/xylazine 80/120 at 20 mg/kg and perfused with 4% paraformaldehyde in 0.1 M phosphate buffer (pH 7.4 at 4°C). Brains from perfused animals were post-fixed

overnight in the same fixative, cryoprotected with 20% sucrose for at least 48 h, snap-frozen in dry ice-cooled isopentane, and stored at -80°C until used.

C57BL/6 adult male, wild-type (+/+) and homozygous (-/-) Cx47EGFP (where Cx47 coding DNA was replaced with enhanced green fluorescent protein, EGFP, reporter gene) were used to characterize Cx47 antibody (Odermatt et al., 2003).

The experimental plan was designed according to the guidelines of the Italian law for care and use of experimental animals (DL 116/92) and approved by the Italian Ministry of Health.

Production of affinity purified anti-CX47 polyclonal antibodies.

To obtain the fusion protein for antibody production we used the cDNA encoding a Cx47 protein fragment of 126 aa corresponding to a sequence within the intracellular loop (IC) of mouse Cx47 (Cx47-IC:

RASEQERRRALRRRPGTRRLPRAQLPPPPPGWPDTTDLGEAEPILALEEDEDEEP GAPEGPGEDTEEERAEDVAAKGGGGDGKTVVTPGPAGQHDGRRRIQREGLMR VYVAQLVVRAAFEVAFLVG; UniProtKB/Swiss-Prot accession number: Q8BQU6). The restriction endonucleases used to generate this fragment were KpnI and PstI. This cDNA was inserted into a bacterial expression vector including a His tail (Qiagen S.p.A., Milan, Italy). His-tagged fusion protein was purified by a Ni(2+)-charged affinity column. Repeat immunization of a chicken with the purified recombinant Cx47-IC protein allowed the production of a high-titer polyclonal antibodies. The antibodiy was extracted from eggs (Tini et al., 2002) and purified by immunoaffinity using the purified antigen immobilized on CNBr-activated Sepharose 4B resin (Sigma-Aldrich, Milan, Italy).

HeLa cells transfection

Human cervix carcinoma HeLa cells were cultured in Dulbecco's modified eagle medium supplemented with 10% fetal bovine serum, 2mM glutamine, 100U/ml

penicillin, and 100µg/ml streptomycin at 37 °C in a humidified CO2-controlled incubator.

The coding region of mouse Cx47 was amplified from cDNA of mouse brain by PCR (primers: F: 5'-AGCTGGAGCTTCCTGACG- 3' and R: 5'-TCAGATCCACACGGTGGC- 3') and subcloned into the expression vector pCDNA3.1-TOPO (Invitrogen Milan, Italy).

HeLa cells were transiently transfected with the obtained construct including Cx47 using the Lipofectamine reagent (Invitrogen Milan, Italy) according to the manufacturer's instructions. Wild-type and transfected HeLa cells were used for Western blot and immunofluorescence analyses.

Enzyme-Linked Immunosorbent Assay (ELISA) procedure

Wells of microtiter plates were coated (18 h, 4 °C) with 2 µg/ml of polyclonal anti-Cx47 antibodies in 50 µl of coating buffer (0.05 M Na2CO3, 0.05 M NaHCO3, pH 9.6) and were then blocked with 2% bovine serum albumin in PBS for 1 h at 37 °C. Decreasing concentrations of Cx47 immunizing antigen (200 µl) were loaded in duplicate and incubated for 2 h at room temperature. HRP-conjugated goat anti-chicken (1:20,000) in blocking buffer was added (1 h, room temperature) and the reaction was visualized by the addition of 50 µl chromogenic substrate (TMB) for 30 min. The

reaction was stopped with 100 µl H2SO4 and absorbance at 450 nm was measured with reduction at 630 nm using ELISA plate reader. Plates were washed five times with washing buffer (PBS, pH 7.4, containing 0.1% (v/v) Tween 20) after each step. Different antigens than the immunizing one were also used as negative controls.

Black Gold staining

Black Gold staining was used to visualize at the light-microscopic level myelin during de- and remyelinization process as previously described (Schmued and Slikker, 1999). A 0.2% solution of Black Gold (Histo-Chem, Jefferson) was prepared according to the

previously published protocol (Schmued and Slikker, 1999). Briefly, mounted sections were Black Gold stained at 60°C in a conventional oven for about 30 min. The staining was intensified by incubation in a solution of 0.2% potassium tetrachloroaureate (Sigma-Aldrich, Milan, Italy) dissolved in 0.9% NaCl for 15 min at 60°C. For fixation, the sections were incubated for 3 min in 2% sodium thiosulfate (Sigma-Aldrich, Milan, Italy) solution. Then the sections were counterstained to localize the cell bodies. These sections were stained for 1.5 min in a 0.1% acetic acid solution of 0.4% malachite green (Sigma-Aldrich Milan, Italy), rinsed in distilled water for 1 min and differentiated in 70% ethanol to remove background staining. Finally, sections were dehydrated in graded ethanol, cleared in xylene, and coverslipped with Entellan (both from Sigma-Aldrich).

Cresyl Violet staining

A standard protocol from Carlton's Histological Technique (1985) was used to stain the sections with Cresyl Violet (Sigma-Aldrich Milan, Italy).

Western blotting.

Tissues and HeLa cells were homogenized in ice-cold 40mM Tris-HCl buffer, ph 7.4, containing 1% NP-40 detergent, 1mM PMSF and aprotinin, leupeptin and pepstatin A each at 5 μg/ml. After homogenization, samples were sonicated for 20 sec. Total protein was determined with the Bio-Rad, Dc protein assay and then resolved by SDS-PAGE. Protein was transferred to 0.25 μm polyvinilylidene difluoride membrane (Bio-Rad, Milan, Italy) in transfer buffer (25mM Tris, 192 mM glycine and 20% v/v methanol) containig 0.05% SDS. Membrane was blocked for 2 h at room temperature (5% dry milk, 1X Tris-buffered saline with 1% Tween 20 [TBST]), and probed with the following primary antibodies: chicken polyclonal anti-Cx47 (1:1000), rabbit polyclonal rabbit anti-Cx47 (1:500, Zymed Laboratories, Inc. USA), polyclonal anti-Cx29 (1:200, Zymed Laboratories, Inc. USA), mouse anti-Cx32 (1:500, Chemicon, Temecula, CA, USA), mouse anti-proteolipid protein (PLP 1:200, Chemicon), mouse anti-2',3'-cyclic nucleotide 3'-phosphodiesterase (CNPase 1:500, Chemicon), rat anti-Myelin Basic Protein (MBP 1:500, Chemicon). Blots were washed for 30 min in 1X TBST and then incubated in 1% dry milk, 1x TBST with the appropriate horseradish peroxidase (HRP) -conjugated secondary antibody (diluted 1:10000, Sigma-Aldrich) for 1h at room

temperature. As a control for protein loading, the same membrane was then incubated with specific anti-actin antibody (1:10.000, Oncogene Research Products, Boston, USA) followed by appropriate peroxidase-conjugated secondary antibody. Blots were washed twice in 1x TBST and once in TBS; antibody binding was detected using ECL (Amersham Pharmacia Biotech, Buckinghamshire, UK) according to the manufacturer's recommendations.

The specificity of Cx47 antibodies were tested by peptide preadsorption as described above. Bands were quantified using the software Gel-Pro Analyzer 3.1.

Immunohistochemistry

Cryostat sections were washed three times in PBS, blocked at room temperature for 1 hr in 1% normal goat serum in PBS, and then incubated overnight with chicken anti-Cx47 (1:200) or rabbit anti-Cx47 (1:100) alone or combined with the following primary antibodies: mouse anti-proteolipid protein (PLP, Sigma-Aldrich; 1:100), rat monoclonal anti-MBP (1:200, Chemicon), mouse anti-glial fibrillary acidic protein (GFAP 1:500, Chemicon), mouse antineuronal nuclei (NeuN, 1:250, Chemicon), monoclonal rat anti-Mac-1 (Cd11b/CD18 1:200, Chemicon). After incubating with the primary antibodies, the slides were washed and incubated with anti-chicken HRP-conjugated secondary antibody (1:1000, Sigma-Aldrich) for single detection of Cx47 or the appropriate fluorescein isothiocyanate- and rhodamine-conjugated donkey cross-affinity-purified secondary antibodies (diluted 1:200, Chemicon) for double-immunofluorescence. The specificity of Cx47 antibodies was tested by peptide preadsorption: 1 μg of anti-Cx47 was preincubated for 1 h at room temperature with or without 100 μg of immunizing peptide and then incubated with tissue sections.

Immunofluorescence analysis on HeLa cells was performed as previously described (Parenti et al. 2002) using anti-Cx47 antibody. Nuclei of HeLa cells were stained with Sytox (Molecular Probes, Eugene, OR).

Fluorescence was examined on a Leica fluorescence microscope equipped with filters for visualization of FITC (excitation, 450-490 nm; emission 515-550 nm) and Cy3 (excitation 541-551 nm; emission, 565-595 nm). Images were captured using a digital camera (Spot, Diagnostic Instruments, Sterling Heights, USA) and adjusted for contrast in Corel Draw version 9.

For confocal analysis, a laser scanning microscopy 510 Zeiss confocal microscope was used. Double-labelled sections of the same area for each fluorochrome were scanned to obtain images of double labelling and images were not manipulated to alter alignment of resulting overlays. Digital images were acquired with a 60× oil-immersion objective lens (numerical aperture, 1.5). Images at 1,024 × 1,024 pixel resolution were captured by using AxioVision 3.0.6 software and assembled in Photoshop 6.0 or Corel Draw 8. Minimal adjustment to brightness and contrast was required.

RESULTS

Cx47 antibody characterization

High-titer polyclonal antibodies were obtained by immunizing a chicken with the purified recombinant Cx47-IC protein, corresponding to Cx47 sequence of the intracellular loop. The antibody was purified by immunoaffinity using the immunizing antigen and was characterized by ELISA test, western blot and immunofluorescence analysis. The ELISA test was performed using the immunizing antigen that showed a titer of 1:20000, while no signal was obtained using different antigens as controls (data not shown). The antibody was tested on HeLa cells. Immunofluorescence analysis with Cx47 antibody on transiently transfected HeLa cells showed a bright fluorescent signal on cell membranes (Fig. 1A), while wild type HeLa cells spontaneously showed neither Cx47 RNA (data not shown) nor protein (Fig.1A1). Furthermore, western blot of transfected HeLa cells and total brain by using Cx47 antibody showed a single band migrating at ~47 kDa, while it was absent in both the heart extract, used as control tissue, and the total brain extract treated with the antibody pre-absorbed with immunizing antigen (Fig.1A1). Cx47 antibody was tested immunohistochemically: histological sections of adult brain were processed with anti-Cx47 or with protein extracts from eggs taken from chicken prior to immunization with the antigen. The sections processed with Cx47 antibody showed labelling that was absent on the sections performed with proteins of non-immunized eggs. No signal was detected when the primary antibody was omitted, thus excluding any unspecific staining by the secondary antibody itself (data not shown).

Immunoprecipitation was performed to demonstrate that antibodies use in this study recognize Cx47 protein target. We used rabbit-Cx47 antibody (Abcam) for precipitation. After, we performed the western blot with our chicken Cx47 antibody. We

carried out western blot on tissues from wild-type (+/+) and null-Cx47 (-/-) mice, in which Cx47 gene was replaced by EGFP (Odermatt et al., 2003). Cx47 was detected by Western blot analysis after immunoprecipitation in brain and spinal cords of Cx47 wild-type (+/+) mice but not in heart or in brain and spinal cords of Cx47 EGFP(-/-) mouse tissues (Fig 1B), as previously described in the senior author's report (Odermatt, et al., 2003).

Our antibodies were compared to the polyclonal antibodies against Cx47 generated in rabbit by Zymed and Abcam. All three antibodies showed one band migrating at ~47 kDa in western blot analysis on spinal cord and brain extracts of both wt and Cx47-KO animals (Fig. 1 C1-C2, data not shown for Abcam antibody). We hypothesized that the antibodies did not detect a specific signal on crude lysate while did following immunoprecipitation, on purified protein. Conversely, in immunohistochemical analysis all three antibodies labeled myelin and oligodendrocytes of the corpus callosum of wt animals but not those of null-Cx47 EGFP(-/-) animals, (Fig. 1 C3-C4, data not shown for Abcam antibody). Our antibodies labelled the myelin, counterstained by the antibody for the MBP (Fig. 1E-E1) as well as the bodies of oligodendrocytes, counterstained by the antibody for the PLP (Fig. 1F-F1). Cells stained by NeuN (neurons) and GFAP (astrocytes) were not labelled by either our or Zymed or Abcam antibodies.

In conclusion, our findings show that our as well as Zymed or Abcam antibodies are useful to be as a probe, even if the quantification of the amount of protein by immunoblotting is not possible.

Analysis of Cx47 protein during development

Immunohistochemical studies show the dynamic expression of Cx47 protein during developmental time.

Prenatal developmental stages were studied at different time intervals from E9.5 to E17.5. At E9.5 no immunopositivity was detected in the brain. At E10.5 a weak immunostaining was found in the mantle layer of hindbrain, in the commissure under the telencephalic vescicle and in the mantle layer of the longitudinal spinal tracts in the spinal cord (Fig. 2A). At E14.5, immunopositivity was found in both sides of the

ventral midline of the pons and the medulla and the medial areas of the cerebellar plate (Fig. 2B). At E15.5 to E17.5 the labelling became more widespread involving the main longitudinal tract of the brain and cerebellar plate (Fig. 2C-C1, D-D1). The immunoreactivity was localised in highly arborized processes typical of oligodendrocytes, while it was not detected in the soma of the corresponding cells. These irregular processes are roughly oriented in the same direction, probably forming axon tracts.

The postnatal development was investigated from P0 to P14. In that time interval Cx47 was expressed in some white matter tracts of different brain regions, such as diencephalon: the thalamo-cortical tract (Tha, Fig. 2E-E1) and the ventral tract of the fornix; the medulla: the hypoglossal nerve roots (hnr, Fig. 2F-F1), the medial longitudinal fascicle (mlf, Fig. 2F-F1), the longitudinal tracts in the tegmental region (see in Fig. 2F the habenulopeduncular tract, hpt), the transversal roots of cranial nerves (Fig. 2G-G1), as well as some disperse fibres in the reticular formation (Rt, Fig. 2G-G1); the white matter of the cerebellum (Fig. 2H-H1) and the white matter of the spinal cord.

In adult life (P28 and P60), Cx47 was expressed in few brain regions. In fact, the immunoreactivity was restricted to the corpus callosum (Fig. 3A), a few areas of the striatum (Fig. 3A-A1), the anterior commissure (AC, Fig. 3A) and some fibre tracts such as the spinal trigeminal tract (sp5, Fig. 3B-B1) and the optic tract (Fig. 1E). A weak labelling took place, involving fibres of cerebellar white matter (Fig. 3B-B2). Finally, Cx47 labelling was diffusely detected in oligodendrocytes of the spinal cord white matter (Fig. 1F).

The temporal expression profile of Cx47, analyzed at different times of the development, was compared to those of Cx32 and Cx29. Western analysis was performed to studying the protein levels of Cx32 and Cx29 (Fig. 4A-B). Cx32 was first detected at E17.5 and its amount progressively increased until P28. Cx29 was detected at P0 and the amount progressively increased until P28 (Fig. 4A-B). Cx47 expression was studied by immunostaining (Fig. 4C). With this aim, we arbitrarily divided the density of staining for microscopic area (20x) in four classes: no staining (-); weak staining (+), middle staining (++) and strong staining (+++). Different densities were usually found in the various areas of single animals. We show in Fig. 4C the greater density found at each age as the mean of the findings reported in the various animals investigated for each age. The diagram showed that the quantitative profile of the

expression of Cx47 is temporally organized. The expression started at E11.5 and progressively increased up to E17.5 and PO and successively decreased to weak level at P28, that is, at adult life (Fig. 4C).

The results show that Cx47 occurred while Cx32 and Cx29 increased suggesting a pioneering role of Cx47 in developmental myelinogenesis. Moreover, since in early postnatal life the decreasing profile of Cx47 occurred in the meantime of the increasing level of the Cx32 and Cx29, it is possible to postulate complementary functional role of these connexins at this age.

Cuprizone animal model

Cuprizone model was used to study demyelination followed by full remyelination (Matsushima and Morell, 2001). The study was carried out over 11 weeks. In the first 5 weeks, termed Cup1w-Cup5w, the animals were submitted to cuprizone diet, the following 6 weeks, Cup1wR-Cup6wR, the animals were fed a normal diet.

i.- Anatomical and neurological features - Progressive brain damage occurred in the time interval Cup1w-Cup5w. It was shown by ventricular enlargement together with a general reduction of the thickness of the upper cerebral cortex, as well as the other brain regions (Fig. 5B,C). As occurs following anatomical injury the animals showed severe neurological deficits which principally involved motor behaviour affecting exploration, locomotion, grooming and feeding. At Cup5w the animals showed more severe clinical condition and some of them died. Surviving animals showed complete anatomical restoration in the time interval of Cup1wR to Cup6wR: the brain regions returned to their normal volumes and the hydrocephalus disappeared. Consequently, neurological functions were completely recovered.

ii.- Oligodendrocyte and myelin injuries - Among the wide range of anatomical injuries of the brain, the myelin of the corpus callosum was particularly affected (Ludwin, 1978; Matsushima and Morell 2001). Myelinated fibres progressively decreased from Cup1w to Cup5w (Fig. 5B: Cup3w; Fig. 5C: Cup5w), as shown by the labelling of the Black-Gold, a marker for both normal and pathological myelin (Schmued and Slikker, 1999). Moreover, at Cup5w, when the demyelination process reached its peak, few oligodendrocytes were stained in the corpus callous which was reduced to a thin layer, and the myelin showed bead-like varicosities within the severed axonal remnants (Fig. 5C, C1), in contrast to the sharply outlined myelinated fibres of control animals (Fig.

5A, A1). Re-myelination of the corpus callosum occurred with the normal diet during Cup1wR-Cup6wR. It consisted of progressive growth of oligodendrocyte cell population in the demyelinated areas up to normal condition. Typical pathological features, such as fibre bubbles, progressively disappeared (Fig. 5F-F1).

iii.- Gliosis - During demyelination, a strong gliosis occured. Immunostaining with Mac-1, a marker for microglia/macrophages, showed that microglia increased in all brain regions, but principally in the demyelinated fibre areas of the corpus callosum at Cup3w mice and more again at Cup5w (Fig. 6B, B1). Thereafter it progressively decreased to return to physiological level during the 6 weeks of recovery.

The density of astrocytes strongly increased from Cup1w to Cup5w and this increment persisted during Cup1wR-Cup6wR. The astrocytosis diffusely involved the CNS, including myelinated bundles, such as the anterior commissure (Fig. 6C) and demyelinated ones, such as the corpus callosum (Fig. 6E). The astrocytes of demyelinated areas showed hypertrophied somata and thick processes, morphological features known as "reactive astrocytosis" (Fig. 6E1), in contrast to the thin and delicate processes of the astrocytes of areas that were not demyelinated.

iiii.- Protein changes - Protein levels of the myelin and the oligodendrocytic cells were analyzed in the cuprizone model during different steps of demyelination (Cup3w and Cup5w), and remyelination (Cup1wR, Cup3wR, and Cup6wR), by using MBP and the CNPase, respectively (Fig. 7). The results were compared to those collected from wt animals, used as control animals (Fig. 7). Western blot analysis was performed on extracts of relatively wide areas of the brain regions including the corpus callosum, as the severe injury of the corpus callosum did not allow selective dissection of the demyelinated areas. Therefore, western blot values reported in this study are mean results of injured tissue and intact surrounding areas.

Both MBP and CNPase protein levels decreased progressively during the treatment with cuprizone and reached lower values at Cup1wR. At this time the myelin, which corresponded to about 25% of normal values, was affected more severely than oligodendrocytes, which corresponded to about 50% of control animals (Fig. 7A-C). Successively, with normal diet, they increased towards baseline, in agreement with Matsushima and Morell (2001), although there were some differences (Fig. 7). In fact, oligodendrocytes returned to normal values (about 100%, in compared to control values) at Cup3wR, while the myelin increased slowly and at Cup6wR it was similar to normal value (Fig. 7A, C). The different temporal profiles of oligodendrocytes and

myelin during the recovery, supports the idea that the re-myelinization occurs in two steps: first, the re-colonization of the demyelinated area by oligodendrocytes and second, the formation of the myelin. (abbrevia e non enfatizzare differenza oligo/mielina così come divisione in two steps)

The expression of Cx47 in the corpus callosum was investigated at the same time intervals as the MBP and CNPase by using the same model reported before. In summary: the discrete immunostaining observed in the corpus callosum of control animals to Cx47 antibody, was scored as (+). The density of staining observed in treated animals was arbitrarily divided into two further levels: moderately increased staining (++) and strongly increased staining (+++). The histographic representation of the expression of Cx47 of these animals reported in Fig.7D, shows the strong increment of the expression (+++) at 3w and 5w, the medium expression (++) at 1wR and 3wR and finally, the return to normal level of expression at 6wR.

The findings, collected from the corpus callosum of treated animals, show that the expression of the myelin and oligodendrocytes, and Cx47, changed differently. The first ones decreased during the treatment, while the second ones increased. The contrary occurred in post-treatment recovery. Since previous findings have reported the expression of Cx47 in myelin and oligodendrocytes, it was surprising to find that all the changes were not parallel. Therefore, we performed an immunoistochemical investigation to study this phenomenon at cellular level. Expression of Cx47 at cellular level - Cx47 was slightly expressed by myelinated fibres of the corpus callosum of wt animals, while in cuprizone treated animals the expression strongly increased in myelinated fibres at Cup3w, as shown by double staining with MBP marker (Fig. 8a A-B). At Cup5w, few myelinated fibres were visualized in the corpus callosum, which was completely disorganized and infiltrated by many astrocytes, as well as the overhanging cortex and the subjacent striatum (Fig. 8a C-D). At this stage Cx47 was expressed by many more cells by microscopic field than wt animals. Most of these cells were also stained by the antibody for the GFAP. The astrocyte nature of these cells was also corroborated by their typical cellular profile. Most of Cx47-positive astrocytes found in the demyelinated area of the corpus callosum (Fig. 8a C1-D1) and in the close surrounding borders (Fig. 8a C2-D2), showed large cell bodies and shorter processes (as typical reactive astrocytes) than resting ones, principally found in brain regions far from demyelinated areas.

Interestingly, Cx47 was very few, if any, expressed in astrocytes of other brain areas, including cortical layer overhanging the demyelinated corpus callosum (Fig. 8b C3-D3) and other non-demyelinated bundles of fibres (Fig. 8b E-F). This condition was largely unchanged at Cup1wR. In the following recovery period (Cup3wR–Cup6wR), despite the large number of reactive astrocytes that persisted in the corpus callosum (Fig. 8b G-H), the quantitative incidence of Cx47-positive astrocytes decreased inversely to the increment of oligodendrocytes and myelin. At Cup6wR Cx47 was almost exclusively expressed by restored myelinated fibres of the corpus callosum (Fig. 8b G1-H), while it was no longer detectable in astrocytes.

Thus, immunohistochemical expression of Cx47 in cuprizone diet showed that Cx47 strongly increased in the first weeks and that such a level persisted at Cup3w and Cup5w. In the successive normal diet, Cx47 slightly decreased at Cup1wR and this level was roughly maintained at Cup3wR and Cup6wR (Fig. 7 D). The comparison of Cx47 with the expression levels of MBP and CNPase, showed that Cx47 increased in the same time period in which both myelin and oligodendrocytes decreased (Cup3w-Cup5w). Thereafter, Cx47 decreased during recovery time (Cup1wR-Cup6wR) maintaining a higher expression level than wt animals (Fig. 7 D). This evidence would support the involvement of Cx47 principally in demyelination, but also in myelin regeneration.

In conclusion, the data shows a dynamic expression profile of Cx47. It was up-regulated by affected myelinated fibres during demyelination process, transiently expressed by reactive astrocytes during the acute time of demyelination in the affected area and in the delimiting borders and finally re-expressed by oligodendrocytes newly forming myelin during remyelination process.

DISCUSSION

The first step of the study consisted in the generation of a new antibody for Cx47. The following considerations can be made.

1) The use of intracellular loop as epitope, unlike commercially available antibodies, which are usually generated against C-teminal sequence, allows for the comparison of immunostaining results obtained by this novel antibody with those obtained by commercially available antibodies. Comparable immunostaining results were obtained by using our antibody, generated in chicken, and the Zymed or Abcam antibodies, generated in rabbit.

The new antibody stained both myelin and oligodendrocyte cell bodies (Fig. 1 E-F), while previous immunohistochemical studies have reported the principal localization of Cx47 in the oligodendrocyte perycaria (Nagy et al., 2003; Menichella et al., 2003; Odermatt et al., 2003). We tentatively attributed the different staining to the different epitopes of the antibodies used in the studies.

2) The generation of antibody in chicken brings several advantages (Tini 2002), because birds exhibit enhanced immunogenicity to mammalian proteins due to their phylogenetic distance (Gassmann et al., 1990). Furthermore, the chicken egg-yolk immunoglobulins (IgY) do not interfere with mammalian IgG because of their different Fc region structure. Therefore, the use of antibody made in chicken usually reduces background noise.

3) The purification by affinity increased the specificity of the antibody.

4) The specificity of antibodies used in this study was tested on wild-type and Cx47 EGFP(-/-) mice, because the use of knockout animal is one of the more efficient ways to demonstrate the specificity of a given antibody (Pradidarcheep et al., 2009). The results showed comparable specificity of all three antibodies for immunoistochemical analysis while they apparently did not recognize any specific band in western blotting analysis. An hypothesis can be proposed to this regard. It is possible that Cx47 protein appears differently in its native conformation (as seen in immunohistochemistry) when compared to the conformation adopted under denaturing condition, as seen on an SDS gel. Finally, immunoprecipitation result suggested that antibodies did not detect specific signal on crude lysate while it did on purified protein. Therefore, single antibodies, are

useful to be used for immunohistochemistry, even if the quantification of the amount of protein by immunoblotting is not possible. Previously has been suggested for single antibodies, possible coexistence of low specificity for Western blots and high specificity for immunohistochemistry (Pradidarcheep et al., 2009; Saper, 2008).

In light of these considerations, immunoistochemical results of this study obtained by our antibodies were systematically confirmed by Zymed or Abcam antibodies, because both of them always show similar results.

Cx47 expression

The expression of Cx47 was very dynamic during both development and de- or re-myelination process in adult brain

a.- Cx47 expression during development

This study first investigated the expression of Cx47 protein in prenatal life. Therefore, it provided some new information on early expression of Cx47 in CNS.

Early expression of Cx47 detectable by immunocytochemistry occurred at E10,5 in the mantle layer of both hindbrain and longitudinal spinal tract in the spinal cord as well as in the commissure under telencephalic vescicle. Since previous studies have shown that oligodendrocyte precursors arise at that developmental time and in the same brain regions (Timsit, Martinez et al., 1995), it was likely that Cx47-positive cells were developing oligodendrocytes. Alternatively, it is also possible that some of the cells expressing Cx47 at that time were pluripotent progenitors, since the generation of neurons and oligodendrocytes from a common precursor cell has previously been reported by Williams (et al., 1991), and was described in mouse brain until P10 (De Vitry et al., 1980). The dynamic pattern demonstrated by successive immunostaining (the ventral midline of the pons and the medulla, the main longitudinal tract of the brain and cerebellar plate) was congruent with the migration of oligodendrocyte progenitors

into developing CNS tissues (Timsit, Martinez et al., 1995; Hardy and Friedrich,1996). This evidence supports the hypothesis that Cx47-positive cells were myelin-forming cells. It is well known that oligodendrocytes are extensively coupled with adjacent cells during myelinogenesis (Venance et al., 1995). The interactions of oligodendrocyte with neurons at the axonal level is required for the maturation of CNS neurons (Brady et al., 1999; Colello et al., 1994; Colello and Schwab, 1994; Mathis et al., 2000), the formation and maintenance of the nodes of Ranvier and the paranodal regions (Arroyo et al., 2001; Mathis et al., 2001). The role of these interactions in the normal brain development has also been suggested by Mathis (et al., 2003) who recently reported that a phenotype with a profound perturbation of the cerebellar cytoarchitecture occurrs after oligodendrocyte ablation. Therefore, it is possible explained by Cx47 involvement in the communication of oligodendrocytes with surrounding cells (Altevogt and Paul, 2004; Nagy et al., 2004;). The role played by Cx47 is further stressed by the fact that it is expressed earlier and stronger than Cx32 and Cx29. Altogether, this evidence would suggest Cx47 has a role of primary importance in the context of direct cell-cell communication in early brain development, and more generally, the importance of the role played by gap unction communication in the correct brain development.

Findings collected by the analysis of Cx47 expression in postnatal life basically corroborate previous studies (Menichella et al., 2003). In fact, the expression level gradually decreased from born to adulthood, when it was restricted to a few specific areas. At that age Cx47 immunolabelling was similar to that of Cx32 and quite different from that of Cx29, according to previous results (Li et al., 2004; Nagy et al., 2004). The similar expression pattern of Cx47 and Cx32 suggested a possible functional cooperation between them. This hypothesis was strengthened by previous results which showed that mice lacking both Cx47 and Cx32, die by postnatal week 6 with severe abnormalities in CNS, characterized by oligodendrocyte cell death, and axonal loss, prominent myelin abnormalities accompanied by a strong action tremor while mice lacking Cx32 or Cx47 alone, are viable and fertile (Odermatt et al., 2003; Menichella et al., 2003).

It is worth noting that all findings of developmental studies, from prenatal time to adulthood, support the expression of Cx47 in a single cell type: oligodendrocyte or myelin. Staining of other cell types has now been excluded. In fact, despite Cx47 mRNA was firstly reported to be restricted to neurons (Teubner et al., 2001), the neuronal localization of Cx47 mRNA was recognized to be incorrect (Odermatt et al.,

2003), and it was definitively demonstrated that Cx47 is expressed exclusively in oligodendrocytes in mouse brain and spinal cord (Li et al., 2004; Nagy et al., 2004).

b.- Cx47 expression in cuprizone model

Cuprizone administration induced the progressive loss of both myelin and oligodendrocytes up to Cup5w in the corpus callosum , when the corpus callosum was reduced to a thin layer, while with normal diet it was restored to normal size in 6 weeks (Fig. 5). The deletion of myelin and oligodendrocytes was shown during cuprizone diet by both Western blot (Fig. 7) and immunohistochemical analyses (Fig. 8), in agreement with previous findings (Dermietzel et al, 1989; Scherer et al., 1995; Nadarajah, 1997; Melanson-Drapeau et al., 2003; Nagy et al., 2003).

Therefore, as Cx47 was expressed by both oligodendrocytes and myelin, the decrement expression of Cx47 during administration of cuprizone was expected. Conversely, it increased during demyelination and the successive recovery process (Fig. 7C). The upregulation of Cx47 suggests that it is involved in both affected and plastic cell remodelling. Moreover, the expression of Cx47 in the corpus callosum was very dynamic. In fact, while in control animals Cx47 was slightly expressed in oligodendrocytes and myelin processes, in cuprizone treatment the expression changed at different time intervals: at Cup3w it was up-regulated in myelin processes (Fig. 8a A-B); at Cup5w and Cup1wR, Cx47 did not stain oligodendrocytes and myelin of the corpus callosum, obviously because they were almost completely absent, conversely it was de-novo and transiently expressed by astrocytes (Fig. 8a C-D); at Cup3wR and Cup6wR, Cx47 was once more expressed by oligodendrocytes and new-formed myelin, while it was absent in astrocytes (Fig. 8b G-H).

Therefore, the transient and de novo expression of Cx47 occurred in astrocyte cells within a precise timeframe. In fact, it occurred only in the time ranging from severe demyelination, Cup5w, to the first week of recovery, Cup1wR. The expression of Cx47 involved principally the astrocytes segregated within the demyelinated area of the corpus callosum plus the surrounding grey matter (Fig. 8a C1-D1, C2-D2) while it did not affect astrocytes located elsewhere, either in grey or white matter (Fig. 8b C3-D3, E-F).

In summary, in wt animals Cx47 was slightly expressed in myelin and absent in astrocytes. Under cuprizone treatment it was over-expressed in myelin during the early affected stage; transiently expressed in astrocytes during severe injury (when

demyelination occurred) and once more expressed by new-formed myelin during the recovery process. Therefore, de novo expression of Cx47 in astrocytes in demyelinated areas, and in close regions, apparently vicariated the no-expression of Cx47 due to loss of myelin.

From this consideration the question arises of the role played by Cx47. Some hypotheses can be proposed. This study shows that the increment of Cx47 occurred alongside anatomical injury. In light of the severe functional defects shown by cuprizone administration, it is likely that protective factors are delivered locally to prevent severe and not more reversible occurrence of injuries. The anatomical segregation of Cx47 in the demyelinated area, suggests that it could be involved in the neuron protective function.

A further hypothesis focused on the transient expression of Cx47 in astrocytes. In fact, previous studies have shown that astrocytes are involved in delivery of factors promoting remyelination (Mason et al., 2001; Matsushima and Morell 2001). Since in these experiments Cx47 was expressed in astrocytes principally located inside the demyelinated area, it is possible that Cx47 may be involved in a network of astrocytes which actively promote the release of factors supporting remyelination.

Legends

Figure 1.

A: Immunofluorescence analysis on transiently transfected HeLa cells with Cx47 cDNA showed bright fluorescent signal on cell membranes. Nuclei were counterstained by Sytox. Scale bar =10 µm. A1: Western blot for Cx47 detection on protein extracts, by using chicken anti-Cx47 (Ch-Cx47). Lane 1, total brain; lane 2, transfected HeLa cells; lane 3, wild-type HeLa cells; lane 4, heart (control tissue). The lane 5 shows the absence of signal on total brain extract when the antibody was pre-absorbed with the immunizing antigen. The antibody detected a single band migrating at 47 kDa in all samples. B: Western blot analysis with Ch-Cx47 antibody after immunoprecipitation with Rb-Cx47 (Abcam) in lysate from Cx47 wild-type (+/+) and Cx47 EGFP(-/-) mouse tissues. Cx47 was found in the brain and spinal cord of wild-type mice. In heart (control tissue) and lysates from Cx47 EGFP(-/-), no bands were detected. C1-C2: Western blot analysis of protein lysates from Cx47 wild-type (+/+) and Cx47 EGFP(-/-) mouse tissues by using both chicken (C1, Ch-Cx47, prepared by us) and rabbit (C2, Rb-Cx47, Zymed) anti-Cx47. Western blot analysis showed a band, at ~ 47 kDa in total brain and spinal cord of wild-type (+/+) and Cx47 EGFP(-/-) mice. C3-C4: Images of corpus callosum immunostained by using both Ch-Cx47 (C3) and Rb-Cx47 (C2) that show EGFP signal (green) as reporter for Cx47-expressing cells. EGFP was shown by Cx47 EGFP(-/-) mice while it was not observed in wild-type tissues (+/+) (not shown). All corresponding micrographs were recorded with the same microscope settings.

E-F: Ch-Cx47 antibody used in this study stained both the myelin, as revealed by double immunohistochemistry with MBP (E-E1) as well as cell bodies of oligodendrocytes, as revealed by double immunohistochemistry with PLP (F-F1). Abbreviations: Opt, optic tract; SC, spinal cord.

Figure 2

Pattern of expression of Cx47 in pre- and post-natal developmental stages. A: Immunostaining of sagittal section 10.5 dpc mouse embryo, showing high expression in the mantle layer of hindbrain (white arrowhead). B: Magnified view of coronal sections 14.5 dpc mouse embryo, showing immunolabelling in cerebellar plate (B-B1) and

medulla (B-B2). C: coronal sections 17.5 dpc mouse embryo, showing immunolabelling in the longitudinal tracts of the midbrain (C-C1 and D-D1) and cerebellar plate (D-D2). E-H: coronal sections of postnatal mouse brain, showing immunolabelling in some axonal tracts: thalamus and hypothalamus (E-E1), medulla (F-F1, G-G1) and white matter of cerebellum (H-H1). Abbreviations: Hnr, hypoglossal nerve roots; hpt, habenulopeduncular tract; Hyp, hypothalamus; Mlf, medial longitudinal fascicle; Rt, reticular formation; Tha, thalamus.

Figure 3

A-B: Pattern of expression of Cx47 in coronal sections of adult mouse brain. Abbreviations: AC, anterior commissure; Cbl, white matter of cerebellum; CC, corpus callosum; Sp5, spinal trigeminal tract; Str, striatum.

Figure 4

A: Western blot for Cx32 and Cx29 detection on protein extracts of total embryo (E9.5 - E11.5) and total brain embryos (E13.5 - P28). Approximately 30 μg of protein extract was applied to each lane. The antibodies used in western blot are described in Material and Methods. Note that the anti-Cx32 detected 27 kDa monomer and its dimer form, migrating at 47 kDa; anti-Cx29 detected 29 kDa protein and a band around 50 kDa, probably Cx29 dimers.

B: Graphical representation of the optical densities of the Cx32 and Cx29 bands from Fig. 1A normalized for loading discrepancies using the β-actin signal, arbitrarily considered equal to 100. Western blots are plotted as single points that are the mean of three samples. Standard deviation was less than 20% (not shown).

C: Temporal expression profile of Cx47. We arbitrarily divided the density of staining for microscopic area (20x) into four classes: no staining (-); weak staining (+), middle staining (++) and strong staining (+++). The greater density found at each age is the mean of the findings reported in the various animals investigated for each age.

Figure 5

Black-Gold staining of corpus callosum obtained from control mice fed with a regular diet (A), 3 weeks (B), 5 weeks (C) of a diet containing cuprizone, or 5 weeks of a diet containing cuprizone followed by 1 (D), 3 (E), or 6 (F) weeks of recovery on a regular diet. Note the ventricular enlargement together with a general thickness reduction of the upper cerebral cortex occurring from Cup3w to Cup1wR (B-D) that disappeared from Cup3wR to Cup6wR (E-F), progressively. Compare the sharply outlined myelinated fibres of the control (A1) with the bead-like varicosities during the severed axonal remnants of Cup5w (C1). Some bubbles persisted until Cup6wR (F1) even if myelin morphology progressively acquired normal features. Magnification : 10x (A-F); 50x (A1, C1, F1).

Figure 6

Gliosis occurred in brain regions of the cuprizone model. A-B: Immunostaining with Mac1 antibody in coronal sections of adult mouse brain was negative in untreated controls (A) and labelled microglia in the corpus callosum (outlined by the dotted line) of Cup5w (B-B1). C-E: Immunostaining with GFAP antibody, labelled myelinated bundles not affected by cuprizone, such as the anterior commissure (C) and those in which demyelination occurred (E), such as the corpus callous, while it was negative in untreated controls (D). Astrocytes localized in demielinated area of the CC showed typical morphological modifications (reactive astrocytosis), which consisted of hypertrophied somata with thick processes (E1). Magnification: 10x (A-B and D); 40x (C); 60x (E1).

Abbreviations: AC, anterior commissure; CC, corpus callosum;

Figure 7

A: Western blot analysis showing the protein levels of the myelin by MBP, and oligodendrocytic cells by CNPase. For each time interval, controls were processed (C3-5w and C1-6wR). Antibodies were used as described in Material and Methods. B-C Graphical representation of the optical densities of the MBP and CNPase bands in

cuprizone and control time intervals from 7A. The densities were normalized to control (corpus callosum obtained from control mice fed with a regular diet), arbitrarily considered equal to 100. Western blots are plotted as single points that are the mean of three samples. Standard deviation was less than 20% (not shown). D: Cx47 expression profile in cuprizone versus control animals in the different time intervals. As in Fig. 4C, we arbitrarily divided the density of staining for microscopic area (20x) into four classes: no staining (-); weak staining (+), middle staining (++) and strong staining (+++). The greater density found at each age is the mean of the findings reported in the various animals investigated for each age.

Figure 8a

Confocal double immunofluorescence showing Cx47 localization in CNS of cuprizone mice. A-B: Fields in corpus callosum show overlapping distributions of fibres double labelled for Cx47 (green fluorescence) and MBP (red fluorescence) at level of affected myelinated fibres at the early stage of demyelination (Cup3w). C-D: double labelling for Cx47 (green fluorescence) and GFAP (red fluorescence) in astrocytes within the affected CC at the acute phase of demyelination (Cup5w). C1-D1: double labelled astrocytes infiltrated in the demyelinated area of corpus callosum. C2-D2: double labelled astrocytes in the borders of demyelinated area of corpus callosum.

Figure 8b

C3-D3 and E-F: Cx47-negative, GFAP-positive (red fluorescence) astrocytes of the cerebral cortex surrounding the demyelinated area of corpus callosum and the anterior commissure (AC). G-H: Cx47 labelling (green fluorescence) did not co-localize with GFAP (red fluorescence) in reactive astrocytes that persisted in the area of corpus callosum at the remyelination period (Cup6wR). G1-I: double labeled fibres for Cx47 (green fluorescence) and MBP (red fluorescence) in the same area of G.

REFERENCES

1. Ahn M, Lee J, Gustafsson A, Enriquez A, Lancaster E, Sul JY, Haydon PG, Paul DL, Huang Y, Abrams CK, Scherer SS. 2008. Cx29 and Cx32, two connexins expressed by myelinating glia, do not interact and are functionally distinct. J Neurosci Res. 86(5):992-1006.

2. Altevogt BM, Paul DL. 2004. Four classes of intercellular channels between glial cells in the CNS. J Neurosci. May 5;24(18):4313-23.

3. Arroyo EJ, Xu T, Poliak S, Watson M, Peles E, Scherer SS. 2001. Internodal specializations of myelinated axons in the central nervous system. Cell Tissue Res 305(1):53-66.

4. Bevans CG, Kordel M, Rhee SK, Harris AL. 1998. Isoform composition of connexin channels determines selectivity among second messengers and uncharged molecules. J Biol Chem 273(5):2808-16.

5. Bittman KS, LoTurco JJ. 1999. Differential regulation of connexin 26 and 43 in murine neocortical precursors. Cereb Cortex 9(2):188-95.

6. Brady ST, Witt AS, Kirkpatrick LL, de Waegh SM, Readhead C, Tu PH, Lee VM. 1999. Formation of compact myelin is required for maturation of the axonal cytoskeleton. J Neurosci 19(17):7278-88.

7. Bruzzone R, White TW, Paul DL. 1994. Expression of chimeric connexins reveals new properties of the formation and gating behavior of gap junction channels. J Cell Sci. Apr;107 (Pt 4):955-67.

8. Bruzzone R, White TW, Goodenough DA. 1996. The cellular Internet: on-line with connexins. Bioessays 18(9):709-18.

9. Carlton HM. 1985. In: 5th Edition, ed. Carlton's Histological Technique. Oxford University Press, New York.

10. Colello RJ and Schwab ME. 1994. A role for oligodendrocytes in the stabilization of optic axon numbers. J Neurosci 14(11 Pt 1):6446-52.

11. Colello RJ, Pott U, Schwab ME. 1994. The role of oligodendrocytes and myelin on axon maturation in the developing rat retinofugal pathway. J Neurosci 14(5 Pt 1):2594-605.

12. Cottrell GT, Burt JM. 2005. Functional consequences of heterogeneous gap junction channel formation and its influence in health and disease. Biochim Biophys Acta. 1711(2):126-41.

13. De Vitry F, Picart R, Jacque C, Legault L, Dupouey P, Tixier-Vidal A. 1980. Presumptive common precursor for neuronal and glial cell lineages in mouse hypothalamus. Proc Natl Acad Sci U S A 77(7):4165-9.

14. Dermietzel R, Traub O, Hwang TK, Beyer E, Bennett MV, Spray DC, Willecke K. 1989. Differential expression of three gap junction proteins in developing and mature brain tissues. Proc Natl Acad Sci U S A 86(24):10148-52.

15. Dermietzel R, Farooq M, Kessler JA, Althaus H, Hertzberg EL, Spray DC. 1997. Oligodendrocytes express gap junction proteins connexin32 and connexin45. Glia. Jun;20(2):101-14.

16. Dermietzel R. 1998 Diversification of gap junction proteins (connexins) in the central nervous system and the concept of functional compartments. Cell Biol Int 22(11-12):719-30.

17. Flanders KC, Thompson NL, Cissel DS, Van Obberghen-Schilling E, Baker CC, Kass ME, Ellingsworth LR, Roberts AB and Sporn MB. 1989. Transforming Growth Factor-β1: Histochemical Localization with Antibodies to Different Epitopes. The Journal of Cell Biology, Vol. 108, No. 2, pp. 653-660

18. Gassmann M, Thömmes P, Weiser T, Hübscher U. 1990. Efficient production of chicken egg yolk antibodies against a conserved mammalian protein. FASEB J 4(8):2528-32.

19. Hardy RJ, Friedrich VL Jr. 1996. Oligodendrocyte progenitors are generated throughout the embryonic mouse brain, but differentiate in restricted foci. Development 122 (7):2059-69.

20. Kamasawa N, Sik A, Morita M, Yasumura T, Davidson KG, Nagy JI, Rash JE. 2005. Connexin-47 and connexin-32 in gap junctions of oligodendrocyte somata, myelin sheaths, paranodal loops and Schmidt-Lanterman incisures: implications for ionic homeostasis and potassium siphoning. Neuroscience.;136(1):65-86.

21. Kleopa KA, Orthmann JL, Enriquez A, Paul DL, Scherer SS. 2004. Unique distributions of the gap junction proteins connexin29, connexin32, and connexin47 in oligodendrocytes. Glia 47(4):346-57.

22. Johnstone S, Isakson B, Locke D. 2009. Biological and biophysical properties of vascular connexin channels. Int Rev Cell Mol Biol. 278: 69-118.

23. Li X, Ionescu AV, Lynn BD, Lu S, Kamasawa N, Morita M, Davidson KG, Yasumura T, Rash JE, Nagy JI. 2004. Connexin47, connexin29 and connexin32 co-expression in oligodendrocytes and Cx47 association with zonula occludens-1 (ZO-1) in mouse brain. Neuroscience 126(3):611-30.

24. Mason JL, Suzuki K, Chaplin DD, Matsushima GK. 2001. Interleukin-1beta promotes repair of the CNS. J Neurosci 21(18):7046-52.

25. Mathis C, Hindelang C, LeMeur M, Borrelli E. 2000. A transgenic mouse model for inducible and reversible dysmyelination. J Neurosci 20(20):7698-705.

26. Mathis C, Denisenko-Nehrbass N, Girault JA, Borrelli E. 2001. Essential role of oligodendrocytes in the formation and maintenance of central nervous system nodal regions. Development 128(23):4881-90.

27. Mathis C, Collin L, Borrelli E. 2003. Oligodendrocyte ablation impairs cerebellum development. Development 130(19):4709-18.

28. Matsushima GK, Morell P. 2001. The neurotoxicant, cuprizone, as a model to study demyelination and remyelination in the central nervous system. Brain Pathol 11(1):107-16.

29. Melanson-Drapeau L, Beyko S, Davé S, Hebb AL, Franks DJ, Sellitto C, Paul DL, Bennett SA. 2003. Oligodendrocyte progenitor enrichment in the connexin32 null-mutant mouse. J Neurosci 23(5):1759-68.

30. Menichella DM, Goodenough DA, Sirkowski E, Scherer SS, Paul DL. 2003. Connexins are critical for normal myelination in the CNS. J Neurosci 23(13):5963-73.

31. Mercier F, Hatton GI. 2001. Connexin 26 and basic fibroblast growth factor are expressed primarily in the subpial and subependymal layers in adult brain parenchyma: roles in stem cell proliferation and morphological plasticity? J Comp Neurol. 431(1):88-104.

32. Nadarajah B, Jones AM, Evans WH, Parnavelas JG. 1997. Differential expression of connexins during neocortical development and neuronal circuit formation. J Neurosci 17(9):3096-111.

33. Nadarajah B, Makarenkova H, Becker DL, Evans WH, Parnavelas JG. 1998. Basic FGF increases communication between cells of the developing neocortex. J Neurosci 18(19):7881-90.

34. Nagy JI, Rash JE 2003. Astrocyte and oligodendrocyte connexins of the glial syncytium in relation to astrocyte anatomical domains and spatial buffering. Cell Commun Adhes 10(4-6):401-6.

35. Nagy JI, Ionescu AV, Lynn BD, Rash JE. 2003. Connexin29 and connexin32 at oligodendrocyte and astrocyte gap junctions and in myelin of the mouse central nervous system. J Comp Neurol 464(3):356-70.

36. Nagy JI, Ionescu AV, Lynn BD, Rash JE. 2003. Coupling of astrocyte connexins Cx26, Cx30, Cx43 to oligodendrocyte Cx29, Cx32, Cx47: Implications from normal and connexin32 knockout mice. Glia. Dec;44(3):205-18.

37. Nagy JI, Dudek FE, Rash JE 2004. Update on connexins and gap junctions in neurons and glia in the mammalian nervous system. Brain Res Brain Res Rev 47(1-3):191-215.

38. Odermatt B, Wellershaus K, Wallraff A, Seifert G, Degen J, Euwens C, Fuss B, Büssow H, Schilling K, Steinhäuser C, Willecke K. 2003. Connexin 47 (Cx47)-deficient mice with enhanced green fluorescent protein reporter gene reveal predominant oligodendrocytic expression of Cx47 and display vacuolized myelin in the CNS. J Neurosci. Jun 1;23(11):4549-59.

39. Orthmann-Murphy JL, Abrams CK, Scherer SS. 2008. Gap junctions couple astrocytes and oligodendrocytes. J Mol Neurosci. May;35(1):101-16.

40. Parenti R, Cicirata F. 2004. Retinoids and binding proteins in the cerebellum during lifetime. Cerebellum 3(1):16-20.

41. Pradidarcheep W , Stallen J, Labruyère WT, Dabhoiwala NF, Michel MC, Lamers WH. 2009. Lack of specificity of commercially available antisera against muscarinergic and adrenergic receptors. Naunyn-Schmied Arch Pharmacol 379:397–402.

42. Prime G, Horn G, Sutor B. 2000. Time-related changes in connexin mRNA abundance in the rat neocortex during postnatal development. Brain Res Dev Brain Res. Jan 3;119(1):111-25.

43. Rozental R, Morales M, Mehler MF, Urban M, Kremer M, Dermietzel R, Kessler JA, Spray DC. 1998. Changes in the properties of gap junctions during neuronal differentiation of hippocampal progenitor cells. J Neurosci 18(5):1753-62.

44. Rozental R, Srinivas M, Gökhan S, Urban M, Dermietzel R, Kessler JA, Spray DC, Mehler MF. 2000. Temporal expression of neuronal connexins during hippocampal ontogeny. Brain Res Brain Res Rev 32(1):57-71.

45. Saper CB. 2009. A guide to the perplexed on the specificity of antibodies. J Histochem Cytochem. Jan;57(1):1-5.

46. Scherer SS, Deschênes SM, Xu YT, Grinspan JB, Fischbeck KH, Paul DL. 1995. Connexin32 is a myelin-related protein in the PNS and CNS. J Neurosci 15(12):8281-94.

47. Schmued L, Slikker W Jr. 1999. Black-gold: a simple, high-resolution histochemical label for normal and pathological myelin in brain tissue sections. Brain Res 837(1-2):289-97.

48. Timsit S, Martinez S, Allinquant B, Peyron F, Puelles L, Zalc B. 1995. Oligodendrocytes originate in a restricted zone of the embryonic ventral neural tube defined by DM-20 mRNA expression. J Neurosci 15(2):1012-24.

49. Tini M, Jewell UR, Camenisch G, Chilov D, Gassmann M. 2002. Generation and application of chicken egg-yolk antibodies. Comp Biochem Physiol A Mol Integr Physiol 131:569–574.

50. Veenstra RD. 1996. Size and selectivity of gap junction channels formed from different connexins. J Bioenerg Biomembr 28(4):327-37.

51. Venance L, Cordier J, Monge M, Zalc B, Glowinski J, Giaume C. 1995. Homotypic and heterotypic coupling mediated by gap junctions during glial cell differentiation in vitro. Eur J Neurosci 7(3):451-61.

52. Williams BP, Read J, Price J. 1991. The generation of neurons and oligodendrocytes from a common precursor cell. Neuron 7(4):685-93

FIGURES

Fig. 1

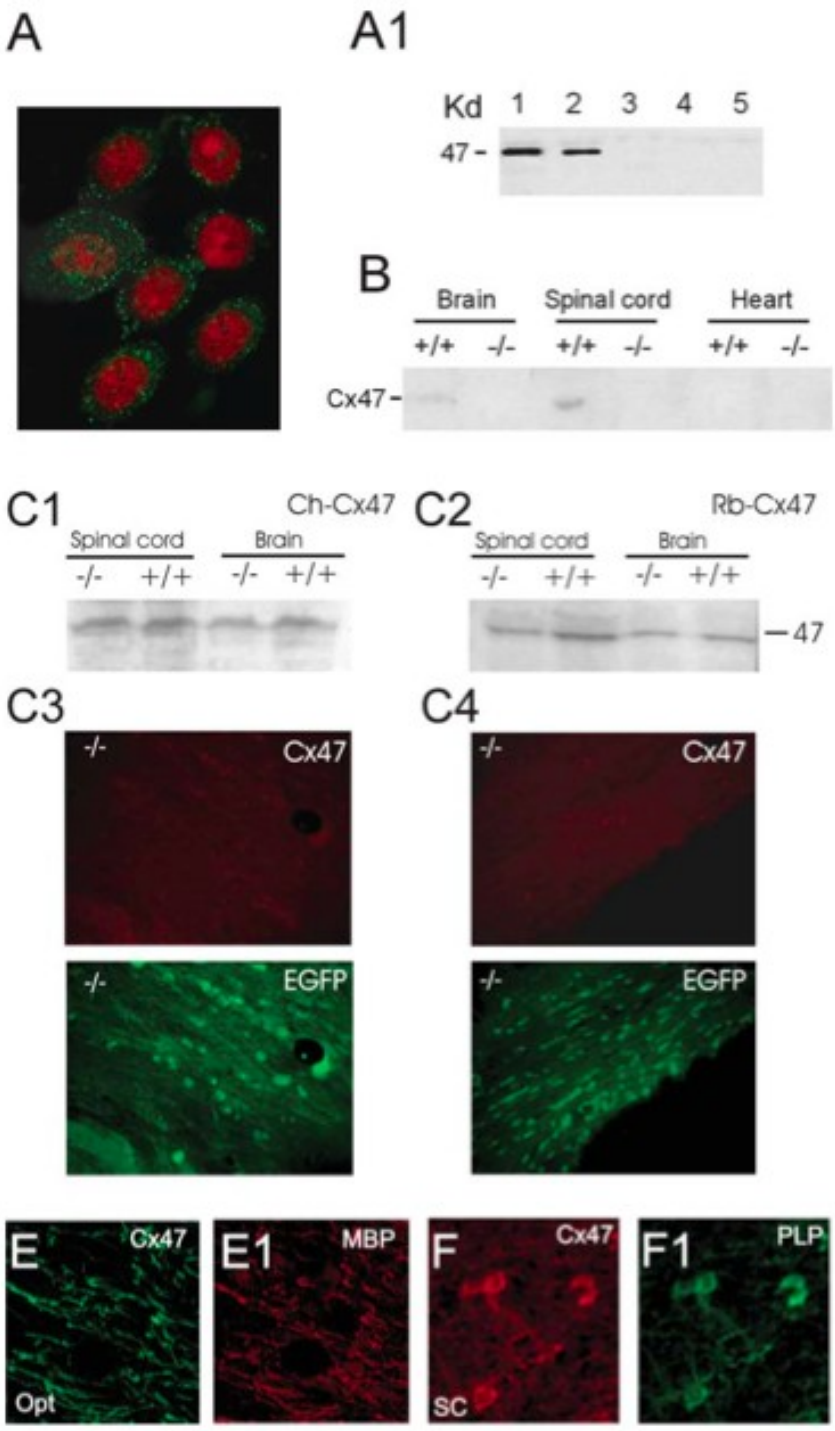

Fig. 2

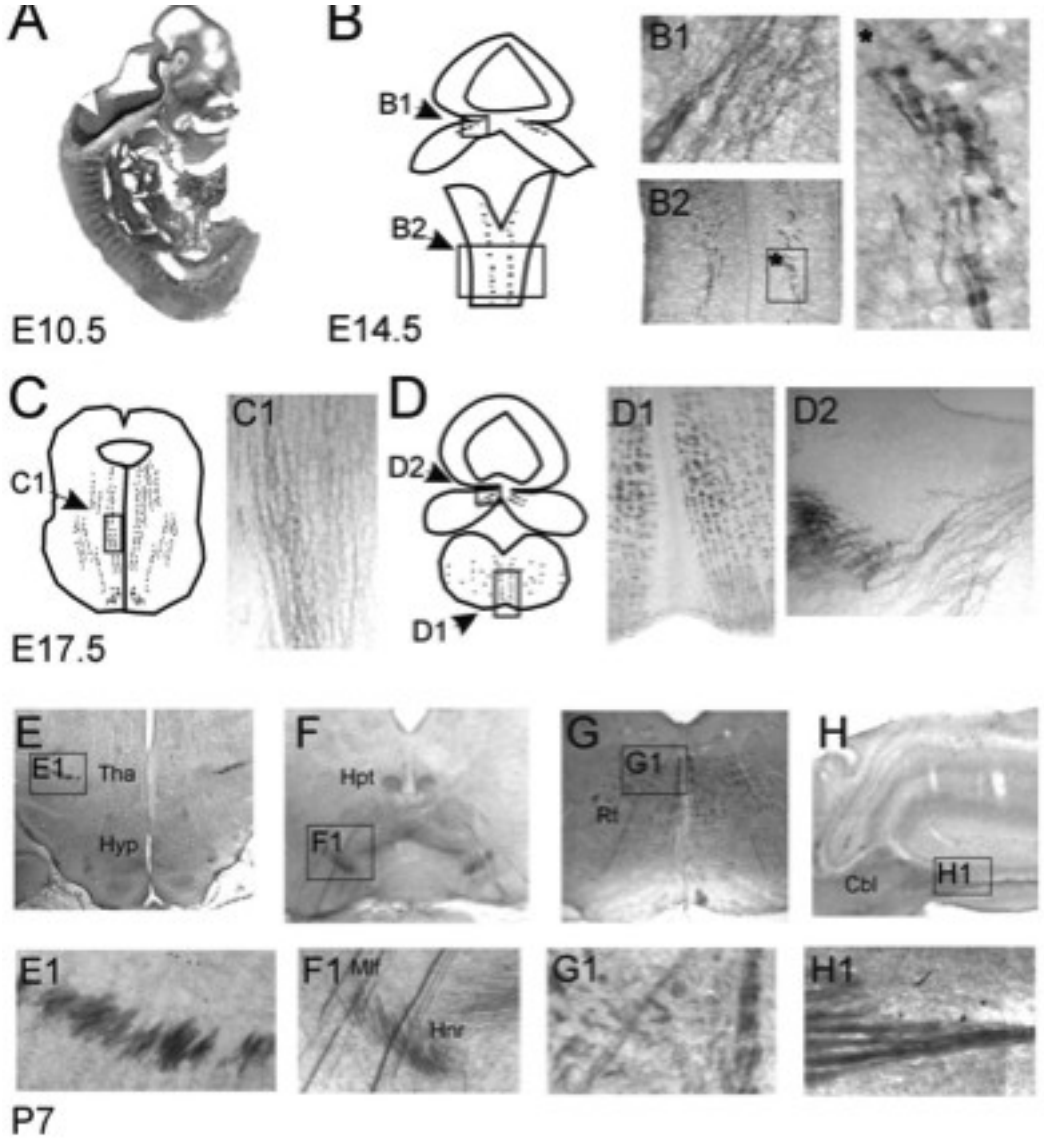
A
E10.5
B
B1
B2
E14.5
B1
B2
C
C1
E17.5
C1
D
D2
D1
D1
D2
E
E1
Tha
Hyp
F
Hpt
F1
G
G1
Rt
H
Cbl
H1
E1
F1
Mf
Hrv
G1
H1
P7

Fig. 3

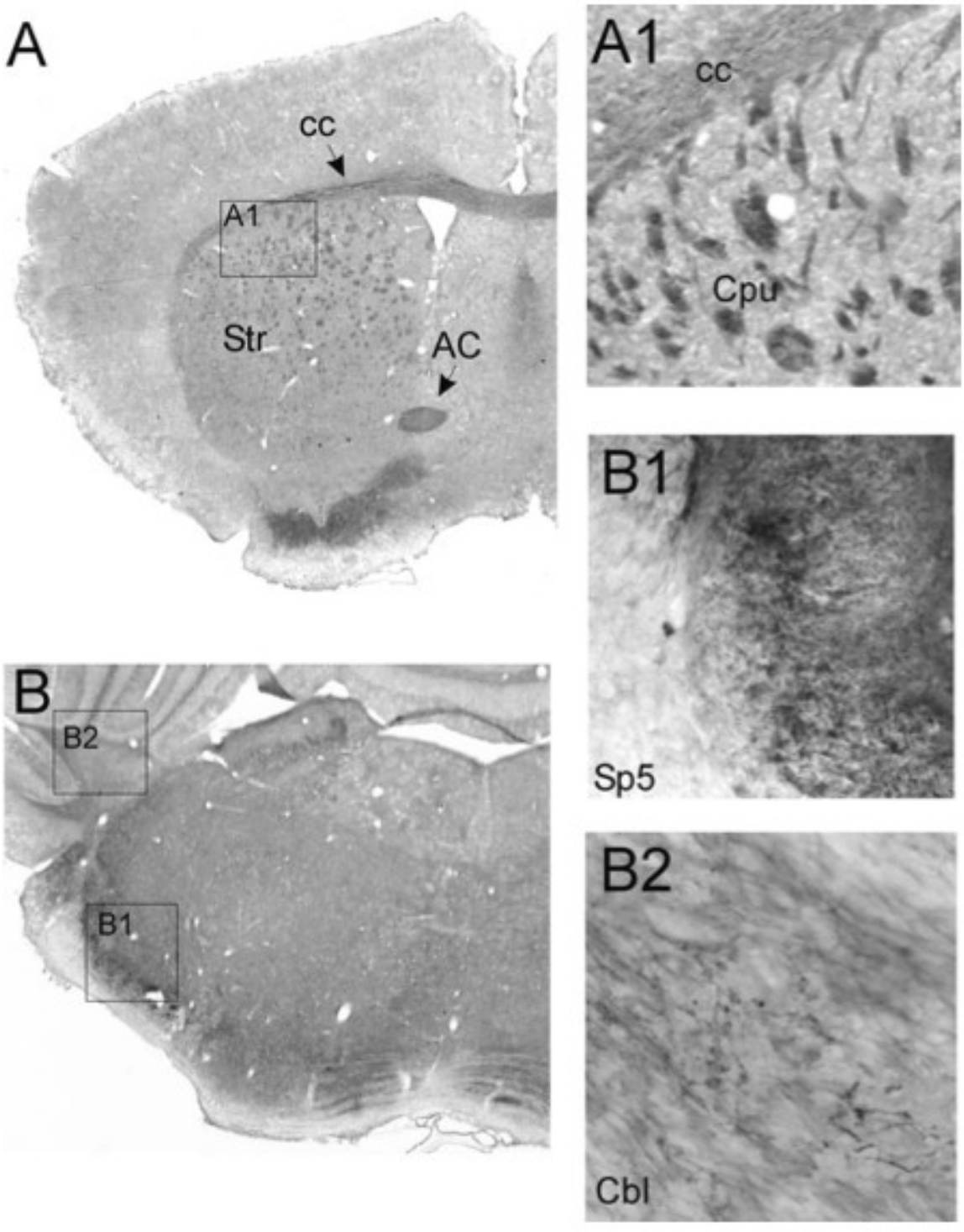

Fig. 4

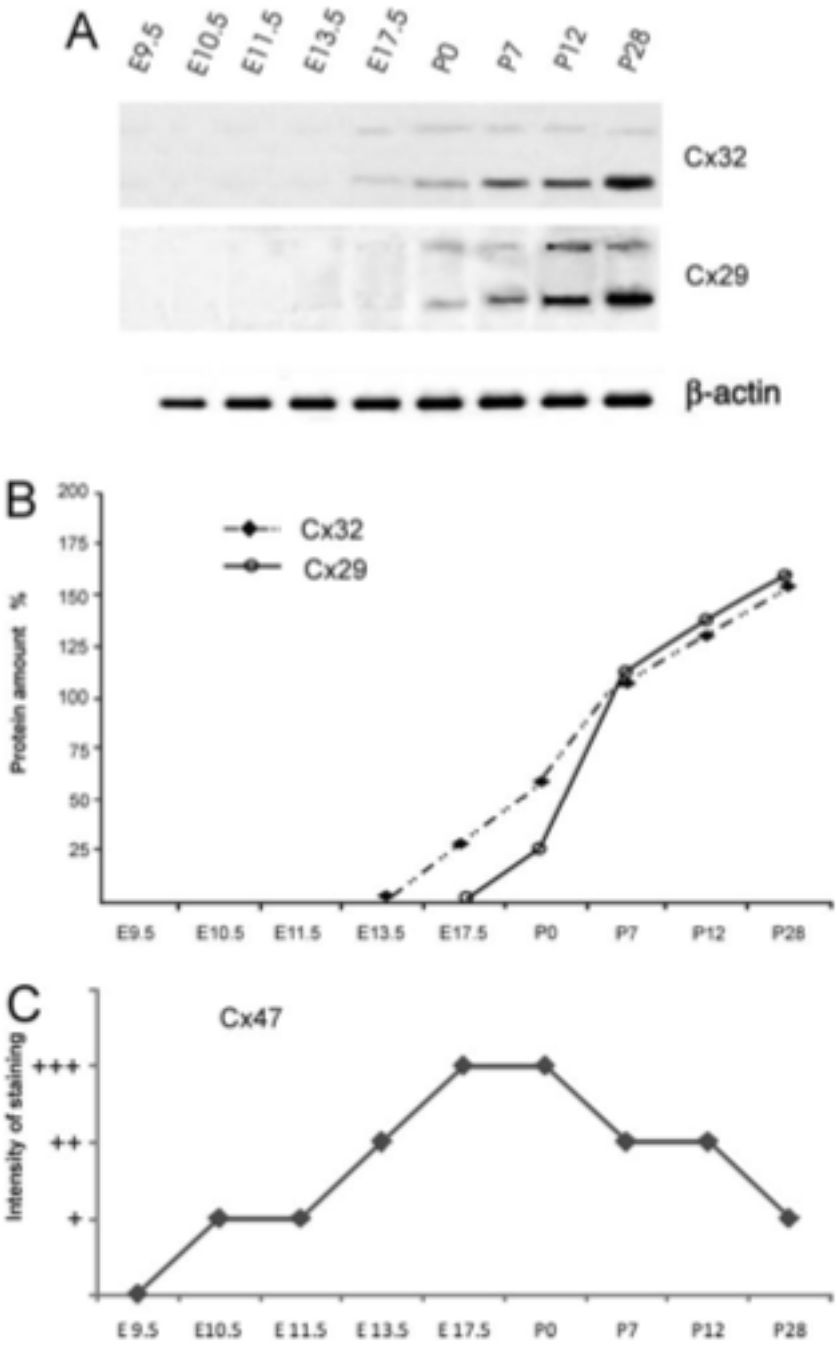
A
E9.5
E10.5
E11.5
E13.5
E17.5
P0
P7
P12
P28
Cx32
Cx29
β-actin
B
Cx32
Cx29
Protein amount %
200
175
150
125
100
75
50
25
E9.5
E10.5
E11.5
E13.5
E17.5
P0
P7
P12
P28
C
Cx47
Intensity of staining
+++
++
+
E 9.5
E10.5
E 11.5
E 13.5
E 17.5
P0
P7
P12
P28

Fig. 5

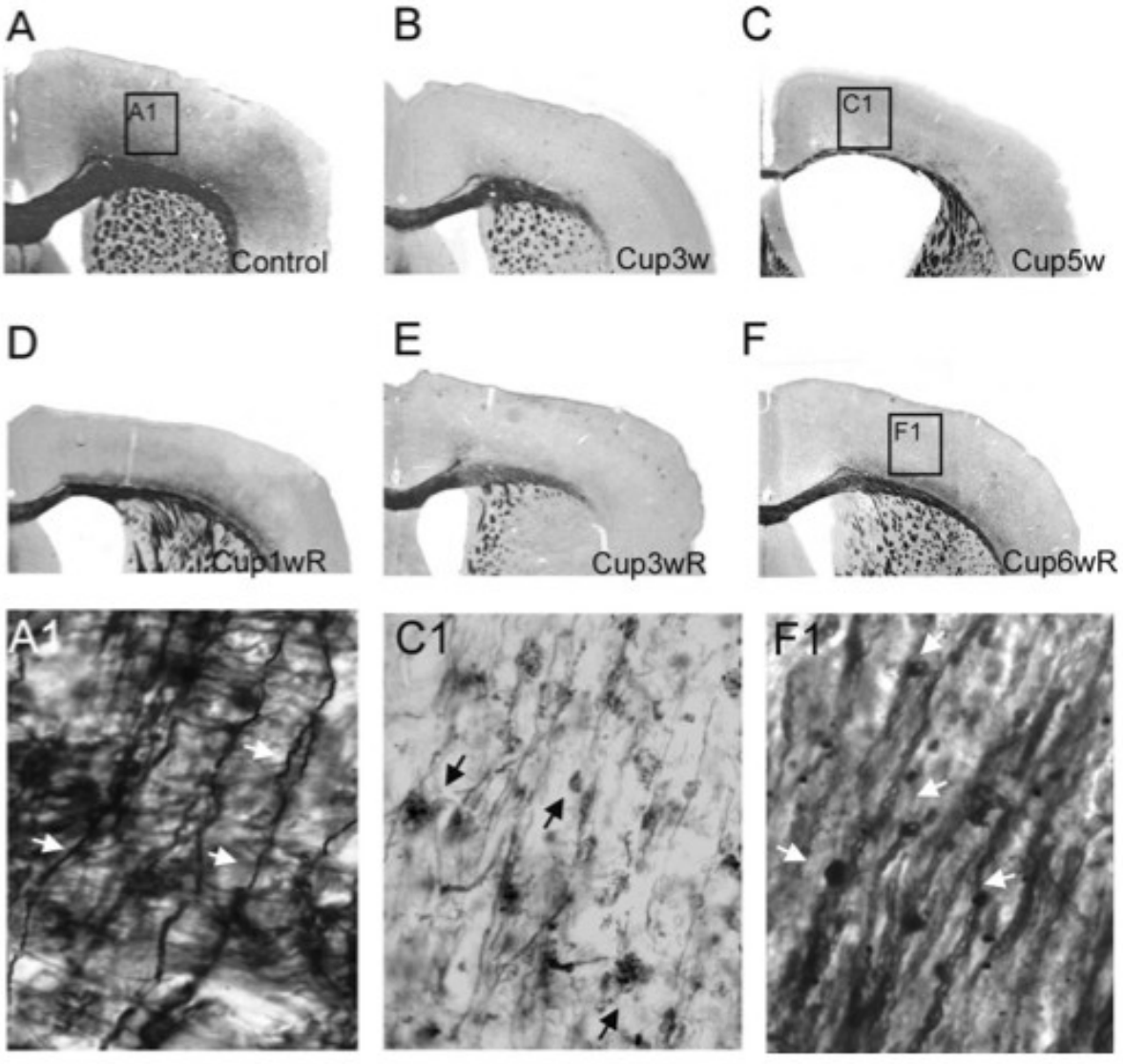
A
A1
Control
B
Cup3w
C
C1
Cup5w
D
Cup1wR
E
Cup3wR
F
F1
Cup6wR
A1
C1
F1

Fig. 6

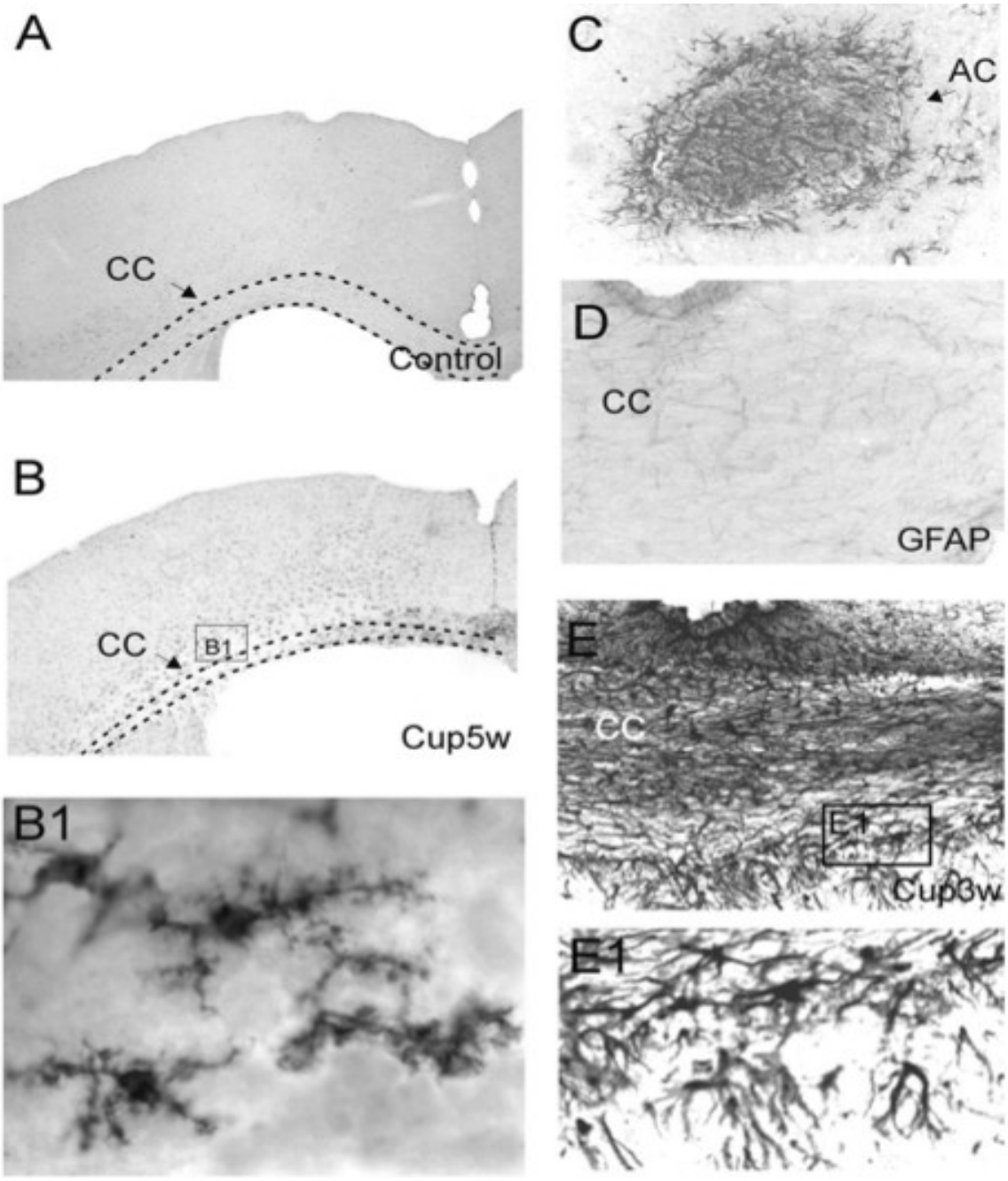

Fig. 7

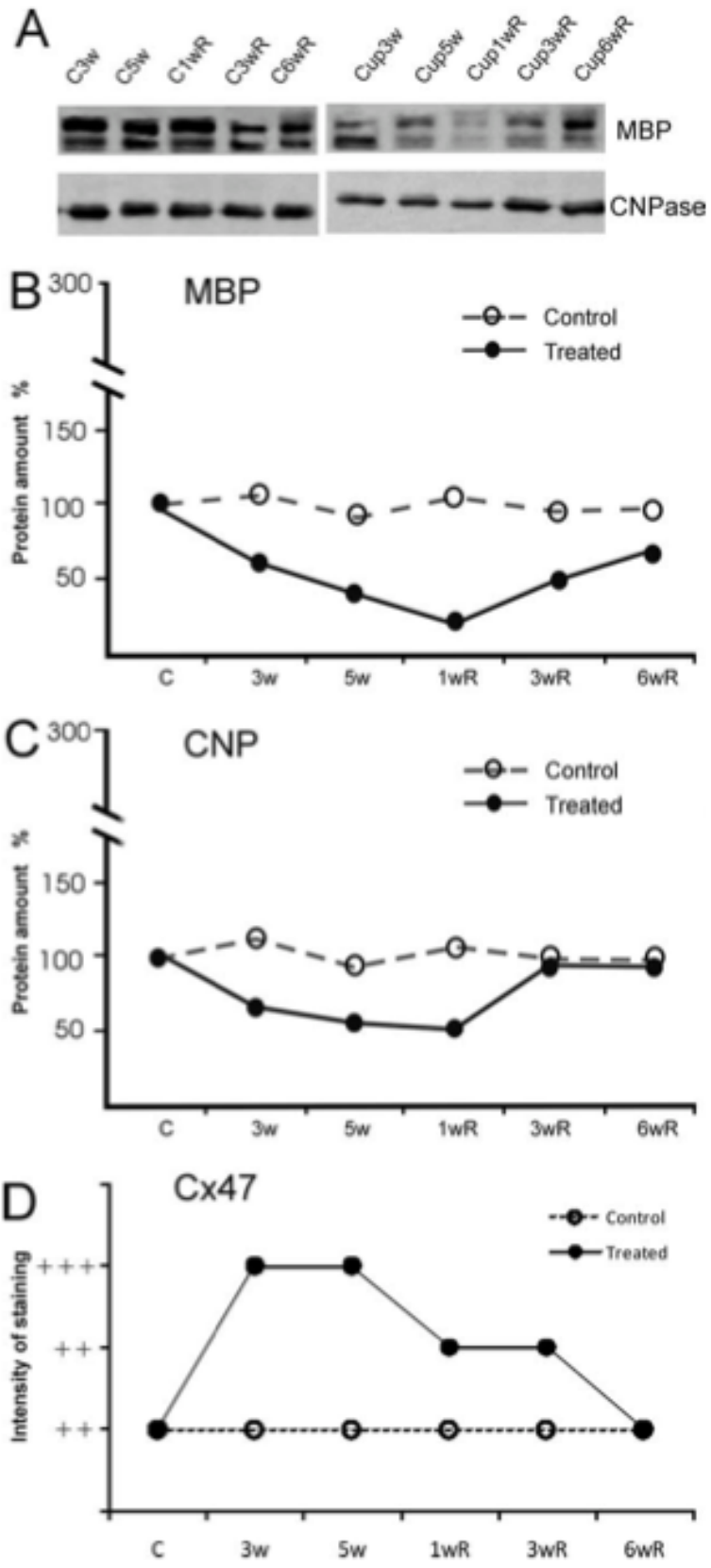
A
C3w
C5w
C1wR
C3wR
C6wR
Cup3w
Cup5w
Cup1wR
Cup3wR
Cup6wR
MBP
CNPase
B
MBP
Control
Treated
Protein amount %
300
150
100
50
C
3w
5w
1wR
3wR
6wR
C
CNP
Control
Treated
Protein amount %
300
150
100
50
C
3w
5w
1wR
3wR
6wR
D
Cx47
Control
Treated
Intensity of staining
+++
++
++
C
3w
5w
1wR
3wR
6wR

Fig. 8a

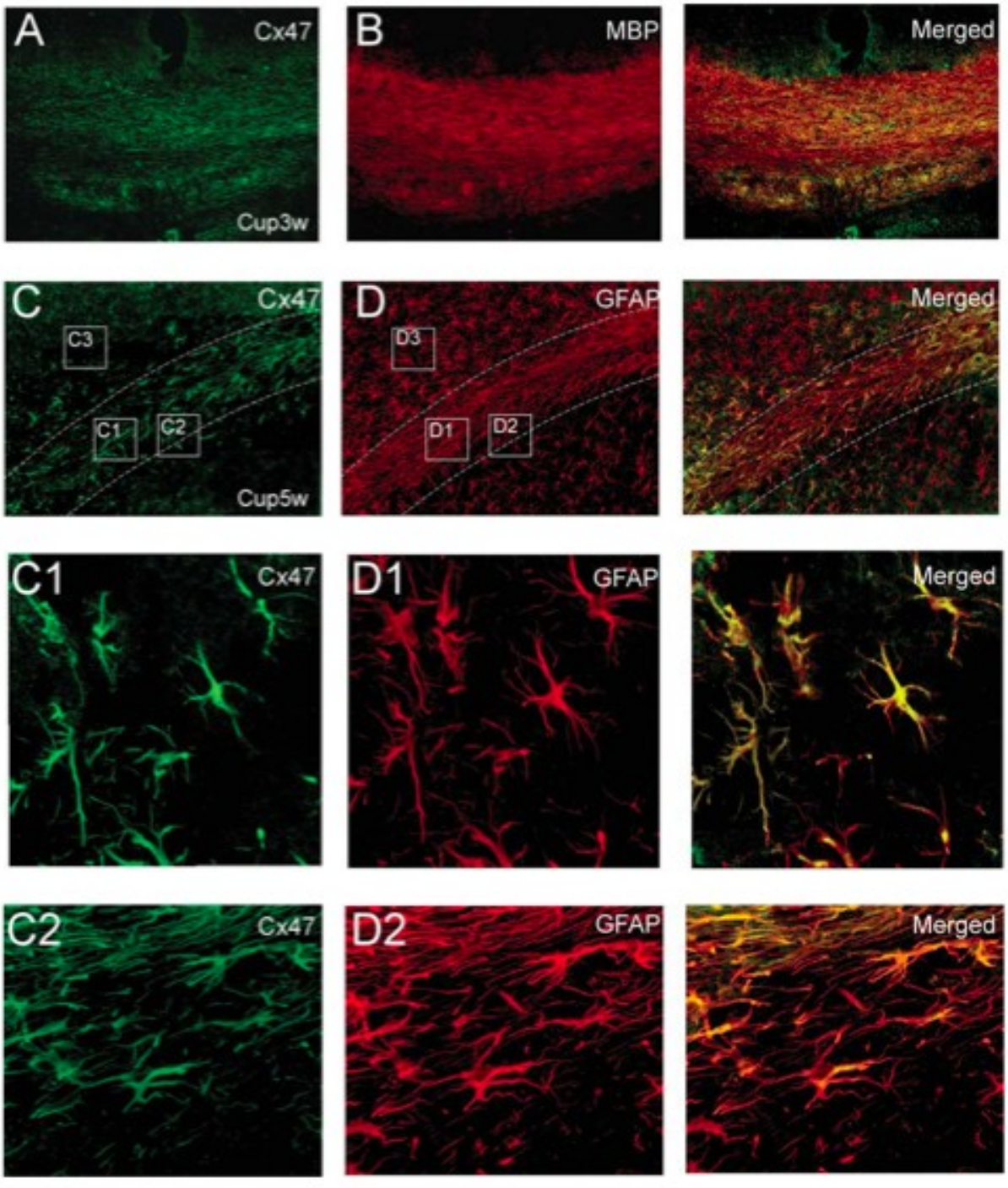
A
Cx47
Cup3w
B
MBP
Merged
C
Cx47
C3
C1
C2
Cup5w
D
GFAP
D3
D1
D2
Merged
C1
Cx47
D1
GFAP
Merged
C2
Cx47
D2
GFAP
Merged

Fig. 8b

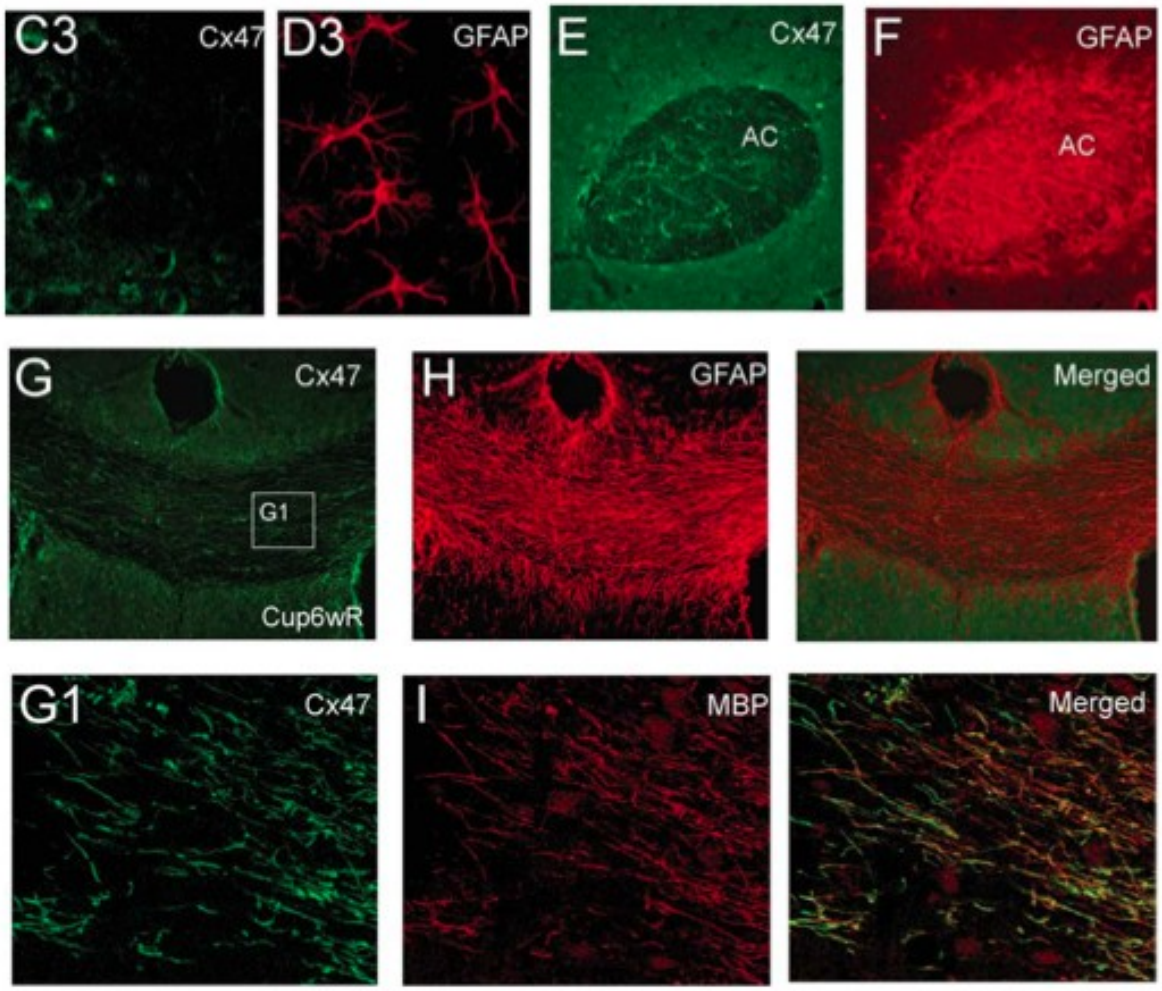
C3
Cx47
D3
GFAP
E
Cx47
AC
F
GFAP
AC
G
Cx47
G1
Cup6wR
H
GFAP
Merged
G1
Cx47
I
MBP
Merged

Chapter 2

Neuroscience 171 (2010) 1–11

Expression of connexin57 in mouse development and in harmaline-tremor model

Agata Zappalà, Rosalba Parenti, Francesco La Delia, Valentina Cicirata and Federico Cicirata*

Department of Physiological Science, University of Catania, Viale A. Doria 6, 95125 Catania, Italy

*Correspondence to: F. Cicirata,

Dipartimento di Scienze Fisiologiche,Viale A. Doria 6

95125 Catania, Italy

tel: (39) 095 7384036

fax: (39) 095 7384217

e-mail: cicirata @ unict.it

Section Editor:

Cellular: Dr. Costantino Sotelo, CNRS UMR 7102, Universite Pierre et Marie Curie, 6eme etage, Bat B, Case 12, 9 Quai St. Bernard, 75005 Paris, France.

ABBREVIATIONS

CNS: central nervous system

Cx: connexin

GJ: gap junction

GJIC: gap junctional intercellular communication

PBS: phosphate buffer saline

BSA: bovine serum albumin

FITC: fluorescein isothiocyanate

GFAP: glial fibrillary acidic protein

mRNA: messenger RNA

NeuN: neuronal nuclei

NGS: normal goat serum

RT-PCR: reverse transcriptase-polymerase chain reaction

SDS: sodium dodecyl

Abstract

Connexin57 (Cx57) was previously reported in retinal cells but not in brain nerve cells. This occurrence was tested in this study, by searching for the expression of Cx57 RNA and protein transcripts during the postnatal development of the mouse CNS. Both the Cx57 RNA (investigated by RT-PCR) and the protein (Western-Blot and immunohistochemistry using a polyclonal antibody generated in chicken) transcripts were firstly expressed in the late postnatal development (P12). The expression of Cx57 in adult life (studied at P28, by in situ hybridization and immunohistochemical analysis) concerned few regions of the brain stem (inferior olive, lateral reticular nucleus and motor trigeminal nucleus), the cerebellum (Purkinje cells and cerebellar nuclei) and the spinal cord (alpha-motoneurons). Double immunohistochemical studies using the Cx57 antibody and antibodies, which specifically labelled neuronal (NeuN) and astrocyte cells (GFAP), showed the expression of Cx57 segregated in neuronal cells. The study also confirmed the expression of Cx57 in the horizontal cells of the retinal outer plexiform layer, reported in previous investigations. Given the expression of Cx57 in the cerebellum and pre-cerebellar nuclei, such as olivary and lateral reticular nuclei, a possible role of Cx57 was hypothesized in the electrical coupling of the cerebellum. This hypothesis was tested by searching for the expression of the Cx57 transcripts in the mouse cerebellum of the harmaline-tremor model. The up-regulation of the Cx57 transcripts reported in this model suggested a possible involvement of Cx57 in the electrotonic coupling of the cerebellar system.

Key words: gap junction, rodent, brain, neurons.

Introduction

Gap junctional intercellular communication (GJIC) plays an important role in the neuronal networks, since it provides the morphological support for direct electrical and biochemical communication between adjacent cells (Evans et al., 2002). Gap junctions (GJ) consist of two hemichannels, termed connexons, and each connexon is built up of six protein subunits called connexins (Cx). A number of studies using electron microscopy, immunocytochemistry, electrophysiology, injection of intercellular tracers and molecular biology have reported the expression of Cxs in various regions of the CNS (Dermietzel et al., 1993; Li et al., 1997; Parenti et al., 2000; Teubner et al., 2000; Rash et al., 2001; Altevogt et al., 2002). GJIC occurs between neurons of brain regions in which temporally correlated activity is important for their function, such as the inferior olive (Llinas et al., 2002), abducens motor nucleus (Gogan et al., 1974), mesencephalic nucleus of the trigeminal nerve (Baker and Llinas, 1971) as well as hippocampal pyramidal neurons (MacVicar and Dudek, 1981) and inhibitory neurons of the cerebellum (Man-Metzer and Yarom, 1999). This study focused on the expression pattern of Cx57 (Manthey et al. 1999) in the development of the mouse brain, because previous studies reported the expression of Cx57 in pre-implantation mouse embryos (Houghton et al., 2002) but its expression during development was not investigated. The Northern blot did not show Cx57 mRNA in total brain extracts of adult mice (Hombach et al., 2004; Manthey et al., 1999), even though the low level of Cx57 mRNA in adult brain was not excluded for the limited detection sensitivity of this method (Hombach et al., 2004). A strong expression of Cx57 in the mouse retina neurons has been shown in adult life (Hombach et al., 2004). The hypothesis of the expression of Cx57 in the mouse brain is supported by the consideration that brain and retina neurons have common origins. To test this hypothesis we investigated the expression of both Cx57 mRNA (by RT-PCR and in situ hybridization) and protein (by Western blot and immunohistochemistry) at different time intervals of the post-natal development. For this purpose, an anti-Cx57 polyclonal antibody was generated in chicken. The Cx57 expression in the cerebellar system (including cerebellum and pre-cerebellar regions) shown in this study suggests a possible role of Cx57 in the cerebellar synchronization. Since over-synchronization of the cerebellum results in somatic tremor and gap-

junctions are involved in cellular network for synchrony (Martin and Handforth, 2006), the involvement of Cx57 was hypothesized in tremor induced by over-synchronization of the cerebellum, as occurred after administration of harmaline. The suppression of harmaline-induced tremors obtained in rodents by the administration of gap junction blockers strengthened this hypothesis (Sinton et al., 1989, Martin et al., 2005, Martin and Handforth, 2006). The possible involvement of Cx57 in the cerebellar synchronization was tested in the last part of this study by searching for the expression pattern of Cx57 in the cerebellum of adult mice treated with harmaline at tremor inducing effective doses.

Experimental procedures

Animals

Outbred CD-1 mice (Charles River, Milan, Italy) were used in this study. Postnatal (P1, P6, P12) and adult mice (P28) were deeply anaesthetized and decapitated. Brains were dissected and tissues were divided in two parts and stored at –80 °C, for RT-PCR and Western blot analyses, respectively.The animals used for immunohistochemical studies were anaesthetized by intraperitoneal injection of ketamine hydrochloride (0.4 ml/Kg, i.p.) and xylazine hydrochloride (1ml/Kg, i.p.) and fixed with paraformaldehyde (PFA) by perfusion through the heart. The brains were removed and post-fixed overnight in the same fixative at 4°C. The tissue was then transferred into a 20% sucrose solution in 0.1 M phosphate buffer saline (PBS), pH 7.4, for cryoprotection, at 4°C for 24-48 hours. Brains were rinsed in PBS, embedded in albumin-gelatin and rapidly frozen in isopentane cooled in liquid nitrogen and stored at –70°C. Brain coronal and sagittal sections were cut at 30 µm with a cryostat, collected in PBS and processed. The experimental plan was designed according to the guidelines of the Italian law for the care and use of experimental animals (DL 116/92) and approved by the Italian Ministry of Health.

Preparation of eyecups and retina

Mice were killed by cervical dislocation. Eyecups were prepared and fixed twice in 2% paraformaldheyde for 15 min at room temperature. After rinsing in PBS, pH 7.4, the eyecups were immersed in 30% sucrose in PBS overnight at 4°C and embedded in Tissue-Tec (Sakura, Zoeterwoude, Netherlands). Vertical cryosections (15 µm) of the eyecups were utilized for the immunolabeling with the Cx57 antibody (1:200), Cx57-immunoreactivity was determined using an anti-chicken-FITC secondary antibody (1:150, Promega, Madison, WI). The sections were then rinsed in PBS and mounted on slides and coverslipped using anti-fade reagent (Molecular Probes, Invitrogen, Milan, Italy). Retina dissection was performed as previously described (Ciolofan et al., 2007)

RT-PCR

RT-PCR was performed on extracts of spinal cord, brain stem, cerebellum, cerebral cortex and retina of adult mouse brain, P1-P28 total brain and HeLa cells. Total RNA was isolated using Trizol reagent according to the manufacturer (Gibco-BRL, Milan, Italy). Reverse transcription (RT) and amplification of cDNA by polymerase chain reaction (PCR) was based, with slight modifications, on the Access Rt-PCR system (Promega). In order to avoid genomic DNA contamination in total RNA preparations, they were treated with RQ-Dnase (Promega). Furthermore, each RNA preparation was tested for the presence of any contaminating genomic DNA by PCR using primers that flank an intron in the β-actin gene (Reaume et al, 1995). All constructs were verified by DNA sequencing. Aliquots of 2 μg of spinal cord, brain stem, cerebellum, cortex and retina total RNA of adult mice, total RNA of postnatal (P1, P6, P12) and HeLa cells were incubated with 2μl of AMV buffer (Promega), 1μl of 25 mM MgSO4, 1μl of RQ-Dnase (1 unit/μl, Promega), 1μl of rNasin (40 units//μl, Promega, Rnase inhibitor) and diethyl pyrocarbonate (DEPC) -treated H2O to a total volume of 10μl and incubated at 37°C for 30 min. Then, RQ-Dnase was inactivated at 75°C for 5 min. The RT reactions were performed with 10μl of DNA-free RNA solution by adding 3μl of AMV buffer, 2.5μl dNTP mix (10 mM each dATP, dCTP, dGTP, dTTP), 1μl of Rnasin, 3μl of AMV-reverse transcriptase ((10 unit/μl, Promega), 1μl of oligo(dT)18 primer (50 pmol), and 5.5 μl of DEPC- H2O for 90 min at 42°C. RT reaction mixtures were stored at –80°C. PCR reaction was performed with 5μl aliquots of the RT reaction mixtures, 4μl of AMV/Tfl buffer, 0.5μl of dNTP mix, 0.5μl of upstream Cx57 primer (50 pmol), 0.5μl of downstream Cx57 primer (50 pmol), 0.5μl of 25 mM MgSO4 , 0.5μl of Tfl polymerase (5 unit/μl, Promega), and DEPC-H2O. Amplification reactions were carried out for 35 cycles in a PTC-100 Thermal Cycler (60s at 94°C, 60s at 58°C, 120s at 72°C). PCR was conducted using the upstream primer 5' - CCCCAAGAATGCAATGTCTCAG - 3' and the downstream primer 5'-GCTGCTTTTACTTACCATCG -3' , leading to an amplicon of 378 bp (pos. 1077-1455, Hombach et al., 2004). The products were visualized on a 1.5% agarose gel stained with ethidium bromide and signals were quantified by densitometry using the

Gel-Pro analyzer 3.1 system (Media Cybernetics, Bethesda, USA). Cx57 expression was standardized to β-actin expression assessed from the same cDNA in separate PCR reactions and run in parallel on separate gels.

β-actin primers: upstream primer 5' – CGTGGGCCGCCCTAGGCAACC -3', downstream primer 5'- TTGGCCTTAGGGTTCAGGGGG -3'. All constructs were verified by DNA sequencing. The values reported in text and figures are the average of the three groups used in each experiment.

Production of affinity purified anti-CX57 polyclonal antibody

To obtain a large quantity of fusion protein for antibody production and biological assay, the cDNA encoding the cytoplasmatic loop of Cx57 (corresponding to amino acids 98-164) was inserted into a bacterial expression vector including a His tail (Qiagen S.p.A., Milano). The His-tagged fusion protein was purified by a Ni(2+)-charged affinity column. Repeated immunization of a chicken with the purified recombinant Cx57-IC protein allowed the production of a high-titer polyclonal antibody. Finally, the antibody was extracted from eggs (Tini, 2002) and purified by immunoaffinity using the purified antigen immobilized on CNBr-activated Sepharose 4B resin (Pharmacia, Milan, Italy).

HeLa cells transfection

Human cervix carcinoma HeLa cells (ATCC, LGC Standards, Milan, Italy) were cultured in Dulbecco's modified eagle medium supplemented with 10% fetal bovine serum, 2mM glutamine, 100U/ml penicillin, and 100µg/ml streptomycin at 37 °C in a humidified CO2-controlled incubator. The coding region of mouse Cx57 (corresponding to the Cx57 sequence described by Hombach et al., 2004) was amplified from cDNA of the mouse brain by PCR and subcloned into the expression vector pCDNA3.1-TOPO (Invitrogen, Milan, Italy). HeLa cells were transiently transfected with plasmid using the Lipofectamine reagent (Invitrogen), according to the manufacturer's instructions and taken for analysis 48h post-transfection. Mock transfected HeLa cells were generated with the empty vector and used as a control.

Western blot

HeLa cells, dissected brains from postnatal and adult mice and retina were homogenized in ice-cold 40 mM Tris-HCl buffer, ph 7.4, containing 1% NP-40 detergent, 1 mM PMSF and aprotinin, leupeptin and pepstatin A each at 5 μg/ml. After homogenization, samples were sonicated for 20 sec. protein concentration were determined after using the protein determination kit with bichinchoninic acid (BCA, Sigma), according to the instructions provided. Aliquots of 30μg per lane were separated by sodium dodecyl sulfate-polyacrylamide gel electrophoresis and transferred to 0.25 μm polyvinilylidene difluoride membrane (Bio-Rad) in transfer buffer (25 mM Tris, 192 mM glycine and 20% v/v methanol) containing 0.05% SDS. The membrane was blocked for 2h in 20 mM Tris, ph 7.4, 150 mM NaCl and 0.2% Tween 20 (TBS-T) containing 5% skim milk powder and incubated with anti Cx57-antibody (at a concentration of 1μg/ml) for 16h at 4°C in TBS-T containing 1% skim milk powder. Blots were washed for 40 min in TBS-T and then incubated for 1h at room temperature in TBS-T containing 1% skim milk powder and anti-chicken horseradish peroxidase-conjugated secondary antibody (1:10000, Chemicon, Temecula, CA, USA), washed and bands revealed by chemiluminescence (GE Healthcare) according to the manufacturer's instructions. As a control for protein loading, the same membrane was then incubated with specific anti-actin antibody (1:10.000, Oncogene Research Products, Boston, USA) followed by appropriate peroxidase-conjugated secondary antibody. The specificity of Cx57 antibody was tested by peptide preadsorption: 1μg of anti-Cx57 was preincubated for 1h at room temperature with or without 100 μg of immunizing peptide and then incubated with blots or tissues. Furthermore, retina was incubated with pre-immune serum as negative control. Ponceau red stained blot was performed for control of equal amounts of protein per sample loaded onto the gel.

***In situ* procedure**

mRNA probe synthesis - The probe was prepared from a 162bp fragment, encoding the cytoplasmatic loop of Cx57 sequence (corresponding to amino acids 98-151) and subcloned in pBluescript KS+ vector (Stratagene, San Diego, CA). The plasmid was linearized with EcoRI or KpnI and transcribed with T7 RNA or T3 RNA polymerase to generate antisense and sense probes, respectively. All constructs were verified by DNA sequencing. In vitro transcription - Riboprobe was transcribed from 1 µg of linearized DNA in a mixture of 10 mM ATP, CTP, GTP, 2 mM UTP, 8 mM digoxigenin (DIG)-11-UTP in 1X transcription buffer (Boehringer-Mannheim) for 2h at 37°C. The labeled RNA was dissolved in 100 µl of 0.01 M Tris, pH 7.5, 0.001 M EDTA, pH 8, 100 µg/ml yeast tRNA, 50 U/ml RNAguard (Pharmacia). To test transcription efficiency, the riboprobe was separated on a denaturing agarose gel, blotted on nitrocellulose and detected with a nucleic acid detection kit (Boehringer-Mannheim). In situ hybridization – Tissue pretreatments consisted of deproteination with 0.2M HCl for 10 min, proteinase K digestion (10µg/ml in 50 mM Tris-HCl/5mMEDTA, pH 8.0) at 37°C for 15 min followed by fixation in 4% phosphate buffered paraformaldehyde for 20 min, acetylation with acetic anhydride 0.25% in 1.5% triethanolamine/0.3 M NaCL, pH 8.0, for 10 min and permeabilization with 0.1% Triton X-100 in PBS for 10 min. Each pretreatment was preceded by brief washes in PBS. Tissue sections were transferred into prehybridisation solution: 50% formamide, 250µ/ml denaturated salmon sperm DNA, 100µg/ml yeast tRNA, 0.05M sodium phosphate, pH 6.5, 4X SSC, 5% dextran sulfate, 0.02% polyvinylpyrrolidone, 0.02% bovine serum albumin, 0.02% Ficoll 400 (1X Denhart solution) for 1-2h at 55°C. Sections were then incubated for 16 h at 55°C with the same solution containing the sense or antisense riboprobe at a final concentration of 1 ng/µl. After hybridization, sections were rinsed twice in 4X SSC at room temperature and treated with ribonuclease a (50µg/ml in 0.5M NaCl, 1mM EDTA, 10mM Tris-HCl buffer, pH 8.0) at 37°C for 20 min. Then sections were rinsed as follows: 2h in 2X SSC at room temperature, 30 min in 0.1X SSC at 55°C, twice for 10 min in 100mM Tris-HCl, 150mM NaCl pH 7.5 (TBS) at room temperature. A pre-incubation in 4% BSA, 0.25% DMSO, 1% Triton X-100 in TBS for 1-2h was followed by the incubation in the alkaline phosphatase-conjugated anti-DIG antibody (Boehringer) diluited 1:1000 in 2% BSA, 0.3% Triton X100 in TBS at 4°C overnight. Sections were then rinsed as follows: four times for 15 min in TBS; twice for 5 min in 100mM Tris-HCl, 100mM NaCl, pH 7.5; twice for 10 min in 100mM Tris-HCl, 100mMNaCl, 50mMMgCl2, pH 9.5. finally, sections were incubated in the last buffer

containing as enzyme substrate nitroblue tetrazolium, NBT and 5-bromo-4-chloro-3-indolyl-phosphate, BCIP (8µl/1.5ml of NBT/BCIP stock solution, Boehringer) with 0.24mg/ml of levamisole (Sigma). Color development proceeded for up to 24-48 h at room temperature initially (2-4 h) and then at 4°C. the accumulation of reaction product was monitored under light microscope. When the staining intensity was reached the reaction was stopped in 10mM Tris-HCl, 1mM EDTA, pH 8.0, rinsed in 10mM Tris-HCl and the sections were mounted on gelatin-coated slides, air-dried and coverslipped in Entellan. Controls including hybridization with sense digoxigenin and Rnase A digestion before hybridization to prevent alkaline phosphatase staining were performed in parallel.

Immunohistochemistry

Immunohistochemical studies were performed on cryostat sections as previously described (Panto, 2004) using anti-Cx57 (1:200) alone or combined with the following primary antibodies: monoclonal mouse anti-GFAP (1:500, Chemicon, Temecula, CA, USA), monoclonal mouse anti-NeuN (1:200, Chemicon, Temecula, CA, USA) in the blocking solution, overnight at 4 °C. Following incubation in primary antibodies, sections were incubated with the anti-chicken peroxidase conjugated secondary antibody (1:1000, Chemicon, Temecula, CA, USA); while anti-chicken-TRITC (1:200, Chemicon, Temecula, CA, USA) or anti-chicken-FITC (1:200, Chemicon, Temecula, CA, USA) together with anti-mouse-Cy3 (1:200, Chemicon, Temecula, CA, USA) were used for immunofluorescence experiments. Immunofluorescence analysis on HeLa cells was performed as previously described (Parenti et al., 2002). Nuclei of HeLa cells were stained with Sytox (Molecular Probes, Eugene, OR). Fluorescence was examined under a Leica fluorescence microscope equipped with filters for visualization of FITC (excitation, 450-490 nm; emission 515-550 nm) and Cy3 (excitation 541-551 nm; emission, 565-595 nm) and under a LSM 510 Zeiss confocal microscope. Images were captured using a digital camera (Spot, Diagnostic Instruments, Sterling Heights, USA) and adjusted for contrast in Corel Draw 9. For each experiment, adjacent cryosections were stained with cresyl violet for morphological reference when viewed under the microscope.Incubation with pre-immune serum and secondary antibody was performed as negative controls.

Drug administration

Administration of harmaline HCL (Sigma-Aldrich, USA) was performed as previously described (Miwa et al., 2006). Briefly, harmaline was dissolved in physiological saline immediately before use and administered intraperitoneally. Two doses (10 and 100 mg/kg) were used. Animals were sacrificed seven days after injection of harmaline. Densitometric analysis was performed after normalization with actin by using an Image Analyzer Software (Kodak, Amsterdam, Netherlands) to quantify the amount of Cx57 mRNA and protein visualized by RT-PCR and immunoblotting respectively.

Statistical analysis

One-way analysis of variance (ANOVA) followed by Bonferroni's t test was performed in order to estimate significant differences among groups. Data were reported as mean values ± SD. Data for each experiment were analyzed using the one-way ANOVA followed by the Tukey's post hoc procedure for multiple comparisons. Differences between groups were considered to be significant at $p<0.05$.

RESULTS

MouseCx57 mRNA expression

Cx57 mRNA was examined by the RT-PCR method using primers localized on Cx57 exon 2. The primers used in the study were drawn over the exon 2 of the Cx57 sequence reported by Hombach, in agreement with Houghton (2002), Shelley (2006), Ciolofan (2007), Dedek (2008), Palacios-Prado (2009), Janssen-Bienhold (2009).

Total RNA was extracted from total brain at P1, P6, P12 and P28 (Fig.1A). RT-PCR analysis was also performed on dissected P28 brain regions: retina, cerebral cortex, cerebellum, brain stem and spinal cord (Fig.1B). The procedure showed positive signals in the retina, spinal cord, brain stem and cerebellum. No signal was detected in the cerebral cortex (Fig.1B). The expression pattern of Cx57 mRNA was also examined by in situ hybridization on coronal sections of adult mice brain. The gene was expressed by the Purkinje cell layer (Fig.1C, C1) and nuclei of the cerebellum (Fig.1D); the inferior olivary complex (Fig.1E), the lateral reticular nucleus (Fig.1F), motor trigeminal nuclei and alpha motoneurons of the spinal cord (Fig.1G, G1). The sense probe for Cx57, used as control, did not show any signal (Fig.1H, I, L, M, N, O).

Cx57 antibody characterization

A high-titer polyclonal antibody was obtained by immunization of a chicken with the purified recombinant Cx57 protein corresponding to the cytoplasmatic loop of the Cx57 sequence. The antibody was purified by immunoaffinity using the immunizing antigen and it was characterized by ELISA test, western blot and immunofluorescence analysis. The ELISA test was performed using the immunizing antigen that showed a titer of 1:15000, while no signal was obtained using different antigens as controls. To test the specificity of the antibody, we transfected HeLa cells with cDNA encoding the Cx57 gene (corresponding to the Hombach's sequence). The transfection was checked by searching for the Cx57 mRNA and protein in cell extracts. They were both absent in non transfected HeLa cells and in mock HeLa cells (Fig.1A, Fig.2A) generated with the empty vector and used as control. Transfected cells showed the expression of Cx57 mRNA through a positive RT-PCR signal (Fig.1A) and the expression of the Cx57

protein through the Western blot (Fig.2A). Western blot analysis performed using spinal cord, brain stem, cerebellar and retina extracts showed a single band migrating at ~57 kDa, while no signal was detected using cortex extract and cerebellar extract treated with the anti-Cx57 pre-incubated with the immunizing antigen (Fig.2A). The Cx57 immunoreactivity pattern was absent in a retina membrane sample incubated with the pre-immune serum (Fig.2B). Immunofluorescence analysis on HeLa cells transiently transfected with Cx57 cDNA showed a bright fluorescent signal (Fig.2C) while no signal was detected in mock HeLa cells (Fig.2D). Finally, histological sections of adult brain were processed with anti-Cx57 or with protein extracts from eggs taken from a hen before immunization with the antigen. Cellular staining was observed with the Cx57 antibody, while no staining was present in brain sections processed with proteins of non-immunized eggs. No signal was detected if the primary antibody was omitted (data not shown).

Cell types stained by Cx57 antibody

The cell type of the Cx57-stained cells was searched using double immunostaining performed on coronal sections of the adult brain, using our antibody to visualize the Cx57 positive cells and the NeuN antibody, which stains neuronal cells, or the GFAP antibody, which stains astrocyte cells. Cx57-positive cells were always co-stained by the NeuN antibody (Fig.2E) but never by the GFAP one (data not showed). These findings shown the neuronal nature of the cells Cx57-positive.

Expression of the Cx57 protein in the development of mouse brain

Proteins extracted from total brains were sampled using Western blot analysis. The expression at the cellular level was investigated through immunohistochemistry on coronal sections at P1, P6, P12 and on both sagittal and coronal sections at P28. Immunoreactive cells were identified according to their position and morphology using adjacent sections stained with cresyl violet to identify the anatomical location of stained cells. At P1 and P6, no positive signals were detected in both Western blot (Fig.3A) and immunohistochemistry (Fig.3B, C, C1, C2), in agreement with the lack of positive signal detected by RT-PCR analysis. At P12 a positive expression was detected by both

Western blot (Fig.3A) and immunohistochemistry (Fig.3D) in agreement with the positive signal detected by RT-PCR analysis. Cellular labeling was visualized in a few brain areas: the Purkinje layer of the cerebellum (Fig.3D1), the lateral reticular nucleus and the inferior olivary complex (Fig.3D2, D2a, D2b). At P28 the expression of the Cx57 protein concerned: the nuclei of the cerebellum (Fig.4A1), the Purkinje cells of the cerebellum (Fig.4A2), the lateral reticular nucleus (Fig.4A3), the inferior olivary complex (Fig.4A4), the motor trigeminal nucleus (Fig. 4A5) and the alpha-motoneurons of the spinal cord (Fig.4A6). Immunohistochemistry performed on horizontal sections of the retina stained the horizontal cells in the outer plexiform layer (Fig.4B, B1). The Cx57 immunoreactivity pattern was absent in retina and brain sections incubated with the pre-immune serum and the secondary antibody (Fig.4B2, C, D, E).

All these findings showed the late expression of Cx57 in the development phase and the segregated topographic expression in CNS of adult mice, which principally concerned cerebellum and precerebellar nuclei, such as the lateral reticular nucleus and the inferior olivary complex.

Expression pattern of Cx57 in the harmaline-tremor mouse model

Systemic administration of harmaline showed generalized tremors in mice in few minutes. Administration of large doses of harmaline (100mg/kg) induced generalized and large amplitude tremors continuously occuring in the head and neck of the animals, while lower doses of harmaline (10 mg/kg) showed slight tremors, in agreement with previously reported behavioural observations in rodents (O'Hearn et al., 1993; Beitz et al., 2004; Miwa et al., 2000, 2006). In the present study we searched for the expression pattern of both Cx57 mRNA and protein in cerebellar extracts of animals treated with harmaline at doses of 10 or 100 mg/Kg and the results were compared in percentage to the corresponding values reported in control animals, which had been given a value of 100. Densitometric analysis was performed after normalization with actin by using an Image Analyzer Software. The expression pattern of mRNA was studied by RT-PCR. As shown in Fig. 5A, A1, the expression of Cx57 mRNA after administration of 10 mg/Kg of harmaline (106% ± 3,26) was weakly increased with respect to control animals but the statistical analysis was not significant ($p>0.05$, $n=5$). Conversely, the administration of 100 mg/Kg of harmaline significantly ($p<0.01$, $n=5$) increased the expression of Cx57 mRNA (115,3% ± 2,05) with respect to control animals (Fig. 5A, A1). The expression pattern of the Cx57 protein was tested by Western blot. Animals

treated with harmaline at a dose of 10 mg/Kg showed an increment of the Cx57expression (118 % ± 3,74; Fig. 5B, B1) with respect to control animals but the statistical analysis was not significant ($p>0.05$, n=5). Mice treated with harmaline at a dose of 100 mg/Kg showed an increased level of the Cx57 protein (143% ± 3,26; Fig. 5B, B1), with respect to control animals, and the statistical analysis was significant ($p<0.01$, n=5). All these findings showed that the expression of both Cx57 mRNA and protein is progressively up regulated by increasing the doses of harmaline administration.

DISCUSSION

The new findings of this study mainly concerned: the expression pattern of the Cx57 during development, the segregated expression in neuronal cells, the topographic expression in discrete regions of adult brain and the involvement in harmaline-induced cerebellar over-synchronization. The study investigated the Cx57 expression from birth to adult life. RT-PCR showed that the Cx57 mRNA is first expressed at a late development stage (P12; Fig.1A). Immunohistochemical studies showed the Cx57 protein in Purkinje cells of the cerebellum and in the pre-cerebellar nuclei: inferior olivary nucleus and lateral reticular nucleus. From this age to adult life the expression expanded to few other regions, principally located in the hindbrain. Houghton (2002) had previously reported the expression of Cx57 in very early embryogenesis, corresponding to the preimplantation rodent embryos. So, both findings showed that Cx57 is expressed at both early and late stages of the development. The Cx57 was exclusively expressed by neuronal cells. In fact, both in situ and immunohistochemistry studies have always shown the expression of Cx57 in neuronal cells but never in the glial ones. So, Cx57 can be included in the short list of Cxs principally, if not exclusively, expressed in neuronal cells. This group also includes Cx26, which is principally expressed in the pre-Botzinger complex of the brain stem; Cx36, which is principally expressed in the inferior olive complex, but also in the spinal cord, in several brainstem nuclei, in the cerebellum, in the cerebral cortex, the hippocampus, the reticular thalamic nuclei and the olfactory bulb (Teubner et al., 2000; Solomon et al., 2003); Cx37 and Cx40, which are expressed in the alpha-motoneurons (Chang et al., 2000); Cx45, in the cerebral cortex, the hippocampal and thalamic neurons (Maxeiner et al., 2003) as well as the alpha-motoneurons (Chang et al., 2000). This study showed for

the first time the expression of Cx57 in neurons of the brain, but it is not the first study showing expression of the Cx57 in neurons, since it was reported in retinal neurons by previous studies (Hombach et al., 2004; Ciolofan et al, 2007; Jassen-Bienhold et al., 2009). Immunoistochemical analysis with fluorescent microscope was used in the study, while no confocal or electron microscopic studies were performed. Our procedure showed relatively high-density expression of Cx57 at citosolic level, but we cannot exclude a more discrete expression on the membrane of terminal processes, because the limit of our methodological procedure, as reported in the retina. In fact, we showed the Cx57 in the cell bodies of neurons of horizontal cells, in agreement to Hombach (2004), Ciolofan (2007) and Jassen-Bienhold (2009), but not on their dendrites and axon terminal processes inside the outer plexiform layer reported in previous studies with the use of different methodological procedures (Ciolofan et al., 2007; Jassen-Bienhold et al., (2009). The expression of the Cx57 in the citosol of the cellular bodies rises the question on the possible involvement of the Cx57 cellular functions independent by formation of gap junction channels. This hypothesis is supported by many studies performed on other connexins, principally the Cx43, which reported their involvement in different cellular functions such as mitochondria activity (Miro-Casas et al., 2009; Boegler et al., 2009), interactions with other membrane channels and trasporters (Chanson et al., 2007), control of cell growth and motility (Cina et al., 2009; Crespin et al., 2010). Obviously, other investigations must be planned to test the specific functional roles played by the Cx57. The effective expression pattern of the Cx57 protein in discrete hindbrain regions showed by immunohistochemical in adult life was strengthened by the topographic coincidence with the in situ hybridization labeling (compare Fig. 1 with Fig. 4).Since the expression of Cx57 concerned brain regions that usually expressed also the Cx36, a comparison for the topographic expression of these Cxs during development can be made. So, while Cx36 was firstly expressed in the forebrain and after in the hindbrain (Gulisano et al., 2000), Cx57 firstly appeared in cerebellar system regions and thereafter the expression expanded only to a few other nuclei of the hindbrain. In the development phase, differences also occurred in the time of expression: the expression of Cx36 occurred early in embryogenesis (E9,5) while the expression of Cx57 occurred in the late stage of the development (P12). The immunohistochemical study of the retina was positive for the horizontal cells of the distal margin of the retina inner layer (Fig.4B1), in agreement with the Hombach's LacZ analysis of Cx-57 deficient mice (Hombach et al., 2004). The expression of Cx57 in the cerebellum and in the pre-cerebellar (inferior olive and lateral reticular) nuclei suggested a possible involvement in the electrical coupling of cerebellar neurons. The

electrical synchronization of the olivocerebellar system plays a key role in the physiological motor program, but also in the pathophysiological mechanism of both the essential tremor in humans (Deuschl et al., 2000; Louis et al., 2002; Pinto et al., 2003) and the experimental model of harmaline-induced tremor (Bernard et al., 1984; Miwa et al., 2000). The rodent model of harmaline-induced tremor has been used as an animal model of essential tremor, one of the most representative disorder in humans (Deuschl et al., 2000; Elble, 1988; Martin et al., 2005; Wilms et al., 1999). The hypothesis of an involvement of Cx57 in the harmaline-tremor model was shown in the present study by a direct relationship between doses of harmaline administered, levels of somatic tremor and levels of expression of the Cx57 transcripts in the cerebellum. More in general, these findings demonstrate that Cx57 could play a role in the electrical coupling of the cerebellar system. In this function a pivotal role is played by the Cx36, that is principally expressed in the olivary nucleus. The olivary projections mainly result in electrical synchronization of the cerebellar cortex (Llinas et al., 1974; Llinas et al., 1981; Marshall et al., 2007), that plays a key role in the cerebellar physiology (Llinas et al., 1981). Deletion of the Cx36 gene impaired electrical coupling in the inferior olive without any obvious deficit in movement, possibly due to still unknown processes of compensation (Placantonakis et al., 2004). The expression of Cx57 in both cerebellum and precerebellar nuclei suggests a possible role of Cx57 in such compensatory processes, but this hypothesis deserves to be tested in specifically devoted investigations. The expression pattern of Cx57 in the central nervous system showed in this study is innovative. In fact, both Manthey (Manthey et al., 1999) and Hombach (Hombach et al., 2004) did not report on it. The apparent contradiction of their results with findings of this study, can be explained as follows. Both Manthey (Manthey et al., 1999) and Hombach (Hombach et al., 2004) searched for the Cx57 expression by Northern blot hybridization on extract of total brain. In agreement with Hombach, we hypothesized that the absence of an mRNA signal in this tissue after Northern blot hybridization was probably due to the low level of Cx57 mRNA and the limited detection sensitivity of the method (Hombach et al., 2004). Hombach (Hombach et al., 2004) generated Cx57-deficient mice by replacing the Cx57 coding region with a lacZ reporter gene expressed under control of the endogenous Cx57 promoter. Since they did not find expression of the lacZ gene in adult brain, he assumed the absence of the Cx57 expression in such tissue. Since Hombach did not report any data on the brain sections investigated and our study showed the expression in discrete brain regions, it is not possible to exclude that these regions were not exhaustively investigated. Moreover, since lacZ is a reporter gene and Cx57 is an endogenous one, it is possible that the two

genes were under different transcriptional and post-transcriptional controls and thus, that the expressions pattern of lacZ did not correspond to the expression of the Cx57 gene (Cui, et al., 1994; Couffinhal, et al., 1997; Kimura et al., 2000).

REFERENCES

Altevogt BR, Kleopa KA, Postma FR, Scherer SS, Paul DL. (2002) Connexin29 is uniquely distributed within myelinating glial cells of the central and peripheral nervous system. J. Neurosci., 22, 6458-6470.

Baker R, Llinas R (1971) Electrotonic coupling between neurones in the rat mesencephalic nucleus. J Physiol., 212 (1), 45-63.

Beitz AJ, Saxon D. (2004) Harmaline-induced climbing fiber activation causes amino acid and peptide release in the rodent cerebellar cortex and a unique temporal pattern of Fos expression in the olivo-cerebellar pathway. J Neurocytol. Jan;33(1):49-74.

Bernard JF, Buisseret-Delmas C, Laplante S. (1984) Inferior olivary neurons: 3-acetylpyridine effects on glucose consumption, axonal transport, electrical activity and harmaline-induced tremor. Brain Res. Nov 26;322(2):382-7.

Boengler K, Stahlhofen S, van de Sand A, Gres P, Ruiz-Meana M, Garcia-Dorado

D, Heusch G, Schulz R. (2009) Presence of connexin 43 in subsarcolemmal, but not ininterfibrillar cardiomyocyte mitochondria. Basic Res Cardiol. Mar;104(2):141-7.

Chang Q, Balice-Gordon RJ. (2000a) Gap junctional communication among developing and injured motor neurons. Brain Res Brain Res Rev., 32 (1), 242-9.

Chang Q, Pereda, A, Pinter MJ, Balice-Gordon RJ. (2000b) Nerve injury induces gap junctional coupling among axotomized adult motor neurons. J Neurosci, 20 (2), 674-684.

Chanson M, Kotsias BA, Peracchia C, O'Grady SM. (2007) Interactions of connexins with other membrane channels and transporters. Prog Biophys Mol Biol.

May-Jun; 94(1-2):233-44. Review.

Cina C, Maass K, Theis M, Willecke K, Bechberger JF, Naus CC. (2009) Involvement of the cytoplasmic C-terminal domain of connexin43 in neuronal migration. J Neurosci. Feb 18;29(7):2009-21.

Ciolofan C, Lynn BD, Wellershaus K, Willecke K, Nagy J.I. (2007) Spatial relationships of connexin36, connexin57 and zonula occludens-1 in the

outer plexiform layer of mouse retina. Neuroscience. Aug 24;148(2):473-88.

Couffinhal T, Kearney M, Sullivan A, Silver M, Tsurumi Y, Isner JM. (1997) Histochemical staining following LacZ gene transfer underestimates transfection

efficiency. Hum Gene Ther. May 20;8(8):929-34.

Crespin S, Bechberger J, Mesnil M, Naus CC, Sin WC. (2010) The carboxy-terminal tail of connexin43 gap junction protein is sufficient to mediate cytoskeleton changes in human glioma cells. J Cell Biochem. Jun 1;110(3):589-97.

Cui C, Wani MA, Wight D, Kopchick J, Stambrook PJ. (1994) Reporter genes in transgenic mice. Transgenic Res. May;3(3):182-94.

Dedek K, Pandarinath C, Alam NM, Wellershaus K, Schubert T, Willecke K, Prusky GT, Weiler R, Nirenberg S. (2008) Ganglion cell adaptability: does the coupling of horizontal cells play a role? PLoS One. Mar 5;3(3):e1714.

Dermietzel R, Spray DC. (1993) Gap Junctions in the brain: where, what type, how many and why?. Treds Neurosci., 16, 186-192.

Devor A, Yarom Y. (2002) Electrotonic coupling in the inferior olivary nucleus revealed by simultaneous double patch recordings. J Neurophysiol, 87 (6), 3048-58.

Deuschl G, Elble RJ. (2000) The pathophysiology of essential tremor. Neurology.; 54 (11 Suppl 4):S14-20. Review.

Elble RJ. (1998) Animal models of action tremor. Mov Disord.;13 Suppl 3:35-9. Review.

Evans WH, Martin PE, (2002) Gap junctions: structure and function (review). Mol. Membr. Biol. Apr-Jun, 19, (2),121-36. Review.

Gogan P, Gueritaud JP, Horcholle-Bossavit G, Tyc-Dumont S. (1974) Electrotonic coupling between motoneurones in the abducens nucleus of the cat. Exp Brain Res, 21 (2), 139-54.

Gulisano M, Parenti R, Spinella F, Cicirata F. (2000) Cx36 is dynamically expressed during early development of mouse brain and nervous system. Neuroreport 11 (17) 3823-8.

Hombach S, Janssen-Bienhold U, Sohl G, Schubert T, Bussow H, Ott T, Weiler R, Willecke K. (2004) Functional expression of connexin57 in horizontal cells of the mouse retina. Eur J Neurosci, 19 (10), 2633-2640.

Houghton FD, Barr KJ, Walter G, Gabriel HD, Grummer R, Traub O, Leese HJ, Winterhager E, Kidder GM. (2002) Functional significance of gap junctional coupling in preimplantation development. Biol. Reprod., 66, 1403-1412.

Janssen-Bienhold U, Trümpler J, Hilgen G, Schultz K, Müller LP, Sonntag S, Dedek K, Dirks P, Willecke K, Weiler R. (2009) Connexin57 is expressed in dendro-dendritic and axo-axonal gap junctions of mouse horizontal cells and its distribution is modulated by light. J Comp Neurol. Apr 1;513(4):363-74.

Kimura C, Yoshinaga K, Tian E, Suzuki M, Aizawa S, Matsuo I. (2000) Visceral endoderm mediates forebrain development by suppressing posteriorizing signals.

Dev Biol. Sep 15;225(2):304-21.

Li J, Hertzberg EL, Nagy JL. (1997) Connexin32 in oligodendrocytes and association with myelinated fibers in mouse and rat brain. J. Comp. Neurol., 379, 571-591.

Llinás R, Baker R, Sotelo C. (1974) Electrotonic coupling between neurons in cat inferior olive. J Neurophysiol. May;37(3):560-71.

Llinás R, Yarom Y. (1981) Properties and distribution of ionic conductances generating electroresponsiveness of mammalian inferior olivary neurones in vitro. J Physiol. Jun;315:569-84.

Llinás R, Leznik E, Makarenko VI. (2002) On the amazing olivocerebellar system. Ann NY Acad Sci., 978, 258-72. Review.

Louis ED, Zheng W, Jurewicz EC, Watner D, Chen J, Factor-Litvak P, Parides M. (2002) Elevation of blood beta-carboline alkaloids in essential tremor. Neurology. Dec 24;59(12):1940-4.

Mac Vicar BA, Dudek FE. (1981) Electrotonic coupling between pyramidal cells: a direct demonstration in rat hippocampal slices. Science, 213, 782-785.

Mann-Metzer P, Yarom Y. (1999) Electrotonic coupling interacts with intrinsic properties to generate synchronized activity in cerebellar networks of inhibitory interneurons. J Neurosci., 19 (9), 3298-306.

Manthey D, Bukauskas F, Lee CG, Kozak A, Willecke K. (1999) Molecular cloning and functional expression of the mouse gapjunction gene connexin-57 in human HeLa cells. J. Biol. Chem., 274, 14716-14723.

Marshall SP, van der Giessen RS, de Zeeuw CI, Lang EJ. (2007) Altered olivocerebellar activity patterns in the connexin36 knockout mouse. Cerebellum. Feb 28:1-13.

Martin FC, Thu Le A, Handforth A. (2005) Harmaline-induced tremor as a potential preclinical screening method for essential tremor medications. Mov Disord., 20(3), 298-305.

Martin FC, Handforth A. (2006) Carbenoxolone and mefloquine suppress tremor in the harmaline mouse model of essential tremor. Mov Disord. Oct;21(10):1641-9.

Maxeiner S, Kruger O, Schilling K, Traub O, Urschel S, Willecke K. (2003) Spatiotemporal transcript of connexin45 during brain development results in neuronal expression in adult mice. Neuroscience, 119 (3), 689-701.

Miro-Casas E, Ruiz-Meana M, Agullo E, Stahlhofen S, Rodríguez-Sinovas A,

Cabestrero A, Jorge I, Torre I, Vazquez J, Boengler K, Schulz R, Heusch G,

Garcia-Dorado D. (2009) Connexin43 in cardiomyocyte mitochondria contributes to mitochondrial potassium uptake. Cardiovasc Res., Sep 1;83(4):747-56.

Miwa H, Nishi K, Fuwa T, Mizuno Y. (2000) Differential expression of c-fos following administration of two tremorgenic agents: harmaline and oxotremorine. Neuroreport., 11(11):2385-90.

Miwa H, Kubo T, Suzuki A, Kihira T, Kondo T. (2006) A species-specific difference in the effects of harmaline on the rodent olivocerebellar system. Brain Res. Jan 12;1068(1):94-101.

Moorby C, Patel M. (2001) Dual functions for connexins: Cx43 regulates growth independently of gap junction formation. Exp. Cell Res., 271, 238-248.

O'Hearn E, Molliver ME. (1993) Degeneration of Purkinje cells in parasagittal zones of the cerebellar vermis after treatment with ibogaine or harmaline. Neuroscience. Jul;55(2):303-10.

Palacios-Prado N, Sonntag S, Skeberdis VA, Willecke K, Bukauskas FF. (2009) Gating, permselectivity and pH-dependent modulation of channels formed by connexin57, a major connexin of horizontal cells in the mouse retina. J Physiol. Jul 1;587(Pt 13):3251-69. Epub 2009 May 11.

Pantò M R, Zappalà A, Tuorto F, Cicirata F. (2004) Role of the Otx1 gene in cell differentiation of mammalian cortex. Eur J Neurosci 19, 2893-2902..

Pinto AD, Lang AE, Chen R (2003) The cerebellothalamocortical pathway in essential tremor. Neurology. Jun 24;60(12):1985-7.

Placantonakis DG, Bukovsky AA, Zeng XH, Kiem HP, Welsh JP. (2004) Fundamental role of inferior olive connexin 36 in muscle coherence during tremor. Proc Natl Acad Sci U S A. May 4;101(18):7164-9.

Rash JE, Yasumura T, Dudek FE, Nagy JL. (2001) Cell-specific expression of connexins and evidence of restricted gap junctional coupling between glial cells and between neurons. J.Neurosci., 21, 1983-2000.

Shelley J, Dedek K, Schubert T, Feigenspan A, Schultz K, Hombach S, Willecke K,

Weiler R. (2006) Horizontal cell receptive fields are reduced in connexin57-deficient mice. Eur J Neurosci. Jun;23(12):3176-86.

Sinton CM, Krosser BI, Walton KD, Llinás RR. (1989) The effectiveness of different isomers of octanol as blockers of harmaline-induced tremor. Pflugers Arch.; 414(1):31-6.

Solomon IC. (2003) Connexin36 distribution in putative CO2-chemosensitive brainstem regions in rat. Respir Physiol Neurobiol, 139 (1),1-20.

Teubner B, Degen J, Sohl G, Guldenagel M, Bukauskas FF, Trexler EB. (2000) Functional expression of the murine connexin36 gene coding for a neuron-specific gap junctional protein. J. Membr. Biol., 176, 249-262.

Tini M, Jewell UR, Camenish G, Chilov D, Gassmann M. (2002) Generation and application of chicken egg-yolk antibodies. Comp Biochem Physiol a Mol Integr Physiol, 131 (3), 569-74. Review.

White TW, Paul DL. (1999) Genetic diseases and gene knockouts reveal diverse connexin functions. Ann. Rev. Physiol., 61, 283-310.

Wilms H, Sievers J, Deuschl G. (1999) Animal models of tremor. Mov Disord., 14(4):557-71. Review.

FIGURES

Fig. 1

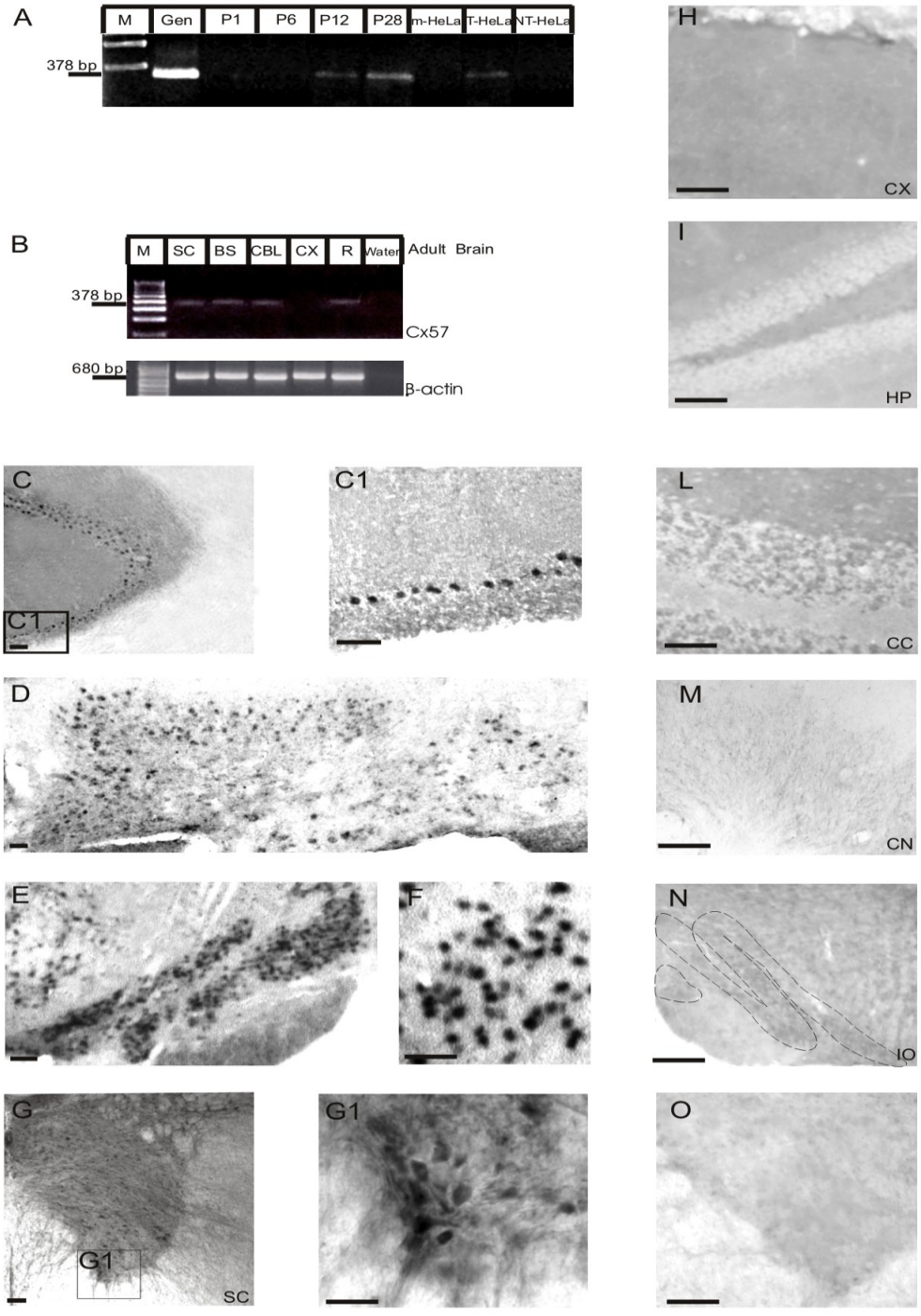

Fig. 2

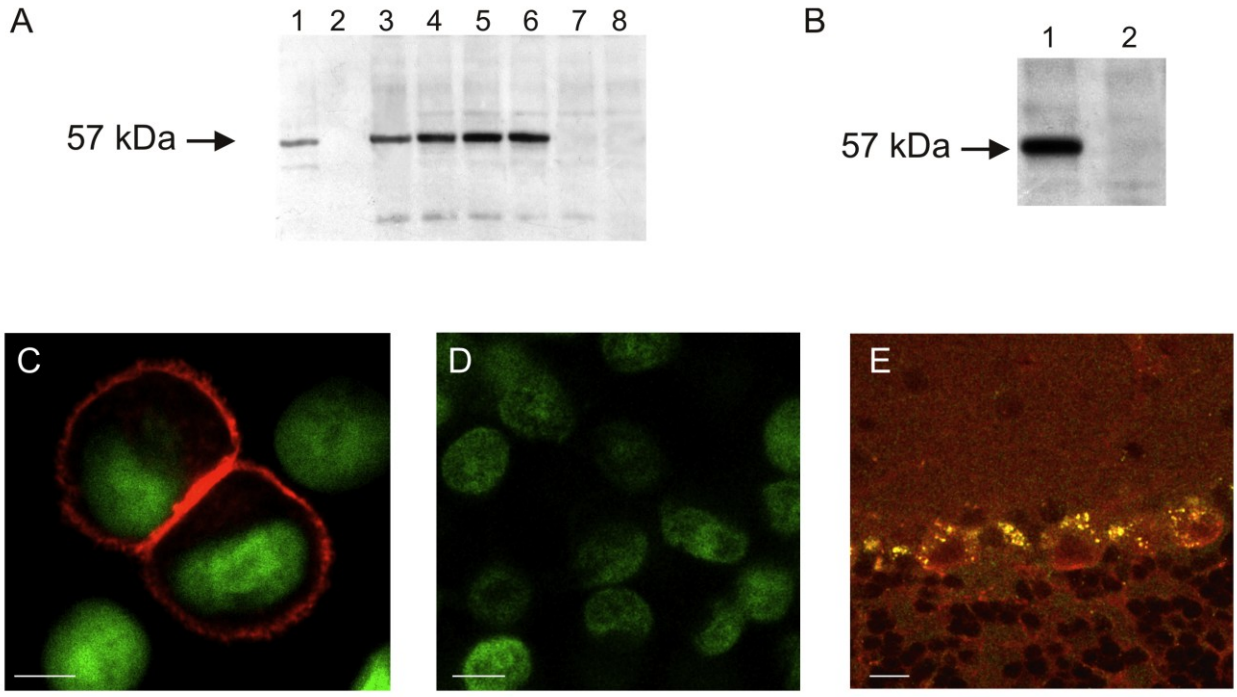

Fig.3

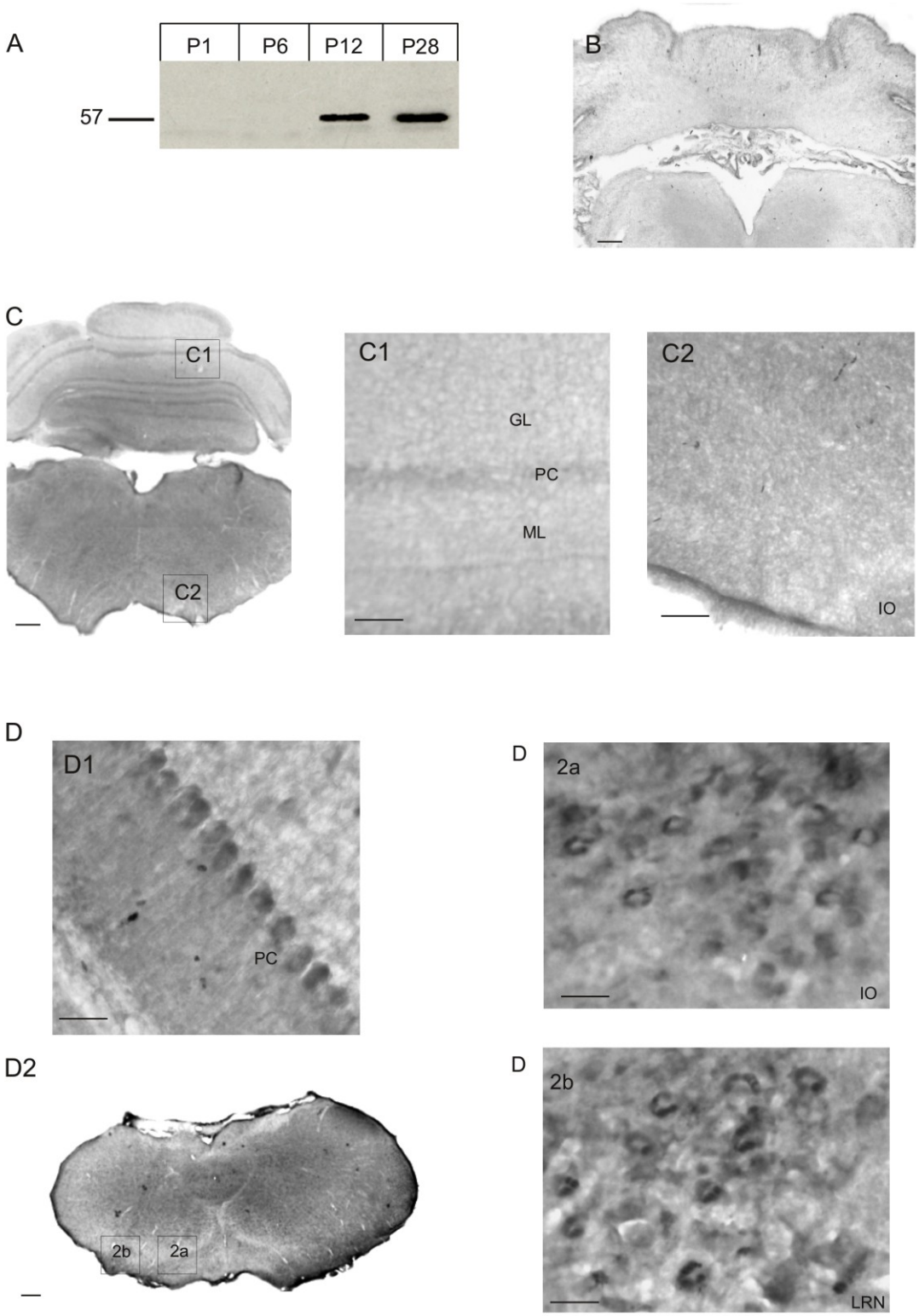
A
P1
P6
P12
P28
57
B
C
C1
C2
C1
GL
PC
ML
C2
IO
D
D1
PC
D
2a
IO
D2
2b
2a
D
2b
LRN

Fig.4

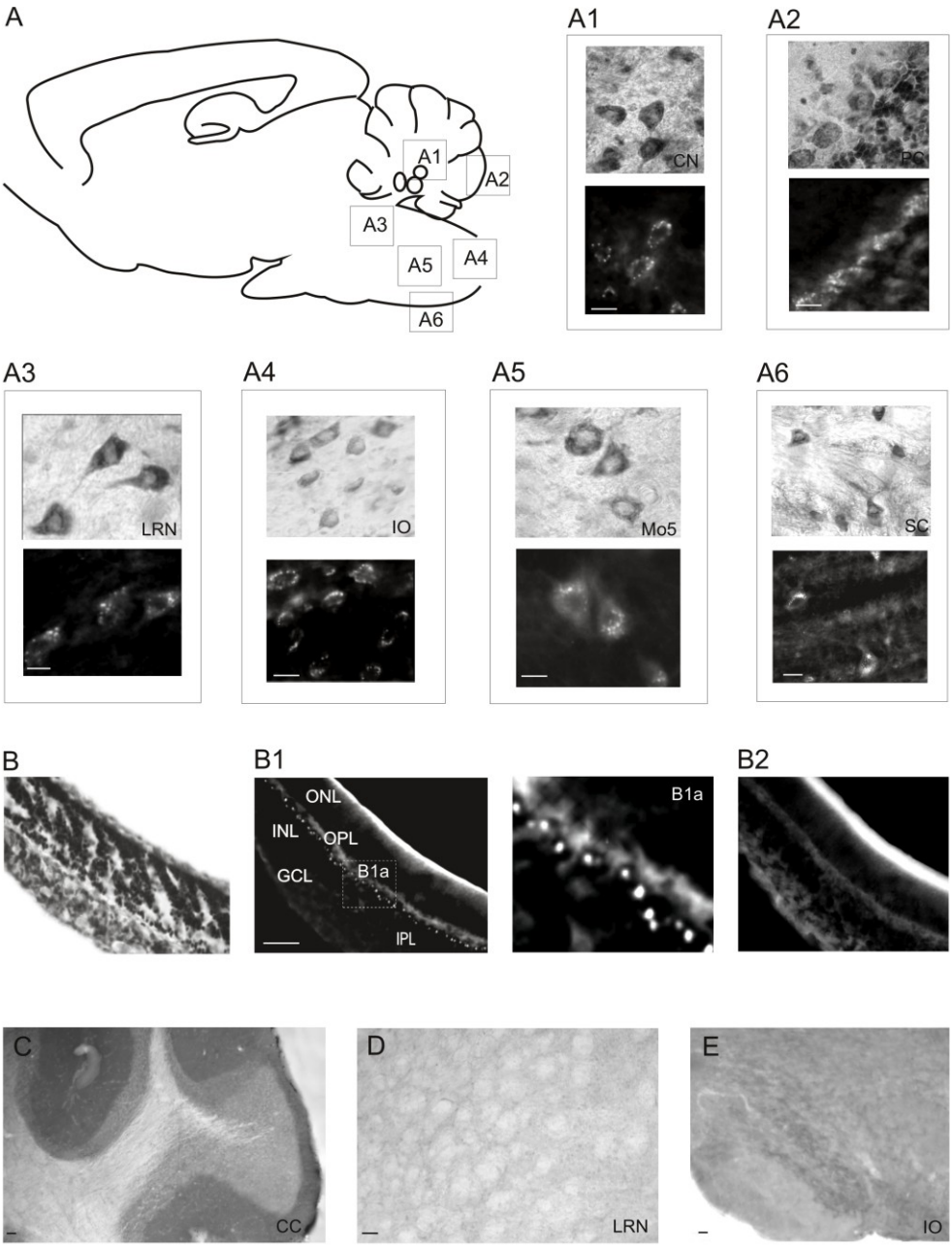
A
A1
A2
A3
A4
A5
A6
CN
PC
LRN
IO
Mo5
SC
B
B1
B2
ONL
INL
OPL
GCL
B1a
IPL
C
D
E
CC
LRN
IO

Fig.5

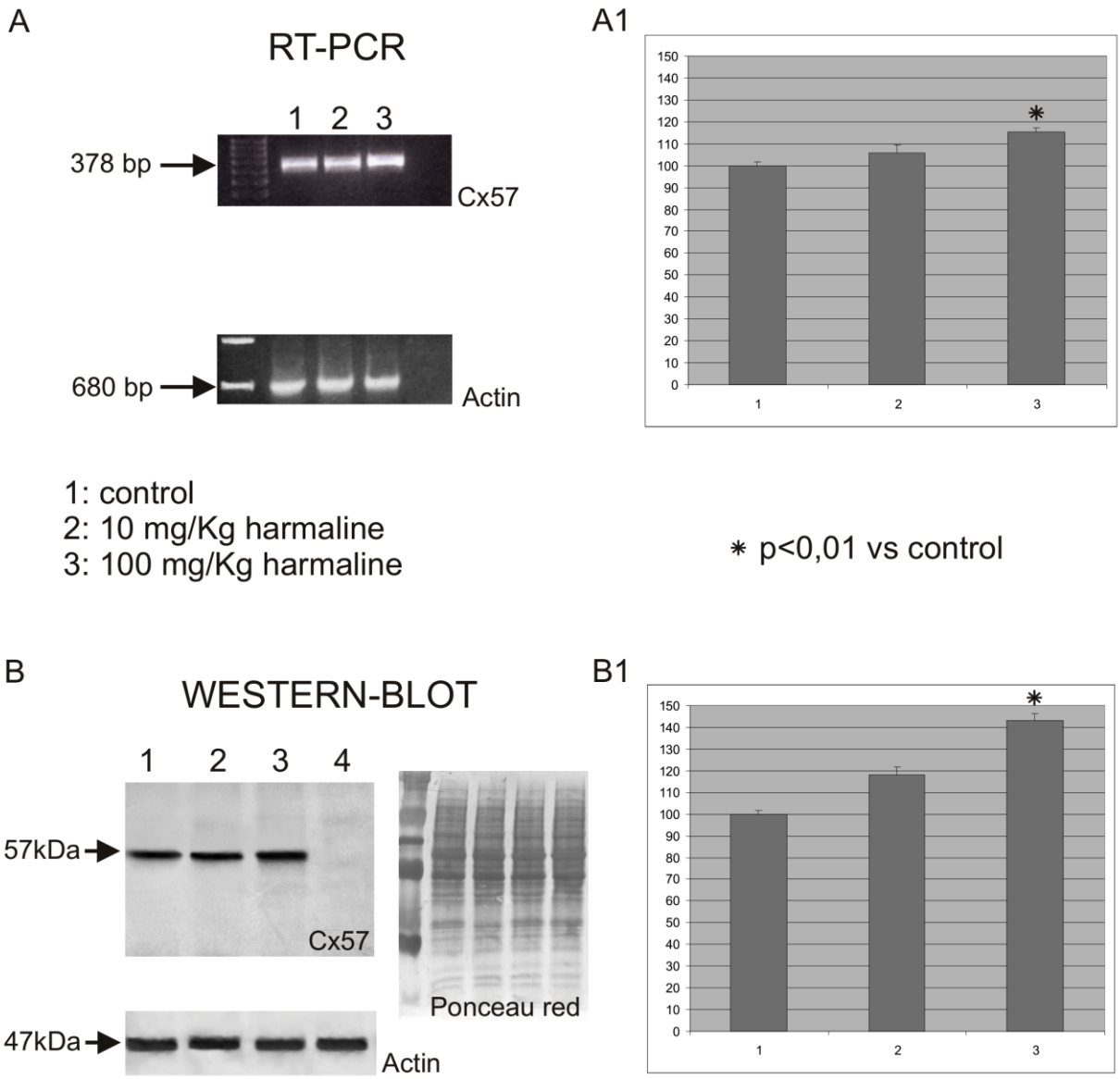
A
RT-PCR
1 2 3
378 bp
Cx57
680 bp
Actin
1: control
2: 10 mg/Kg harmaline
3: 100 mg/Kg harmaline
A1
150
140
130
120
110
100
90
80
70
60
50
40
30
20
10
0
1
2
3
* p<0,01 vs control
B
WESTERN-BLOT
1 2 3 4
57kDa
Cx57
Ponceau red
47kDa
Actin
B1
150
140
130
120
110
100
90
80
70
60
50
40
30
20
10
0
1
2
3

LEGEND

FIG.1 A: RT-PCR detection of Cx57 mRNA on postnatal stages (P1-P28: total brain), mock HeLa cells, transfected HeLa cells and non transfected HeLa cells. M: 100-bp ladder; Gen: Genomic DNA. The 378-bp band represents the Cx57 PCR product.

B: RT-PCR detection of Cx57 mRNA in different adult mouse tissues and retina. SC: spinal cord; BS: brainstem; CBL: cerebellum; CX: cerebral cortex; R: retina.

PCR (680-bp product) with β-actin specific primers has been used for normalization.

C-G: photomicrographs showing the localization of Cx57 mRNA using digoxigenin-labelled antisense riboprobe in brain regions. C, C1: Purkinje cells of the cerebellar cortex. D: cerebellar nuclei. E: inferior olivary complex, F: Lateral reticular nucleus. G, G1: thoracic spinal cord.

The sense probe for Cx57, used as control, did not show any signal (H-O; CX: cortex; HP: ippocampus; CC: cerebellar cortex; CN: cerebellar nuclei; IO: inferior olivary complex; SC: spinal cord)

Scale bar: 100 μm (C-O).

FIG.2 A: Wester blot analysis of the Cx57 immunoreactivity pattern showed by: transfected HeLa cells (1), mock HeLa cells (2), spinal cord (3), brain stem (4), cerebellum (5), retina (6), cortex (7), preadsorbed Cx57 antibody with the immunizing peptide (8).

B: The retina Cx57 immunoreactivity pattern (1) was absent in a retina sample incubated with the pre-immune serum (2).

C: Immunofluorescence analysis on transiently transfected HeLa cells with Cx57 cDNA showed a bright fluorescent signal.

D: No signal was detected in mock HeLa cells transfected with the empty vector and used as control.

E: Neuronal expression of the Cx57 protein was shown by co-staining with a NeuN monoclonal antibody in the Purkinje cells of the cerebellar cortex.

Scale bar: 100 μm (C-E).

FIG.3 A: Western blot for the Cx57 detection on postnatal stages (P1-P28: total brain) by using the polyclonal chicken anti-Cx57 generated in our laboratory. Detectable signals were shown at P12 and P28.

B-C: photomicrographs showing the immunohistochemistry on coronal brain section at P1 (B) and P6 (C) with the polyclonal anti-Cx57. C1, higher magnification of the cerebellar cortex (GL: granular layer, PC: Purkinje cell layer; ML: molecular layer). C2, higher magnification of the inferior olive (IO).

D: photomicrographs showing the immunohistochemistry on coronal brain section at P12. D1: Purkinje cells; D2: brainstem with insets showing the inferior olivary complex (2a) and the lateral reticular nucleus (2b).

Note that the Purkinje cells and the cells of the inferior olive and lateral reticular nuclei were stained at P12 (D) but not at P1 (B) and P6 (C).

Scale bar: 100 μm (B-D).

FIG. 4 A: drawing of sagittal section of adult brain showing the regional distribution of Cx57 labeling.

A1-A6: photomicrographs showing the immunohistochemistry on sagittal brain sections with the polyclonal anti-Cx57. A1: cerebellar nuclei; A2: Purkinje cells; A3: lateral reticular nucleus; A4: inferior olivary complex; A5: motor trigeminal nucleus; A6: spinal cord.

B-B1: photomicrographs showing immunolabeled horizontal cells in the retinal outer plexiform layer. B1a: three-fold magnification of the outer plexiform layer.

Each photomicrograph of immunoistochemical labeling has been coupled to the photomicrograph at the same magnification of the corresponding area of the contiguous histological sections stained with cresyl-violet.

B2, C-E: The Cx57 immunoreactivity pattern was absent in retina (B2) and brain sections (C, D, E) incubated with the pre-immune serum and the secondary antibody (CC: cerebellar cortex, IO: inferior olivary complex, LRN: lateral reticular nucleus).

Scale bar: 200 μm.

FIG.5 Cx57 expression pattern as both mRNA and protein was studied in cerebellum after systemic administration (10 or 100 mg/kg) of harmaline.

A, A1: Cx57 mRNA after administration of 10 mg/Kg of harmaline (106% ± 3,26) was weakly increased with respect to control animals but the statistical analysis was not significant ($p>0.05$, n=5). Conversely, the administration of 100 mg/Kg of harmaline significantly ($p<0.01$, n=5) increased the expression of Cx57 mRNA (115,3% ± 2,05) with respect to control animals.

B, B1: Western blot analysis showed that animals treated with harmaline at a dose of 10 mg/Kg showed an increment of the Cx57 protein expression (118 % ± 3,74) with respect to control animals but the statistical analysis was not significant ($p>0.05$, n=5). Mice treated with harmaline at a dose of 100 mg/Kg showed an increased level of the Cx57 protein (143% ± 3,26), with respect to control animals, and the statistical analysis was significant ($p<0.01$, n=5). Ponceau red stained blot was performed for control of equal amounts of protein per sample loaded onto the gel.

Densitometric analysis was performed after normalization with actin by using an Image Analyzer Software. Data are expressed as means ± SD. Images shown are representative of five separate experiments (n=5).

Chapter 3

EXPRESSION PATTERN OF CONNEXINS AND PANNEXINS IN PRIMARY HUMAN ASTROGLIAL CELL CULTURES EXPOSED TO GLUTAMATE OR LIPOPOLYSACCHARIDE

Nicolosi S.[a], Cicirata V[b], Campisi A[c]., Corsaro V[a]., Ragusa M[d]., Perciavalle V[e]., Di Pietro C[d]., Cicirata F[a*].

Departments of [a]Biomedical Sciences, Physiology Section, of [b]Drug sciences, PhD program in Neuropharmacology, University of Catania, and of [c]Drug Sciences, Biochemistry Section, viale Andrea Doria 6 95125, Catania University, Catania, Italy. [d]Department Gian Filippo Ingrassia, Biology, Genetic, Cellular and Molecular Genomic Giovanni Sichel, University of Catania, via Santa Sofia, 95125 Catania Italy.[e] Department Formative Processes, University of Catania, via Biblioteca 2, 95124 Catania

Corresponding Author:

[a*]Prof. Federico Cicirata

Department of Biomedical Sciences, Physiology Section, University of Catania,

Viale Andrea Doria, 6

95125 Catania, Italy

Phone: +39-095-7384031

e-mail: cicirata@unict.it

---

[a]Nicolosi S. and [b]Cicirata V. contributed equally to the work

Acknowledgments

Valentina Cicirata is supported by the International PhD program in Neuropharmacology, University of Catania, Medical School, Catania, Italy

Abstract

The effects of the administration of LPS (1,10, 100 μg/ml) or glutamate (10, 50, 100 μM) for different time intervals (12, 24 and 48 h) were tested in human astrocytes. Four parameters were compared: cytological modification, cell viability, level of ROS and GSH, the level of mRNA of connexins (Cxs): Cx26, Cx30, Cx43 and pannexins (Panx): Panx 1 and Panx2. Main findings were:1) the stressors (LPS and glutamate) increased the mRNA level of Cx26 and Cx30, while Cx43, Panx1 and Panx2 were not significantly modified; 2) the level of Cx26 and Cx30 increased strongly at lower doses of stressors while increasing the doses of the stressors, the increment of Cx26 and Cx30 progressively lowered. Conversely, the level of the ROS increased with the doses of the stressors; 3) an inversed relation occurred between level of Cxs (Cx26 and Cx30) and grade of injury of the cells (as proved by astrocytosis and by MTT test). These evidences suggested that the gene expression of the Cx 26 and Cx30 are under the control of factors related to cell suffering, while the levels of the ROS were uninfluent. New findings also concerned the demonstration that human astrocytes can evolves in astrogliosis in cultures essentially free of microglia cells, as previously reported in rat by Hamby (2012). The variable level of Cx 26 and Cx30 at increasing level of cell injury suggested that they are likely involved in the so called kiss-of-life or kiss-of-death, in relation to the grade of injury.

Highlights

- mRNA expression of connexins and pannexins in primary human astrocytes were assessed
- Glutamate or lypopolysaccaride as stressor agents were used
- An overexpression induced by the stressor agents of Connexins 26 and 30 was found
- No significant changes in Connexin43 and Pannexins 1 and 2 expression were observed
- The increase of connexins expression might be related to the grade of injury.

Keywords

Gap juctions, primary human astrocytes, connexins, pannexins, glutamate, lipopolysaccharide.

Abbreviations

AGS, Astroglial Growth Factor; Ct, threshold cycle; Cx43, connexin 43, Cx26, connexin 26; Cx30, connexin 30; DCF, 2′,7′-dichlorofluorescein; DCFH-DA, 2′,7′-dichlorofluorescein diacetate; DIV, days *in vitro*; BME, Basal Essential Medium; FBS, heat inactivated Fetal Bovine Serum; GJ, Gap junction; GAPDH, Glyceraldehyde-3-phosphate dehydrogenase; GFAP, Glial Fibrillary Acidic Protein; GSH, reduced glutathione; LPS, lipopolysaccharide; MTT, 3(4,5-dimethyl-thiazol-2-yl)2,5-diphenyl-tetrazolium bromide; Panx1, pannexin 1; Panx2, pannexin 2; qRT-PCR, Quantitative real-time Polimerase Chain Reaction; ROS, reactive oxygen species;

1. Introduction

Gap junction (GJ) channels represent an important form of intercellular communication and are considered the anatomical substrate of electrical synapses (Bennett, 2000; Galarreta and Hestrin, 2001). GJ channels are formed by two hemichannels, each of which consists of subunits of transmembrane proteins. Different families of proteins have been identified. In vertebrates the most numerous and studied class of proteins is constituted by connexins (Cxs) (Nagj and Rash, 2000; Rash et al., (2001); Nakase and Nauss, 2004; Lee et al., (2005). Recently, a new important class of GJ proteins has been recognized in vertebrates, the pannexins (Panxs), which are considered homologous to the innexins of the invertebrates. Phylogenetic analysis revealed that Panxs are highly conserved in *Nematoda, Mollusca, Arthropoda* and also in mammals (Panchin et al. 2000). The high maintenance of the Panxs in classes which are so distant in terms of phylogenesis suggests the importance of their functions (Baranova et al. 2004). Three Panxs and more than 20 Cxs were cloned in mammals. The set of Cxs and Panxs expressed in single cells is functionally important because their combination in GJ channels is critical for permeability to specific signaling molecules or ions (Maeda et al. 2010). Each cell type expresses a given set of GJ proteins, but their expression pattern is not stable in time. In fact, the pattern expressed in resting condition usually changed after injury both in vitro (Eugenín et al. 2001) or in vivo models (Rouach et al. 2002), suggesting altered permeability to signaling molecules in suffering conditions.

It is well known that astrocytes, the most representative cells present in the brain, are involved in acute and chronic brain damages. In particular, a brief exposure to

glutamate of differentiated astrocytes causes cell swelling, whereas a prolonged incubation (excitotoxicity) induces cell damage (Matute et al. 2002). This phenomenon causes alterations in glutamate transport, glutathione (GSH) depletion, inducible nitric oxide synthase (iNOS) activation, and macromolecular synthesis. Consequently, several calcium-dependent enzymes may be activated, causing mitochondria impairment, decrease in ATP levels, reactive oxygen species (ROS) production and subsequent neuronal cell death (Li CY et al. 2004). Furthermore, in several brain diseases lipopolysaccharide (LPS) stimulation in cultured astrocytes induces iNOS expression (Murakami et al. 2003) and proinflammatory cytokines (Faure et al. 2001;Martin et al. 2006), including TNF-a and interleukin-6 (Suto et al. 1993).

It has been reported that astrocytes express Cxs and Panx. In particular, Cx43, Cx26, Cx30, Panx1 and Panx2 was shown in astrocytes of both humans (Ahmed et al. 2009; Nagy et al. 1999; Thompson et al. 2008) and rodents (Orthmann-Murphy et al. 2008; Rash and Nagj, 2001; Nagy, 1999). Previous studies also reported the dynamic expression of single Cxs and Panxs in astrocytes submitted to different types of injuries (Hinkerohe et al. 2010; Figiel et al. 2007; Zappalà et al. 2007, Parenti et al. 2010). However, no information are available on some aspects of the expression pattern of Cxs and Panxs in astrocytes. This study was planned to study: 1) the inter-individual variability of expression of a set of gap junction genes (Cx43, Cx26, Cx30, Panx1, Panx2) after different types of injury; 2) the level of single Cxs and Panxs at increasing grade of injury; 3) the possible role of the ROS as an inducer of gene expression of Cxs and Panxs. In this aim we searched for the amount of mRNA of Cx43, Cx26, Cx30, Panx1 and Panx2 by quantitative Real-Time, in primary human astroglial cell cultures exposed to glutamate or LPS. We also evaluated the morphological modification of astrocyte cells to stressors, the cell viability by MTT test and the intracellular oxidative status by testing the levels of reactive oxygen species (ROS) and glutathione (GSH).

2. Results

The effects of the administration of different concentrations of LPS (1,10, 100 μg/ml) or glutamate (10, 50, 100 μM) for different time intervals (12, 24 and 48 h) were tested. Light and fluorescent microscopes were used to study morphological modification of astrocyte cells induced by stressors. Astrocytes undergo morphological changes referred as reactive gliosis in large amount of cell after treatment with 1 μg/ml LPS or 10 μM glutamate, and virtually in all cell population after treatment with 10 or 100 μg/ml as well as 50 or 100 μM glutamate. Fluorescent microscope and MTT assay were used to asses cell viability (Table 1). Both test showed no significant changes in the viability of astroglial cell cultures exposed to 1 or 10 μg/ml LPS as well as 10 or 50 μM glutamate, at both 12, 24 and 48 hour of intervals. Higher concentrations of LPS (100 μg/ml) and glutamate (100 μM) induced a significant reduction of cellular viability (Table 1).

2.1 ROS and GSH levels - After 24 hours of sham treatment. the ROS levels were of 27.40 ± 0.72 (see Methods, Fig.1) and the GSH levels were of 137.3 ± 4.22 (see Methods, Fig.2). These valued were used as control to compare ROS and GSH levels reported after treatment with stressors. The treatment of the astroglial cell cultures with 10 μM glutamate for 24 h induced a significant increase of ROS levels and a significant reduction of GSH levels (Fig 1). The treatment with 50 μM glutamate for 24 h induced a further, high significant increase of ROS and decrease of GSH (Fig. 2). After treatment with 100 μM glutamate the levels of ROS and GSH were grossly similar to what reported after treatment with 50 μM glutamate (Fig.2). The treatment of the astroglial cell cultures with 1 μg/ml LPS for 24 h induced a significant increase of ROS (Fig.1) and decrease of GSH (Fig. 2). The altered redox status is consistent with a transporter-mediated toxicity evoked by *oxidative stress* (Matute et al., 2002). Furthermore, the comparison of both MTT test (Table 1), ROS (Fig.1) and GSH levels (Fig.2) in astrocytes after treatment with 1 μg/ml LPS and 10 and 50 μM Glutamate suggests a comparable level of cellular injury. This finding is functionally important in the light of the expression of some Cxs under the same experimental conditions.

2.2 Amount of Cxs or Panxs analysis of transcripts

Figure 3 reported the amount of Cxs or Panxs analysis of transcripts evaluated by qRT-PCR in primary human astroglial cell cultures exposed to 1 μg/ml LPS or 10, 50, 100 μM glutamate for 24 h. The relative amount of transcript for each Cxs or Panxs was standardized with respect to the amount of GAPDH mRNA levels and normalized with respect the untreated cells, according to the 2-ΔΔCT method. The level of mRNA of both Cx30 and Cx26 were dramatically changed by the treatment. The level of Cx30 increased more than 10 folds (10.64 assuming 1 as a control; *t*-test: <0.001) after treatment with 1 μg/ml LPS, more than 6 folds (6.06; *t*-test: <0.001) with 10μM glutamate, more than 5 folds (5.4; *t*-test: <0.001) with 50 μM glutamate, while the 100 μM glutamate decreased the expression of -42% (*t*-test: >0.001 <0.05)(Fig.3). The expression of Cx26 increased more than 5 folds (5.21; *t*-test: <0.001) after treatment with 1 μg/ml LPS, more than 3 folds (3.38; *t*-test: <0.001) with 10μM glutamate, more than 2 folds (2.84; *t*-test: <0.001)with 50 μM glutamate, while the 100 μM glutamate decreased the expression of -39% (*t*-test: >0.001 <0.05) (Fig. 3). Cx43, Panx1 and Panx 2 were differently modified by LPS and glutamate. The treatment with 1 μg/ml of LPS decreased moderately (*t*-test: >0.001 <0.05) the expression of Cx43(-36%), Panx1 (-42%) and Panx2 (-51%), while no significant changes (*t*-test: >1) were observed in the expression of Cx43, Panx1 and Panx2 after treatment with glutamate at different doses, in spite of a general down-regulation shown by their expression (Fig.3) .

3. Discussion

In this study LPS and glutamate were used as stressors. The LPS is a canonical innate inflammatory mediator used extensively to study cellular response to inflammation (Raetz and Whitfield, 2002; Daginakatte et a., 2008; Hamby et al., 2012). For many time was assumed that LPS could affect astrocytes only in cultures including microglia. Conversely, Hamby (2012) recently showed in cortical astrocyte cultures of rat essentially free of microglia and other cell types, that LPS control molecular networks and pathways associated in particular with immune signaling and regulation of cell injury, death, growth, and proliferation. The present report is the first demonstration that also human astrocytes can be activated by LPS in cultures free of microglia. The glutamate is concerned in the astrocytic communication (Conti et al., 1996; Schipke et al., 2001; Lalo et al., 2006; Zhang et al., 2003; Lee et al., 2010). It involves the induction of an intracellular calcium wave (Cornell-Bell et al., 1990) that can result in dysfunction and death of astrocytes, at least partially mediated by excessive stimulation of NMDA receptors (Lee et al., 2010). These results enhance the role that NMDA receptors may play in facilitating glial signaling in normal, healthy environment, as well as their potential involvement in neuropathological conditions (Su et al., 2003; Teismann et al., 2004).The study compared four parameters: cytological modification of astrocytes to injuries, cell viability, level of ROS and GSH and level of mRNA of Cxs and Panx. The cytological modification and the cellular viability show the profile of the cellular reactivity to the increasing concentration of the stressors. The other two parameters: ROS/GLU and level of mRNA of Csx and Panx, express the functional reactivity of astrocytes to the injury. The main new findings can be summarized as follows. The study showed the over regulation of Cx26 and Cx30 and the down regulation of Cx43, Panx1 and Panx2 after treatment with LPS and glutamate (Fig. 3). The over-regulation of the Cx26 was firstly shown in this study while the over-regulation of the Cx30 reported in this study extended the finding of Gosejacob et al. (2011), who showed that Cx30 is more abundant than previously thought in the hippocampus where it makes a substantial contribution to interastrocytic gap junctional communication. Our findings implemented such conclusion because the work of Gosejacob et al. (2011) investigated the wild type hippocampus, while our findings reported the strong increment of the Cx30, as well as the Cx26, after injury in respect to resting conditions. The trend shown by the Cx26 and Cx30 genes is reminiscent of the so called inducible genes, which starting from (relatively) low level of expression in resting conditions, increase strongly their expression after activation. A further new

finding concerned the different effects elicited by the stressors. In fact, the administration of 1 μg/ml LPS and 10μM glutamate elicited different effects in spite of the similar level of cellular injury, as shown by comparable level of MTT (Tab1) as well as ROS and GSH test (Figs.1, 2). The level of Cx26 and Cx30 was much stronger after treatment with LPS than after treatment with glutamate (Fig.3) and, moreover, only LPS decreased significantly the level of both Cx43, Panx1 and Panx2 (Fig.3). These evidences suggest the level of mRNA of the two Cxs cannot be generically related to the level of injury, independently to the nature of the stressors as generally assumed, but more finely to the molecular mechanisms specifically interfered by the single stressors. More in general, the specific arrangement of the expression pattern of gap junction genes in relation to the nature of the stressors reported in the study is in agreement with the large body of observation that the expression of single Cxs is differently regulated in different experimental conditions. The findings of this study suggests to extend the research to other toxic agents, to search for possible different (at limit also individualized) pattern of expression of gap junction genes. In addition, we observed that the levels of expression of the Cx26 and Cx30 were dose-dependent to the glutamate added to the culture. In fact, their expression progressively decreased at increasing the doses of glutamate (Fig. 3), that is at the increasing level of injury, as shown by ROS and GSH test (Fg.1,2), MTT assay (Tab.1) and astrogliosis. This evidence raised the question if the expression of the Cx30 and Cx26 was under the direct control of the ROS. This hypothesis was denied by opposite trends of the level of ROS and of Cx30/Cx26 at increasing level of injury. In fact, the level of the ROS increased from glutamate 10 to 50 μM and remained stable at 100 μM glutamate (Fig.1); conversely, the levels of mRNA of Cx26 and Cx30 showed the opposite trend: they showed the greater level at lover doses of glutamate (10 μM) while, increasing the doses of glutamate, the level of mRNA of Cx26 and Cx30 decreased progressively (Fig.3). The “early” expression of Cx26 and Cx30 reported in this study suggests that the communication between astrocytes through GJ or hemichannels principally occurs at precocious stages of cellular suffering. Since the ROS were not concerned in the primary control of the gene expression of the Cx26 and Cx30, new candidate must be searched. One potential candidate could be the ATP, which control the opening of the Panx or Cxs hemichannels, as shown in cultures of spinal astrocytes after treatment with acid fibroblast growth factor. The treatment release ATP from astrocytes, and ATP causes the opening of Panx hemichannels, which then release further ATP. Subsequently, Cxs hemichannels are also opened. Release of ATP appears to become self-sustaining through action of P2X7 receptors to open Panx and Cxs hemichannels,

both of which are ATP permeable (Garrè et al., 2010; Bennet et al., 2012). The hypothesis that ATP could control the expression of the Panxs and Cxs genes, besides the opening of the hemichannels, must be tested in future investigations. Finally, assuming that to the increased level of mRNA of Cx26 and Cx30 corresponds an increased level of the proteins and that they form GJ or hemichannels, some speculations can be done about the nature of the messages that are carried along. The question is, obviously, of utmost interest. Two opposite point of view have been proposed for the gap junction communication system: or the gap junction channels carry signalling molecules that sustain injured cells to overcome the lesions (this role of the GJ channels has been imaginatively defined as "kiss-of-life"; Andrade-Rozental et al. 2000), or they carry signalling molecules that spread the injury from the affected cells to the other to whom they are connected (and in this case they were defined as "kiss-of-death"; Andrade-Rozental et al. 2000). Passing to our model, we have not direct evidences of the nature of the signalling molecules carried along the gap junction channels. Nevertheless, the levels of the expression pattern of the Cx26 and Cx30 at increasing doses of glutamate (Fig.3) can suggests the nature of the messages. The lower levels of expression at the higher level of injury (glutamate 100 μM) can be interpreted as a protective strategy to reduce the number of gap junction channels and thus to decrease the spread of noxious signaling molecules from injured cells to surrounding ones. In the same way, the strong over-expression of the Cx26 and Cx30 at the lower levels of injury (glutamate 10 μM) can be interpreted as a strategy to increase the spread of "positive" signaling molecules to the net of connected cells. In this hypothesis the gap junction channels formed in our models are either kiss-of-life or kiss-of-death in relation to the grade of injury.

4. **Experimental procedure**

4.1 Materials

Cryo-preserved human cortex astroglial cell lines, and astrocyte growth supplement (AGS) were purchased from Innoprot (Derio, Bizkaia, Spain). Heat Inactivated Foetal Bovine Serum (FBS), Eagle's Basal Medium (EBM), L-glutamine, antibiotics (penicillin-streptomycin) and 0.05% trypsin/EDTA 1X solution were from Invitrogen (Milan, Italy). Poly-L-lisine, glutamate, lypopolisaccaride (LPS), phenylmethylsulfonyl fluoride (PMSF), and other chemical reagents were obtained from Sigma (Milan, Italy). Glial Fibrillary Acidic Protein (GFAP) was from Chemicon (Prodotti Gianni, Milan, Italy). Bradford kit was from (Bio-Rad, Richmond, CA). RT-PCR real time Taqman primer and probe for human Cxs an Panxs were provided from Applied Biosystem. Qiamp RNA blood mini kit for RNA extraction was from Qiagen (Milan, Italy), High Capacity RNA-to-cDNA Kit for cDNA synthesis, Taq Man Gene Expression Master Mix and TaqMan probes for different human connexins were from Applied Biosystem s(Foster City, CA,USA).

4.2 Methods

4.2.1 Cell cultures

Human cortex astrocytes were suspended in EBM, containing 10% FBS (vol/vol), 2 mM glutamine, streptomycin (50 µg/ml) and penicillin (50 U/ml) and AGS, plated at a density of $1x10^6$ cells/100 mm dish pretreated with 10 µg/ml poly-L-lysine. Cells were maintained at 37°C in a 5% CO2/95% air humidified atmosphere for two weeks and medium exchanged every two days. Some cultures, approximately 90% confluent, were incubated at 37°C for 5 min. with trypsin/EDTA solution (0.05%), and neutralized at room temperature with FBS (vol/vol 1:1). Cell suspension was then centrifuged at 200 x g for 5 min, suspended in the medium and plated at a density of $1x10^6$ cells/100 mm dish pretreated with 10 µg/ml poly-L-lysine, and maintained at 37°C in a 5% CO2/95% air humidified atmosphere for one week and medium exchanged every two days.

Astroglial cells purity was determined by immunofluorescence analysis with antibodies against GFAP (specific for astrocytes) and CD68 (for microglia). More than 95% of the cells stained positive for GFAP while we did not detect any staining for CD68 (data not shown).

4.2.2 Treatment of the cells

Primary human astroglial cell cultures, approximately 90% confluent, were replated on to 16-mm diameter 10 μg/ml poly-L-lysine coated glass coverslips at a final density of $1x10^4$ cells/coverslip, and fed in fresh complete medium. In preliminary experiments, we exposed astroglial cell cultures for 12, 24 or 48 h to glutamate (10, 50, 100 μM) or to LPS (1, 10, 100 μg/ml), in order to establish the optimal concentrations and their exposure times of stressors. For this purpose, MTT test, morphological, and immunocytochemical characterization were utilized. These sets of experiments showed that a non-toxic concentration for the cells was 10 μM of glutamate and 1 μg/ml of LPS and the optimal exposure time was 24 h.

4.2.3 MTT Bioassay

To monitor cell viability, primary human astroglial cell cultures were set up 60x 10^4 cells/well of a 96-multiwell flat-bottomed 200-μl microplates (Mossman, 1983). Cells were incubated at 37°C in a humidified 5% CO_2–95% air mixture. At the end of treatment time, 20 μl MTT, 0.5%, in phosphate buffer saline were added to each multiwell. After 1 h of incubation with the reagent, the supernatant was removed and replaced with 200 μl dimethylsulfoxide. The optical density of each well sample was measured with a microplate spectrophotometer reader (Titertek Multiskan; Flow Laboratories, Helsinki, Finland) at 570 nm. The 24 h exposure of astroglial cell cultures to 10 μM glutamate or 1μg/ml LPS did not significantly affect cell function and viability, as revealed by MTT reduction assay, evaluating mitochondrial dehydrogenase activity.

4.2.4 Glutathione measurement

Astroglial cell cultures were scraped off and lysed in 50 μM sodium phosphate buffer, pH 7.4. The protein concentration in cell extracts was determined by Bradford assay (Campisi et al. 2004). Then, total glutathione intracellular content (GSH+GSSG), was chemically determined as described by Chen et al. (2000).

4.2.5 ROS determination

Reactive species determination was performed by using DCFH-DA as a fluorescent probe. Briefly, 100 μM of DCHF-DA was dissolved in 100% methanol, added to the cellular medium, and cells were incubated at 37°C for 30 minutes. Under these conditions, the acetate group was not hydrolyzed (Campisi et al. 2004). After incubation, astrocytes were lysed and centrifuged at 10,000 x *g* for 10 min. The fluorescence (corresponding to the radical-species–oxidized 2′,7′-dichlorofluorescein; DCF) was monitored spectrofluorometrically (excitation, λ = 488 nm; emission, λ = 525 nm), using an F-2000 spectrofluorimeter (Hitachi). Values are expressed as fluorescence intensity/mg protein. Protein concentration was measured, according to Bradford (1976).

4.2.6 Quantitative real-time PCR (qRT-PCR)

The mRNA of Cx43, Cx26, Cx30, Panx1 and Panx2 was searched in extracts of astroglial cells, either native (i.e. wt, used as control) or exposed to 1 μg/ml LPS as well as to different concentrations of or glutamate (1, 10, 50 μM), used as stressor agent. Total RNA was isolated using Qiamp RNA blood mini kit and reverse-transcribed using the Thermoscript RT-PCR kit, according to the manufacturer's instructions. RNA was quantified using GENESYS 10 Spectrophotometers at 260 nm. 1 μg of total RNA was reverse-transcribed at a final concentration of 50 ng/μl using the High Capacity RNA-to-cDNA Kit. The mixture was incubated in Biometra ThermaCycler for 10 min at 70°C, followed by 60°C for 60 min and 95°C for 5 min. Synthesized cDNA was stored at -20°C. Real Time PCR was performed using Applied Biosystems 7900HT Fast Real-Time PCR System. 20 ng of cDNA were added to each well in a 96 well plates and the reactions were heated at 95°C for 10 min and amplified with 40 cycles of 95°C for 15s and 60°C for 1 min. Quantitative real-time PCR was performed according to the manufacturer's instructions by using TaqMan Gene Expression Mastermix. The TaqMan assays for Cx43, Cx26, Cx30, Px1, Px2, Glyceraldehyde-3-phosphate dehydrogenase (GAPDH) were purchased from Applied Biosystems. GAPDH was used as normalizator gene. The threshold cycle (Ct), defined as the cycle number at which a significant increase in fluorescence is first detected, was obtained for each gene in each sample. The Ct for each gene in each sample was normalized to the Ct of control genes (GAPDH) and then compared to Ct of the calibrator sample (untreated cells), according to the 2-ΔΔCT method. These analysis were performed by using RQ manager software

from Applied Biosystems. All experiments were performed in triplicate. The data were presented as RQ (relative quantity).

4.3 Statistical analysis

The findings reported in treated cells were compared to corresponding ones shown in sham treated cells. Statistical analysis were performed to test the significant expression levels in treated cells vs control ones. All data were analyzed statistically using one-way ANOVA, followed by Newman–Keuls post hoc test. All values are presented as mean ± SD of 5 separated experiments. The Student's t-test was used to compare the values of each assay; differences were considered statistically significant at $*p < 0.05$ and $**p<0.001$.

FIGURES

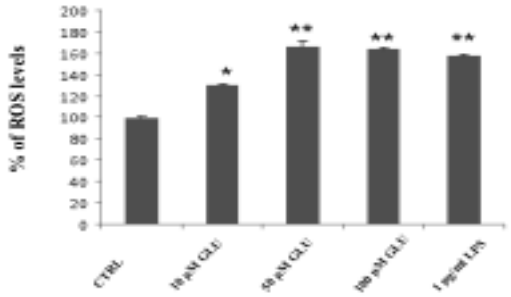

Fig. 1: ROS levels in primary human astroglial cell cultures exposed to glutamate (10, 50, 100 μM) or LPS (1 μg/ml) for 24h. ROS levels are expressed as % of nmoles of dichlorofluorescein produced/30 min/mg protein.Values are mean ± S.D. of four experiments performed in duplicate. Statistically significant vs control : *$p < 0.05$ and **$p<0.001$.

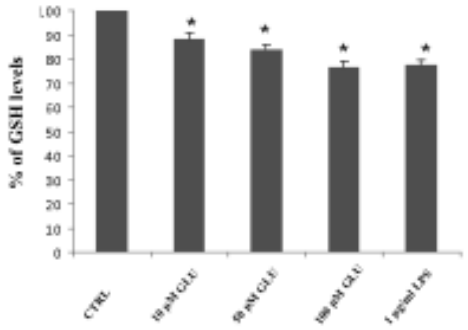

Fig. 2: GSH levels in primary human astroglial cell cultures exposed to glutamate (10-100 μM) or LPS (1 μg/ml) for 24h. GSH levels are expressed as % of nmol of GSH/mg protein. Values are mean ± S.D. of four experiments performed in duplicate. Statistically significant vs control: *$p < 0.05$.

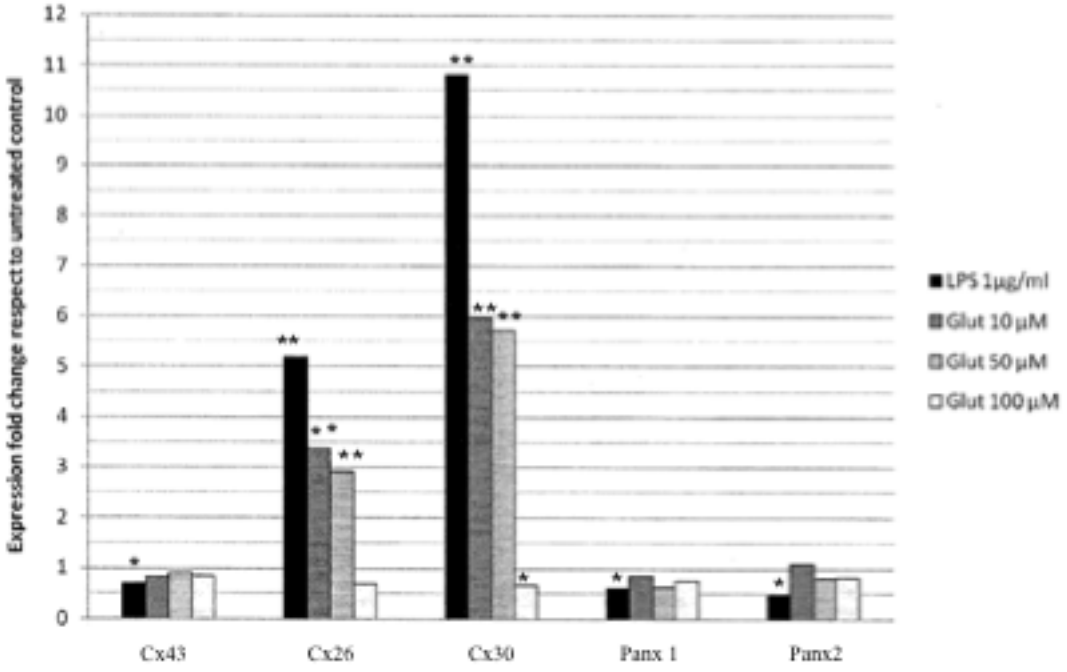

Fig. 3: Amount of Cxs or Panxs analysis of transcripts evaluated by quantitative Real-Time PCR in human primary astroglial cell cultures exposed to 1 µg/ml LPS or 10, 50, 100 µM glutamate for 24 h. The relative amount of transcript for each Cxs or Panxs was standardized with respect to the amount of GAPDH mRNA levels and normalized with respect the untreated cells, according to the 2-ΔΔCT method. Values are mean ± S.D. of four experiments performed in duplicate. Statistically significant vs control: **$p<0.001$, *$p < 0.05$.

Table 1

	% of cell viability		
Treatment	**12 h**	**24 h**	**48 h**
control	**100 ± 2**	**100 ± 1**	**100 ± 1**
+ 10 µM glutamate	**99 ± 2**	**98 ± 3**	**99 ± 1**
+ 50 µM glutamate	**98 ± 1**	**99 ± 2**	**96.5 ± 5**
+ 100 µM glutamate	**85 ± 3***	**75 ± 6***	**70 ± 1***
+ 1 µg/ml LPS	**100 ± 4**	**98 ± 1**	**97 ± 2**
+ 10 µg/ml LPS	**99 ± 1**	**98 ± 3**	**94.5 ± 3**
+ 100 µg/ml LPS	**83 ± 2***	**74 ± 5***	**69 ± 1***

Table 1: Cell viability in primary human astroglial cell cultures unexposed or exposed to different concentrations of glutamate (1, 10, 100 µM) or LPS (1, 10, 100 µg/ml) for 12, 24 or 48 h. Values are mean ± S.D. of four experiments in duplicate. Statistically significant versus control: *$p < 0.001$

References

Ahmed, S., Tsuchiya, T., Nagahata-Ishiguro, M., Sawada, R., Banu, N., Nagira, T., 2009. Enhancing action by sulfated hyaluronan on connexin-26, -32, and -43 gene expressions during the culture of normal human astrocytes. J. Biomed. Mater Res. 90, 713-719.

Andrade-Rozental, A.F., Rozental, R., Hopperstad, M.G., Wu, J.K., Vrionis, F.D., Spray, D.C., 2000. Gap junctions: the "kiss of death" and the "kiss of life". Brain Res. Brain Res. Rev. 32, 308-315.

Baranova, A., Ivanov, D., Petrash, N., Pestova, A., Skoblov, M., Kelmanson, I., Shagin, D., Nazarenko, S., Geraymovych, E., Litvin, O., Tiunova, A., Born, T.L., Usman, N., Staroverov, D., Lukyanov, S., Panchin, Y., 2004. The mammalian pannexin family is homologous to the invertebrate innexin gap junction proteins. Genomics. 83, 706-716.

Bennett, MV., 2000. Seeing is relieving: electrical synapses between visualized neurons. Nat. Neurosci. Review. 3, 7-9.

Bennett MV, Garré JM, Orellana JA, Bukauskas FF, Nedergaard M, Sáez JC., 2012. Connexin and pannexin hemichannels in inflammatory responses of glia and neurons. Brain Res. http://dx.doi.org/10.1016/j.brainres.2012.08.042

Campisi, A., Caccamo, D., Li Volti, G., Currò, M., Parisi, G., Avola, R., Vanella, A., Ientile, R., 2004. Glutamate-evoked redox state alterations are involved in tissue transglutaminase upregulation in primary astrocyte cultures. 578, 80-4

Chen, C.J., Liao, S.L., Kuo, J.S., 2000. Gliotoxic action of glutamate on cultured astrocytes. J.Neurochem. 75, 1557-65

Conti, F., DeBiasi, S., Minelli, A., Melone, M., 1996. Expression of NR1 and NR2A/B subunits of the NMDA receptor in cortical astrocytes. Glia. 17, 254-258.

Cornell-Bell, A.H., Finkbeiner, S.M., Cooper, M.S., Smith, S.J., 1990. Glutamate induces calcium waves in cultured astrocytes: long-range glial signaling. Science. 247, 470-473.

Daginakatte, G.C., Gadzinski, A., Emnett, R.J., Stark J.L., Gonzales, E.R., Yan, P., Lee, J.M., Cross, A.H., Gutmann, D.H., 2007. Expression profiling identifies a molecular signature of reactive astrocytes stimulated by cyclic AMP or proinflammatory cytokines. Exp Neurol. 210, 261-267.

Eugenín, E.A., Eckardt, D., Theis, M., Willecke, K., Bennett, M.V., Saez, J.C., 2001. Microglia at brain stab wounds express connexin 43 and in vitro form functional gap junctions after treatment with interferon-gamma and tumor necrosis factor-alpha. Proc. Natl. Acad. Sci. USA 98, :4190-4195.

Faure, E., Thomas, L., Xu, H., Medvedev, A., Equils, O., Arditi, M., 2001. Bacterial lipopolysaccharide and IFN-gamma induce Toll-like receptor 2 and Toll-like receptor 4 expression in human endothelial cells: role of NF-kappa B activation. J Immunol. 166,2018-24

Figiel, M., Allritz, C., Lehmann, C., Engele, J., 2007. Gap junctional control of glial glutamate transporter expression. Mol. Cell. Neurosci. 35, 130-137.

Galarreta, M., Hestrin, S., 2001. Electrical synapses between GABA-releasing interneurons. Nat. Rev. Neurosci. 2, 425-433.

Garré JM, Retamal MA, Cassina P, Barbeito L, Bukauskas FF, Sáez JC, Bennett MV, Abudara V. 2010. FGF-1 induces ATP release from spinal astrocytes in culture and opens pannexin and connexin hemichannels. PNAS 107:22659-22664.

Gosejacob, D., Dublin, P., Bedner, P., Hüttmann, K., Zhang, J., Tress, O., Willecke, K., Pfrieger, F., Steinhäuser, C., 2011. Theis M. Role of astroglial connexin30 in hippocampal gap junction coupling. Glia. 59, 511-519.

Hinkerohe, D., Smikalla, D., Schoebel, A., Haghikia, A., Zoidl, G., Haase, C.G., Schlege, l.U., Faustmann, P.M., 2010. Dexamethasone prevents LPS-induced microglial activation and astroglial impairment in an experimental bacterial meningitis co-culture model.Brain Res. 1329, 45-54.

Hamby, M.E., Coppola, G., Ao, Y., Geschwind, D.H., Khakh, B.S., Sofroniew, M.V., 2012. Inflammatory mediators alter the astrocyte transcriptome and calcium signaling elicited by multiple g-protein-coupled receptors. J Neurosci. 32, 14489-14510.

Lalo, U., Pankratov, Y., Kirchhoff, F., North, R.A., Verkhratsky, A., 2006. NMDA receptors mediate neuron-to-glia signaling in mouse cortical astrocytes. J Neurosci. 26, 2673-2683.

Lee, M.C., Ting, K.K., Adams, S., Brew, B.J., Chung, R., Guillemin, G.J., 2010. Characterisation of the expression of NMDA receptors in human astrocytes. PLoS One. 5, 14123.

Lee, I.H., Lindqvist, E., Kiehn, O., Widenfalk, J., Olson, L., 2005. Glial and neuronal connexin expression patterns in the rat spinal cord during development and following injury. J Comp Neurol. 489, 1-10.

Li, C.Y., Chin, T.Y., Chueh, S.H., 2004. Rat cerebellar granule cells are protected from glutamate-induced excitotoxicity by S-nitrosoglutathione but not glutathione. Am. J. Physiol. Cell. Physiol. 286, 893-904.

Maeda, S., Tsukihara, T., 2010. Structure of the gap junction channel and its implications for its biological functions. Cell. Mol. Life Sci.

Martin, K., Viera, K., Petr, C., Marie, N., Eva, T., 2006. Simultaneous analysis of cytokines and co-stimulatory molecules concentrations by ELISA technique and of probabilities of measurable concentrations of interleukins IL-2, IL-4, IL-5, IL-6, CXCL8 (IL-8), IL-10, IL-13 occurring in plasma of healthy blood donors. Mediators Inflamm. 5 ,65237.

Matute, C., Alberdi, E., Ibarretxe, G., Sánchez-Gómez, M.V., 2002. Excitotoxicity in glial cells. Eur. J. Pharmacol. 447, 239-246.

Mosmann, T., 1983. Rapid colorimetric assay for cellular growth and survival: Application to proliferation and cytotoxicity assays. J. Immunol. Methods 65, 55-63.

Murakami, A., Matsumoto, K., Koshimizu, K., Ohigashi, H., 2003. Effects of selected food factors with chemopreventive properties on combined lipopolysaccharide- and interferon-gamma-induced IkappaB degradation in RAW264.7 macrophages. Cancer Lett. 195, 17-25.

Nagy, J.I., Patel, D., Ochalski, P.A., Stelmack, G.L., 1999. Connexin30 in rodent, cat and human brain: selective expression in gray matter astrocytes, co-localization with connexin43 at gap junctions and late developmental appearance.Neuroscience. 88, 447-468.

Nagy, J.I., Rash, J.E., 2000. Connexins and gap junctions of astrocytes and oligodendrocytes in the CNS. Brain Res Brain Res Rev. 32, 29-44.

Nakase ,T., Naus, C.C., 2004. Gap junctions and neurological disorders of the central nervous system. Biochim. Biophys. Acta. 1662, 149-158.

Orthmann-Murphy, J.L., Abrams, C.K., Scherer, S.S., 2008. Gap junctions couple astrocytes and oligodendrocytes. J. Mol. Neurosci. 35, 101-116.

Panchin, Y., Kelmanson, I., Matz, M., Lukyanov, K., Usman, N., Lukyanov, S., 2000. A ubiquitous family of putative gap junction molecules. Curr. Biol. 10, 473 -474.

Parenti, R., Cicirata, F., Zappalà, A., Catania, A., La Delia, F., Cicirata, V., Tress, O., Willecke, K., 2010. Dynamic expression of Cx47 in mouse brain development and in thecuprizone model of myelin plasticity. Glia. 58, 1594-1609.

Raetz, C.R., Whitfield, C., 2002. Lipopolysaccharide endotoxins. Annu Rev Biochem.71, 635-700.

Rash, J.E., Yasumura, T., Dudek, F.E., Nagy, J.I., 2001. Cell-specific expression of connexins and evidence of restricted gap junctional coupling between glial cells andbetween neurons. J. Neurosci. 21, 1983-2000.

Rash, J.E., Yasumura, T., Davidson, K.G., Furman, C.S., Dudek, F.E., Nagy, J.I., 2001. Identification of cells expressing Cx43, Cx30, Cx26, Cx32 and Cx36 in gap junctions of rat brain and spinal cord. Cell. Commun. Adhes. 8, 315-320.

Rouach, N., Avignone, E., Même, W., Koulakoff, A., Venance, L., Blomstrand, F., Giaume, C., 2002. Gap junctions and connexin expression in the normal and pathological centralnervous system. Biol. Cell. 94, 457-75.

Schipke, C.G., Ohlemeyer, C., Matyash, M., Nolte, C., Kettenmann, H., Kirchhoff, F., 2001. Astrocytes of the mouse neocortex express functional N-methyl-D-aspartate receptors. FASEB J. 15, 1270-1272.

Suto, N., Ikura, K., Sasaki, R., 1993. Expression induced by interleukin-6 of tissue-type transglutaminase in human hepatoblastoma HepG2 cells. J Biol Chem. 268, 7469-73.

Su, Z.Z., Leszczyniecka, M., Kang, D.C., Sarkar, D., Chao, W., Volsky, D.J., Fisher, P.B., 2003. Insights into glutamate transport regulation in human astrocytes: cloning of the promoter for excitatory amino acid transporter 2 (EAAT2). Proc Natl Acad Sci U S A. 100, 1955-1960.

Teismann, P., Schulz, J.B., 2004. Cellular pathology of Parkinson's disease: astrocytes, microglia and inflammation. Cell Tissue Res. 318, 149-161.

Thompson, R.J., Macvicar, B.A., 2008. Connexin and pannexin hemichannels of neurons and astrocytes. Channels (Austin). 2, 81-86.

Zhang, Q., Hu, B., Sun, S., Tong, E., 2003. Induction of increased intracellular calcium in astrocytes by glutamate through activating NMDA and AMPA receptors. J Huazhong Univ Sci Technolog Med Sci. 23, 254-257.

Zappalà, A., Li Volti, G., Serapide, M.F., Pellitteri, R., Falchi, M., La Delia, F., Cicirata, V., Cicirata, F., 2007. Expression of pannexin2 protein in healthy and ischemized brain of adult rats. Neuroscience. 148, 653-667.

Chapter 4

Effects of lithium treatment in the expression of Cx43, Cx30 and Cx26 by using both *in vitro* and *in vivo* models of Alzheimer's pathological conditions

Cicirata V. et al., *In Preparation*

Introduction

Alzheimer disease (AD), one of the most common neurodegenative disease, is characterized by a progressive deterioration of cognitive abilities, eventually leading to the individual's death. (Toledo et al.2010). The disease is due to widespread destruction of neurons (neuronal depopulation), casused by the deposition of beta-amyloid-42. This pathological form of beta amyloid tends to deposit in extracellular aggregates called senile plaques and, furthermore, triggers the hyperphosphorylation of Tau protein and then the alteration of its function. So we have two pathological events: 1) the deposition of beta amyloid which is deposited in plaques and 2) the hyperproduction of hyperphosphorylated tau protein that deforms the neurons and they assembled in "neurofibrillary tangles". A hallmark of neurodegenerative disease is the reactive gliosis characterized by a phenotypic change in astrocyte and microglia (Koulakoff et al. 2011). This glial response is associated with modifications in the expression and function of connexins (Cxs). Cxs are the molecular constituent of gap junctions, which are cluster of intracellular channels that allow the direct intercellular exchange of ions and small molecules (e.g. IP_3, ATP, glutamate and energy metabolites) between neighborig cells (Bruzzone et. Al 1996). Increased Cx expression is detected in most reactive astrocyte located at amyloid plaques and this data suggest that astrocyte connexin partecipate in the neurodegenerative process of Alzheimer's disease (ref.).

Lithium compounds are used in the treatment of various bipolar spectrum disorders, and have been shown to have neuroprotective effects against various insults (ref.). In particular It has been shown to inhibit glycogen-synthase kinase 3-beta (GSK3b), a key kinase for the phosphorylation of tau (ref.). Indeed, it is kniwn that lithium treatment in mice expressing the P301L human tau mutation reduceds hyperphosphorylated tau (Noble W, et al. 2005). Furthermore, literature data shows that the concentration and the time course of LiCl treatment may play an important role in regulating Cx43 expression and gap-junctional communication in skeletal myoblasts (Du et al.2012). The LiCl regulates Cx43 expression not mainly at transcriptional level but also via phosphorylated modification (Du et al.2012). Nevertheless, nothing is known about the modalities underlying the recruitment of the Cx in the neuroprotective effect of Lhitium. Thus, aim of the present study was to determine what impact the lithium chloride treatment would have in the expression of Cx43, Cx30 and Cx26 by using both *in vitro* and *in vivo* models of Alzheimer's pathological conditions.

Experiment were performed using an experimental model of amnesia induced by Aβ peptide (AB 1–42) administered intracerebroventricularly in mice. Animals were tested to assess the impact of lithium chloride in learning and memory process with different by using the passive avoidance test. Then, the expression of Cx43, Cx30 and Cx26 was evaluated in different brain areas. The effect of lithium treatment on the expression of Cx43, Cx30 and Cx26 was also evaluated in a model of primary human astroglial cell culture exposed at different cytotoxic stimuli (glutamate or LPS).

MATERIALS AND METHODS

2.1 Experimental procedures *in vitro*

2.1.1 Materials

Cryo-preserved human cortex astroglial cell lines, and astrocyte growth supplement (AGS) were purchased from Innoprot (Derio, Bizkaia, Spain). Heat Inactivated Foetal Bovine Serum (FBS), Eagle's Basal Medium (EBM), L-glutamine, antibiotics (penicillin-streptomycin) and 0.05% trypsin/EDTA 1X solution were from Invitrogen (Milan, Italy). Poly-L-lisine, glutamate, lypopolisaccaride (LPS), phenylmethylsulfonyl fluoride (PMSF), and other chemical reagents were obtained from Sigma (Milan, Italy). Glial Fibrillary Acidic Protein (GFAP) was from Chemicon (Prodotti Gianni, Milan, Italy). Bradford kit was from (Bio-Rad, Richmond, CA).

2.1.2 Cell cultures

Human cortex astrocytes were suspended in EBM, containing 10% FBS (vol/vol), 2 mM glutamine, streptomycin (50 µg/ml) and penicillin (50 U/ml) and AGS, plated at a density of $1x10^6$ cells/100 mm dish pretreated with 10 µg/ml poly-L-lysine. Cells were maintained at 37°C in a 5% CO2/95% air humidified atmosphere for two weeks and medium exchanged every two days. Some cultures, approximately 90% confluent, were incubated at 37°C for 5 min. with trypsin/EDTA solution (0.05%), and neutralized at room temperature with FBS (vol/vol 1:1). Cell suspension was then centrifuged at 200 x g for 5 min, suspended in the medium and plated at a density of $1x10^6$ cells/100 mm dish pretreated with 10 µg/ml poly-L-lysine, and maintained at 37°C in a 5% CO2/95% air humidified atmosphere for one week and medium exchanged every two days.

Astroglial cells purity was determined by immunofluorescence analysis with antibodies

against GFAP (specific for astrocytes) and CD68 (for microglia). More than 95% of the cells stained positive for GFAP while we did not detect any staining for CD68 (data not shown).

2.1.3 Treatments

Primary human astroglial cell cultures, approximately 90% confluent, were replated on to 16-mm diameter 10 μg/ml poly-L-lysine coated glass coverslips at a final density of $1x10^4$ cells/coverslip, and fed in fresh complete medium. We exposed astroglial cell cultures for 12, 24 or 48 h to glutamate (10, 50, 100 μM) , to LPS (1, 10, 100 μg/ml) and to LiCl (0.5, 1.0, 1.5, 10, 100 mM), in order to establish the optimal concentrations and their exposure times of stressors. Afterwards two groups of cells were treated with 1.5mM of lithium chloride and 30 minutes later we expose this pretreated cell cultures at different concentration of LPS and glutamate at cell cultures for 12, 24 or 48h. For this purpose, MTT test, morphological, and immunocytochemical characterization were utilized. These sets of experiments showed that a non-toxic concentration for the cells was 10 μM of glutamate, 1 μg/ml of LPS, 1.5mM of LiCl and the optimal exposure time was 24 h.

2.1.4 MTT Bioassay

To monitor cell viability, primary human astroglial cell cultures were set up 60x 10^4 cells/well of a 96-multiwell flat-bottomed 200-μl microplates (Mossman, 1983). Cells were incubated at 37°C in a humidified 5% CO_2–95% air mixture. At the end of treatment time, 20 μl MTT, 0.5%, in phosphate buffer saline were added to each multiwell. After 1 h of incubation with the reagent, the supernatant was removed and replaced with 200 μl dimethylsulfoxide. The optical density of each well sample was measured with a microplate spectrophotometer reader (Titertek Multiskan; Flow Laboratories, Helsinki, Finland) at 570 nm. The 24 h exposure of astroglial cell cultures to 10 μM glutamate or 1μg/ml LPS did not significantly affect cell function and viability, as revealed by MTT reduction assay, evaluating mitochondrial dehydrogenase activity

2.2 Experimental procedures *in vivo*

2.2.1 Animals

Swiss mice (40–50 g) were purchased from Charles River (Italy). For at least 1 week prior to the experiments, the animals were housed four per cage at a constant temperature of 21 °C, under a 12-h light/dark cycle (lights on between 8:00 and 20:00), with food and water ad libitum. All animals were sacrificed at the end of behavioral procedures. All behavioral tests took place in an experimental room with the same light–dark cycle and the environmental conditions, such as humidity and temperature levels inside the room, similar to those of the housing facility. All experiments were carried out according to the European Community Council Directive 86/609/EEC and efforts were made to minimize animal suffering and to reduce the number of animals used. Rationale, design and methods of this study were approved by the Ethical Committee for Animal Research, University of Catania.

2.2.1 Drugs and experimental amnesia

The lithium chloride was dissolved in bi-distilled water and administered intraperitoneally (i.p.) at different doses (50, 150, 300,600 and 1000 mg/kg) in a total volume of 0.1 ml/ 100 g body weight. The dose of lithium was selected based on results of previous experiments (Suddth et al.2012). The β-Amyloid 1–42 fragment (BAP 1–42, Sigma, USA) was prepared as stock solutions in sterile 0.1 M phosphate-buffered saline (pH 7.4). The proper volume was freshly prepared and used. Sterile 0.1 M phosphate-buffered saline was injected into control animals. The Aβ peptide 1–42 (400 pmol) was administered i.c.v. in mice using a microsyringe with a 28- gauge stainless-steel needle 3.0 mm long (Hamilton). In brief, the needle was inserted unilaterally 1 mm to the right of the midline point equidistant from each eye, at an equal distance between the eyes and the ears, and perpendicular to the plane of the skull (Maurice et al., 1996; Mazzola et al., 2003). The β-Amyloid peptide or the vehicle solution (2 µl/mouse) was delivered gradually within 3s. We have used only data obtained from mice exhibiting a correct insertion at histological examination. The lithium solution (50, 150-300- 600 and 1000 mg/kg) was administered i.p. for 11 days, starting on day 3 after BAP 1–42 **i**njection. On day 14, mice were submitted to the passive avoidance task.

2.2.2 Passive avoidance test

The apparatus for the step-through passive-avoidance test was an automated shuttle-box

(Cat. 7551 Passive Avoidance Controller and Cat. 7553 Passive Avoidance Mouse Cage, Basile, Italy), divided into an illuminated compartment and a dark compartment of the same size by a wall with a guillotine door. In the experimental session, each mouse was trained to adapt to the step-through passive avoidance apparatus (Venault et al., 1986). The animal was put into the illuminated compart- ment, facing away from the dark compartment. After 10 s, the door between these two boxes was opened and the mouse was allowed to move into the dark compartment freely. The latency to leave the illuminated compartment was recorded. Two hours after the adaptation trial, the mouse was again put into the illuminated compartment. The learning trial was similar to the adaptation trial except that the door was closed automatically as soon as the mouse stepped into the dark compartment and an inescapable foot-shock (0.2 mA, 2 s) was delivered through the grid floor. The retention of passive avoidance response was measured 1 and 7 days after the learning trial. Each animal was again put into the illuminated compartment and the latency to re-enter the dark compartment was recorded. No foot-shock was delivered while the retention test was performed. The maximum cut-off time for step-through latency was 300 s (Venault et al., 1986).

2.2.3. Plasma lithium concentration

Steady state concentrations of lithium were measured in separated groups of mice treated (n=5 per group) with the same dosage and for the same time as animals tested in the behavioral model of amnesia induced by the i.c.v. injection of AB 1-42 . Terminal blood collections were performed under full general anesthesia by cardiac puncture. Blood collections were performed 1h post the last lithium injection. Lithium plasmatic concentrations were measured by atomic spectrophotometry.

2.2.4 Real Time – PCR

Expression of Cx , 43, 30 and 26 will be detected in the PFC and Hippocampus of treated mice. These experiments are in progress.

3. Statistical analysis of data

Data were analyzed using one- or two-factor ANOVA for repeated measures and the post hoc Tukey's for multiple comparisons. A level of $P<0.05$ was considered as indicative of statistical significance.

4. Results

4.1. Lithium cloride protects primary human astroglial cell cultures from cytotoxic effects induced by glutamate or LPS

Primary human astroglial cell culture were used to assess the cytoprotective role of lithium chloride after the exposure to glutamate or LPS. In preliminary experiments, in the basis of both observations through fluorescent microscope and MTT assay, we estabilished the concentration of lithium chloride, glutamate or LPS, which didn't produce toxic effect and the optimal time of their exposure. No significant changes in cell viability was found in culture exposed to glutamate for 12h, 24h or 48h in the range of concentration between 1 and 10μM (Table 1); As well as no toxic effect was showed in cell culture exposed to LPS for 12h, 24h or 48h in the range of concentration between 0,5 and 1,5 μg/ml, when compared with the respective controls (Table 2). As shown in Table 1 and 2, we found that higher concentrations of Glutamate (100μM) or LPS (100μg/ml) produced significantly toxic effects for all exposure times. The exposure of cultures to 10μM glutamate or 1μg/ml LPS in absence or in presence of LiCl don't induce LDH release both in untreated and treated Lithium Chloride for 24h, demonstrating that the stressors didn't cause necrotic cell death.

4.2. Effects of lithium chloride on passive avoidance response of mice subjected to amnesia induced by AB-1-42

As shown in Fig. 1, the i.c.v. injection of BAP 1–42 (400 pmol/ mouse) 14 days prior to the learning trial induced a reduction of latency to re-enter the dark box in comparison to i.c.v. injection of the vehicle alone (control vs. BAP vehicle-treated group). This effect was observed in both retention tests, made 1 ($P < 0.001$) and 7 ($P < 0.001$) days after the learning trial. Repeated administration of the LiCl solution both at 150 mg/kg/day and 300 mg/kg/day for 11 days prior to the learning trial, inhibited the amnesic effect of BAP 1–42 by increasing the latency to re-enter the dark box in the first (150 mg/kg, $P < 0.01$; 300 mg/kg, $P < 0.01$) and second (150 mg/kg, $P < 0.01$; 300 mg/kg, $P < 0.01$) retention test. The repeated administration of the LiCl solution at 50 mg/kg/day for 11 days prior to the learning trial did not inhibit the amnesic effect of

BAP 1–42 both in the first (P = NS) and second (P = NS) retention test. The LiCl solution injected at both 600 mg/kg /day and 1000 mg/kg/day induced the death of treated animal few hours later. The injection of lithium cloride per se at the doses of 50, 150 and 300 mg/kg did not improve the memory capacity of control mice in the passive avoidance paradigm (data not shown).

4.3. Plasma concentration of lithium injected at the doses of 50, 150 and 300 mg/kg after 11 days period of treatmnent

Fig.2 shows the plasma concentrations of lithium (50, 150 and 300 mg/kg) measured in separated groups of mice (n=5 per group) treated intraperitoneally for 11 days . The mean of the plasma concentration of lithium 1 h after the last lithium injection at the dose of 50 mg/kg/day was 0.40 mequiv. L^{-1}. After 11 days of 150 mg/kg lithium the mean of the plasma concentration was 0.70 mequiv. L^{-1}. Finally, the mean of the plasma concentration levels at 300 mg/kg/day lithium was 1.40 mequiv. L^{-1}. Since, the therapeutic plasmatic concentrations are in the range of 0.2–1.5 mequiv. L^{-1} (Schou, 1976), our results were below toxic concentrations and in the range of therapeutic concentration.

4.4. Expression of Cx43, Cx30 and Cx26 in the PFC and Hippocampus of mice subjected to amnesia induced by AB 1-42.

These experiments are in progress.

Tables and Figures

Table 1

	% of cell viability		
Treatment	12 h	24 h	48 h
control	100 ± 2	99 ± 1	99 ± 1
+ 0.5 mM Lithium chloride	100 ± 1	100 ± 2	100 ± 3
+ 1.0 mM Lithium chloride	100 ± 1	100 ± 4	100 ± 4
+ 1.5 mM Lithium chloride	100 ± 3	100 ± 5	100 ± 4
+ 10 mM Lithium chloride	88.45 ± 1	81± 3*	78.63 ± 4
+ 100 mM Lithium chloride	18.03 ± 1*	13± 5	11.90 ± 3
+ 10 µM glutamate	97.89 ± 4	97± 3	96.5 ± 5
+ 10 µM glutamate + 0.5 mM Lithium chloride	98.67 ± 2	98 ± 3	97.78 ± 4
+ 10 µM glutamate + 1.0 mM Lithium chloride	99.24 ± 5	98.9± 2	98.37 ± 3
+ 10 µM glutamate + 1.5 mM Lithium chloride	99.99 ± 1	99± 3	98.92 ± 2
+ 10 µM glutamate + 10 mM Lithium chloride	45.02± 1	41 ± 3	38.7± 2
+ 10 µM glutamate + 100 mM Lithium chloride	0.0 ± 1	0.01 ± 3	0.0 ± 2

Tab. 1. Cell viability in human astroglial cell cultures untreated or lithium treated unexposed or exposed to 10 µM glutamate for 12, 24 or 48 h. Values are mean ± S.D. of four experiments in duplicate. * Statistically significant versus control $p<0.001$.

Table 2

	% of cell viability		
Treatment	12 h	24 h	48 h
control	100 ± 2	100 ± 1	100 ± 1
+ 0.5 mM Lithium chloride	100 ± 1	100 ± 2	100 ± 3
+ 1.0 mM Lithium chloride	100 ± 1	100 ± 4	100 ± 4
+ 1.5 mM Lithium chloride	100 ± 3	100± 5	100 ± 4
+ 10 mM Lithium chloride	88.45 ± 1	81 ± 3	78.63 ± 4
+ 100 mM Lithium chloride	18.03 ± 1	13± 5	11.90 ± 3
+ 1 µg/ml LPS	97.89 ± 4	97± 3	96.87 ± 5
+ 1 µg/ml LPS + 0.5 mM Lithium chloride	98.67 ± 2	98 ± 1	98.78 ± 4
+ 1 µg/ml LPS + 1.0 mM Lithium chloride	99.24 ± 5	99.1 ± 2	98.37 ± 3
+ 1 µg/ml LPS + 1.5 mM Lithium chloride	99.99 ± 1	100± 3	98.92 ± 2
+ 1 µg/ml LPS + 10 mM Lithium chloride	52.99 ± 1	50 ± 3	47.92 ± 2
+ 1 µg/ml LPS + 100 mM Lithium chloride	0.0 ± 1	0.01 ± 3	0.0 ± 2

Tab. 2. Cell viability in human astroglial cell cultures untreated or lithium treated unexposed or exposed to 1 µg/ml LPS for 12, 24 or 48 h. Values are mean ± S.D. of four experiments in duplicate. * Statistically significant versus control $p<0.001$.

Figure 1

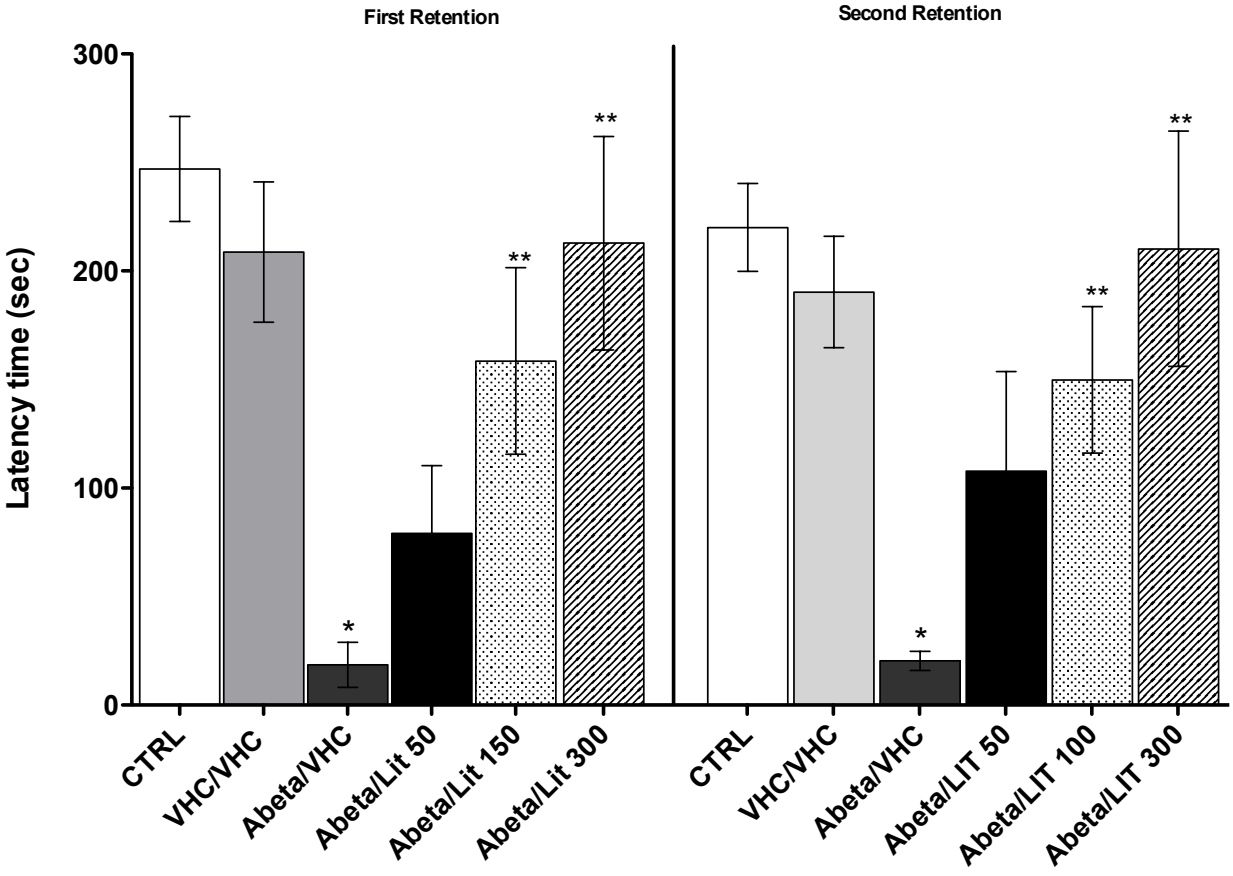

Fig.1 Effects of repeated treatment (11 days) with lithium on passive-avoidance response of mice subjected to amnesia induced by Abeta 1-42. Values are means ± S.E.M. *P < 0.001 vs. VHC/VHC; ** P < 0.01 vs. BAP/VHC.

Figure 2

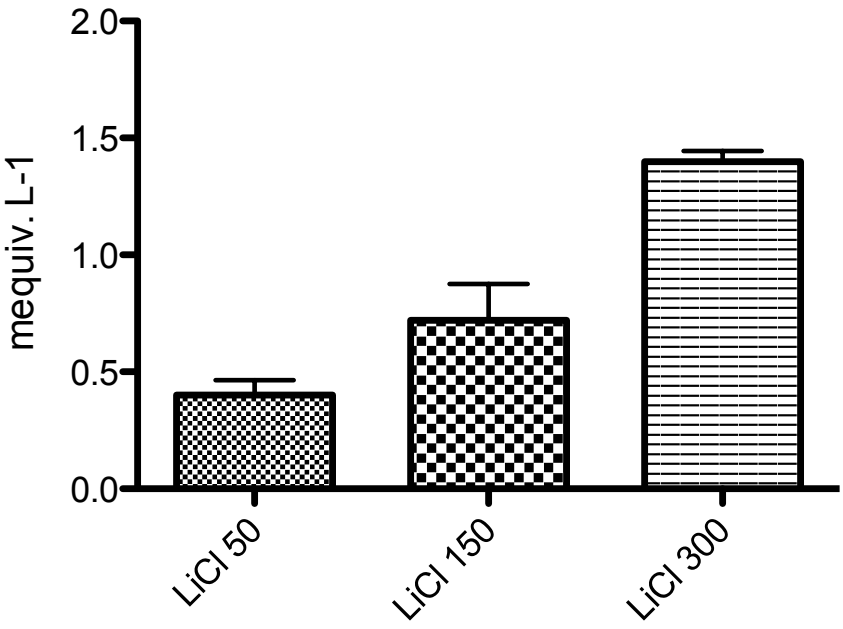

Fig. 2 Plasma concentrations of lithium 50, 150 and 300 mg/kg measured in separated groups of mice (n=5 per group) treated intraperitoneally for 11 days. Values are means ± S.E.M.

REFERENCES

Toledo EM and Inestrosa NC. Activation of Wnt signaling by lithium and rosiglitazone reduced spatial memory impairment and neurodegeneration in brains of an APPswe/PSEN1DE9 mouse model of Alzheimer's disease. Molecular Psychiatry (2010) 15, 272–285

Koulakoff A., Mei X., Orellana J.A., Sáez J.C., Giaume C. Review Glial connexin expression and function in the context of Alzheimer's disease. Biochimica et Biophysica Acta 1818 (2012) 2048–2057.

Bruzzone, R., White, T.W., Paul, D.L., 1996. Connections with connexins: the molecular basis of direct intercellular signal- ing. Eur. J. Biochem. 238, 1–27

Noble W, Planel E, Zehr C, Olm V, Meyerson J, Suleman F, et al. (2005). Inhibi- tion of glycogen synthase kinase-3 by lithium correlates with reduced tauopathy and degeneration in vivo. Proc Natl Acad Sci U S A 102: 6990–6995.

Sudduth T.L., Wilson J.G., Everhart A., Colton C. A., Wilcock D.M. Lithium Treatment of APPSwDI/NOS22/2 Mice Leads to Reduced Hyperphosphorylated Tau, Increased Amyloid Deposition and Altered Inflammatory Phenotype. PLoS ONE 7(2): e31993. doi:10.1371/journal.pone.0031993.

DU W.J., LI J.K., WANG Q. Y., HOU J. B., YU B.1. Lithium Chloride Regulates Connexin43 in Skeletal Myoblasts In Vitro: Possible Involvement in Wnt/b-Catenin Signaling. Cell Communication and Adhesion, 15: 261□271, 2008

Maurice, T., Lockhart, B.P., Privat, A., 1996. Amnesia induced in mice by centrally administered beta-amyloid peptides involves cholinergic dysfunction. Brain Res. 706, 181-193.

Mazzola, C., Micale, V., Drago, F., 2003. Amnesia induced by β-amyloid fragments is counteracted by cannabinoid CB1 receptor blockade. Eur. J. Pharmacol. 477, 219–225.

Venault, P., Chapouthier, G., de Carvalho, L.P., Simiand, J., Morre, M., Dodd, R.H., Rossier, J., 1986. Benzodiazepine impairs and beta-carboline enhances performance in learning and memory tasks. Nature 321, 864–866

General Discussion and Conclusion

A common feature of several CNS diseases is the phenotypic transformation of glial cells, that are engaged in the activation process resulting, in reactive gliosis. In most of these pathologies, in situ studies have established that this glial response is associated with a change in Cx expression.

Table 1

Pathology	Experimental models		Connexin expression	Gap junction coupling (GJC) / Hemichannel activation (HCA)
Alzheimer disease	*In vivo*	Human PM biopsies	⬀ Cx43 IR at Aβ plaques [94]	NT
		APP/PS1 mice	⬀ Cx43, Cx30 IR at Aβ plaques[95, 110]	HCA astrocytes at plaques [110]
		PDAPP mice	NT	GJC ⬀ cortex [83] GJC no change Hip[83] GJC no change Hip[100]
		PDGFAPPSwInd	NT	GJC no change [26]
	In vitro	Aβ -treated astrocytes	No change Cx43[22, 26]	GJC ⬂ [100]
		Aβ-treated microglia	⬀ Cx43[22]	HCA[22]
		Aβ-treated Hip slices	NT	HCA astrocytes and microglia [22]
Parkinson disease		MPTP mice	⬀ Cx43 striatum [123]	GJC no change [123]
		Rotenone rat	⬀ Cx43 basal ganglia [124]	
Huntington disease		Post-mortem human biopsies	⬀ Cx43 caudate nucleus,no change globus pallidus [124, 125]	NT
Multiple sclerosis		EAE mouse	⬂ Cx43 in inflamed WM [126]	NT
		EAE guinea pig	⬂ Cx43 demyelinated WM [127] ⬀ Cx43 remyelinating WM [127]	NT

IR: immunoreactivity; NT: not tested; Hip: hippocampus; EAE: experimental autoimmune encephalomyelitis; MPTP: 1-methyl-4-phenyl-1,2,3,6-tetrahydropyridine; PM post-mortem; WM: white matter.

Table 1:(Image adapted from Koulakoff A. et al. 2012)

The function of gap junctions and the different expression of the connexins have been well studied in the CNS. Neuronal gap junctions may play an important role in the regulation of the

periodic synchronized activity between neurons. Astrocytes exchange ions and metabolic substrates, such as inositol 1,4,5-triphosphate and ATP, through gap junctions. Gap junctions of oligodendrocytes play a critical role in maintaining normal myelination. Recent studies have described that macrophages may influence the expression of astrocytic gap junctions and that activated microglia may communicate with each other through gap junctions. Passing to our model, we have not direct evidences of the nature of the signalling molecules carried along the gap junction channels. Nevertheless, we find that the levels of the expression pattern of the Cx26 and Cx30 at increasing doses of glutamate can suggests the nature of the messages. The lower levels of expression at the higher level of injury (glutamate 100 μM) can be interpreted as a protective strategy to reduce the number of gap junction channels and thus to decrease the spread of noxious signaling molecules from injured cells to surrounding ones. In the same way, the strong over-expression of the Cx26 and Cx30 at the lower levels of injury (glutamate 10 μM) can be interpreted as a strategy to increase the spread of "positive" signaling molecules to the net of connected cells. In this hypothesis the gap junction channels formed in our models are either kiss-of-life or kiss-of-death in relation to the grade of injury. In the Cuprizone model of mielin plasticity, in wt animals Cx47 was slightly expressed in myelin and absent in astrocytes. Under cuprizone treatment it was over-expressed in myelin during the early affected stage; transiently expressed in astrocytes during severe injury (when demyelination occurred) and once more expressed by newly-formed myelin during the recovery process. Therefore, de novo expression of Cx47 in astrocytes in demyelinated areas and in close regions, apparently vicariated the no- expression of Cx47 due to loss of myelin.

From this consideration the question arises of the role played by Cx47. Some hypotheses can be proposed. This study shows that the increment of Cx47 occurred alongside anatomical injury. In light of the severe functional defects shown by cuprizone administration, it is likely that protective factors are delivered locally to prevent severe and not more reversible occurrence of injuries. The anatomical segregation of Cx47 in the demyelinated area, suggests that it could be involved in the neuron protective function. A further hypothesis focused on the transient expression of Cx47 in astrocytes. In fact, previous studies have shown that astrocytes are involved in delivery of factors promoting remyelination [239, 240]. Since in these experiments Cx47 was expressed in astrocytes principally located inside the demyelinated area, it is possible that Cx47 may be involved in a network of astrocytes which actively promote the release of factors supporting remyelination. In neurodegenerative diseases as Alzheimer disease, it is also important to evaluate the inflammatory response because exhibit inflammation in the lesion. Indeed, antinflammatory drugs may reduce the incidence of AD and delay the progression of the disease. As mentioned previously, activated microglia express gap junctions composed of Cx43. Moreover, activated macrophages decreased the expression of astrocytic gap junctions. Therefore, further investigation of the possible gap junctional

neuroprotective role of glial cells and inflammatory cells in neurodegenerative diseases is warranted. It is important to be able to understand the gap junctional network in the entire neuronal system in the pathological condition. Then, the regulation of gap junctions in the nervous system may contribute to the development of new therapies for neurological diseases. The question is, obviously, of utmost interest. Two opposite point of view have been proposed for the gap junction communication system: or the gap junction channels carry signalling molecules that sustain injured cells to overcome the lesions (this role of the GJ channels has been imaginatively defined as "kiss-of-life"; [241]), or they carry signalling molecules that spread the injury from the affected cells to the other to whom they are connected (and in this case they were defined as "kiss-of-death"; [241]). Further investigation must be done to to answer to all these questions.

REFERENCES

1. Panchin, Y., Kelmanson, I., Matz, M., Lukyanov, K., Usman, N., Lukyanov, S., 2000. A ubiquitous family of putative gap junction molecules. Curr. Biol. 10, 473 -474 .

2. Baranova, A., Ivanov, D., Petrash, N., Pestova, A., Skoblov, M., Kelmanson, I., Shagin, D., Nazarenko, S., Geraymovych, E., Litvin, O., Tiunova, A., Born, T.L., Usman, N., Staroverov, D., Lukyanov, S., Panchin, Y., 2004. The mammalian pannexin family is homologous to the invertebrate innexin gap junction proteins. Genomics. 83, 706-716.

3. Nestler, E.J., Molecular basis of long-term plasticity underlying addiction. Nat Rev Neurosci, 2001. 2(2): p. 119-28.

4. Scemes, E., D.C. Spray, and P. Meda, Connexins, pannexins, innexins: novel roles of "hemi-channels". Pflugers Arch, 2009. 457(6): p. 1207-26.

5. Maeda, S., Tsukihara, T., 2010. Structure of the gap junction channel and its implications for its biological functions. Cell. Mol. Life Sci

6. Eugenín, E.A., Eckardt, D., Theis, M., Willecke, K., Bennett, M.V., Saez, J.C., 2001. Microglia at brain stab wounds express connexin 43 and in vitro form functional gap junctions after treatment with interferon-gamma and tumor necrosis factor-alpha. Proc. Natl. Acad. Sci. USA 98, :4190-4195.

7. Rouach, N., Avignone, E., Même, W., Koulakoff, A., Venance, L., Blomstrand, F., Giaume, C., 2002. Gap junctions and connexin expression in the normal and pathological centralnervous system. Biol. Cell. 94, 457-75.

8. Willecke, K., et al., Structural and functional diversity of connexin genes in the mouse and human genome. Biol Chem, 2002. 383(5): p. 725-37.

9. Phelan, P., Innexins: members of an evolutionarily conserved family of gap-junction proteins. Biochim Biophys Acta, 2005. 1711(2): p. 225-45.

10. Kumar, N.M. and N.B. Gilula, The gap junction communication channel. Cell, 1996. 84(3): p. 381-8.
11. Yeager, M., V.M. Unger, and M.M. Falk, Synthesis, assembly and structure of gap junction intercellular channels. Curr Opin Struct Biol, 1998. 8(4): p. 517-24.

12. Grahame, N.J. and C.L. Cunningham, Intravenous self-administration of ethanol in mice. Curr Protoc Neurosci, 2002. Chapter 9: p. Unit 9 11

13. Sohl, G. and K. Willecke, Gap junctions and the connexin protein family. Cardiovasc Res, 2004. 62(2): p. 228-32.

14. Unger, V.M., et al., Three-dimensional structure of a recombinant gap junction membrane channel. Science, 1999. 283(5405): p. 1176-80.
15. Elenes, S., et al., Heterotypic docking of Cx43 and Cx45 connexons blocks fast voltage gating of Cx43. Biophys J, 2001. 81(3): p. 1406-18.

16. Boassa, D., et al., Pannexin1 channels contain a glycosylation site that targets the hexamer to the plasma membrane. J Biol Chem, 2007. 282(43): p. 31733-43.

17. Falk, M.M., et al., Cell-free synthesis and assembly of connexins into functional gap junction membrane channels. EMBO J, 1997. 16(10): p. 2703-16.

18. Harris, A.L., Connexin channel permeability to cytoplasmic molecules. Prog Biophys Mol Biol, 2007. 94(1-2): p. 120-43.

19. Rackauskas, M., et al., Gating properties of heterotypic gap junction channels formed of connexins 40, 43, and 45. Biophys J, 2007. 92(6): p. 1952-65.

20. Gaietta, G., et al., Multicolor and electron microscopic imaging of connexin trafficking. Science, 2002. 296(5567): p. 503-7.

21. Laird, D.W., Life cycle of connexins in health and disease. Biochem J, 2006. 394(Pt 3): p. 527-43.

22. Lauf, U., et al., Dynamic trafficking and delivery of connexons to the plasma membrane and accretion to gap junctions in living cells. Proc Natl Acad Sci U S A, 2002. 99(16): p. 10446-51.

23. Falk, M.M., et al., Gap junction turnover is achieved by the internalization of small endocytic double-membrane vesicles. Mol Biol Cell, 2009. 20(14): p. 3342-52.

24. Kjenseth, A., et al., Regulation of gap junction intercellular communication by the ubiquitin system. Cell Signal, 2010. 22(9): p. 1267-73.

25. Jordan, K., et al., The origin of annular junctions: a mechanism of gap junction internalization. J Cell Sci, 2001. 114(Pt 4): p. 763-73.

26. Dobrowolski, R. and K. Willecke, Connexin-caused genetic diseases and corresponding mouse models. Antioxid Redox Signal, 2009. 11(2): p. 283-95.

27. Firouzi, M., et al., Polymorphisms in human connexin40 gene promoter are associated with increased risk of hypertension in men. J Hypertens, 2006. 24(2): p. 325-30.

28. Gerido, D.A. and T.W. White, Connexin disorders of the ear, skin, and lens. Biochim Biophys Acta, 2004. 1662(1-2): p. 159-70.

29. Simon, A.M. and D.A. Goodenough, Diverse functions of vertebrate gap junctions. Trends Cell Biol, 1998. 8(12): p. 477-83.

30. White, T.W. and D.L. Paul, Genetic diseases and gene knockouts reveal diverse connexin functions. Annu Rev Physiol, 1999. 61: p. 283-310.

31. Bosco, D., J.A. Haefliger, and P. Meda, Connexins: key mediators of endocrine function. Physiol Rev, 2011. 91(4): p. 1393-445.

32. Ebihara, L., Physiology and biophysics of hemi-gap-junctional channels expressed in Xenopus oocytes. Acta Physiol Scand, 2003. 179(1): p. 5-8.

33. Goodenough, D.A. and D.L. Paul, Beyond the gap: functions of unpaired connexon channels. Nat Rev Mol Cell Biol, 2003. 4(4): p. 285-94.

34. Kar, R., et al., Biological role of connexin intercellular channels and hemichannels. Arch Biochem Biophys, 2012. 524(1): p. 2-15.

35. Goldberg, G.S., P.D. Lampe, and B.J. Nicholson, Selective transfer of endogenous metabolites through gap junctions composed of different connexins. Nat Cell Biol, 1999. 1(7): p. 457-9.

36. Valiunas, V., E.C. Beyer, and P.R. Brink, Cardiac gap junction channels show quantitative differences in selectivity. Circ Res, 2002. 91(2): p. 104-11.

37. Weber, P.A., et al., The permeability of gap junction channels to probes of different size is dependent on connexin composition and permeant-pore affinities. Biophys J, 2004. 87(2): p. 958-73.

38. Maeda, S. and T. Tsukihara, Structure of the gap junction channel and its implications for its biological functions. Cell Mol Life Sci, 2011. 68(7): p. 1115-29.

39. Gonzalez, D., J.M. Gomez-Hernandez, and L.C. Barrio, Molecular basis of voltage dependence of connexin channels: an integrative appraisal. Prog Biophys Mol Biol, 2007. 94(1-2): p. 66-106.

40. Revilla, A., M.V. Bennett, and L.C. Barrio, Molecular determinants of membrane potential dependence in vertebrate gap junction channels. Proc Natl Acad Sci U S A, 2000. 97(26): p. 14760-5.

41. Bukauskas, F.F. and V.K. Verselis, Gap junction channel gating. Biochim Biophys Acta, 2004. 1662(1-2): p. 42-60.

42. Verselis, V.K., C.S. Ginter, and T.A. Bargiello, Opposite voltage gating polarities of two closely related connexins. Nature, 1994. 368(6469): p. 348-51.
43. Musa, H., et al., Amino terminal glutamate residues confer spermine sensitivity and affect voltage gating and channel conductance of rat connexin40 gap junctions. J Physiol, 2004. 557(Pt 3): p. 863-78.
44. Neyton, J. and A. Trautmann, Physiological modulation of gap junction permeability. J Exp Biol, 1986. 124: p. 993-114.
45. Peracchia, C., Chemical gating of gap junction channels; roles of calcium, pH and calmodulin. Biochim Biophys Acta, 2004. 1662(1-2): p. 61-80.
46. Gonzalez-Nieto, D., et al., Regulation of neuronal connexin-36 channels by pH. Proc Natl Acad Sci U S A, 2008. 105(44): p. 17169-74.
47. Harris, A.L., Emerging issues of connexin channels: biophysics fills the gap. Q Rev Biophys, 2001. 34(3): p. 325-472.
48. Trexler, E.B., et al., Rapid and direct effects of pH on connexins revealed by the connexin46 hemichannel preparation. J Gen Physiol, 1999. 113(5): p. 721-42.
49. Moreno, A.P. and A.F. Lau, Gap junction channel gating modulated through protein phosphorylation. Prog Biophys Mol Biol, 2007. 94(1-2): p. 107-19.
50. Saez, J.C., et al., Regulation of gap junctions by protein phosphorylation. Braz J Med Biol Res, 1998. 31(5): p. 593-600.
51. Shah, M.M., A.M. Martinez, and W.H. Fletcher, The connexin43 gap junction protein is phosphorylated by protein kinase A and protein kinase C: in vivo and in vitro studies. Mol Cell Biochem, 2002. 238(1-2): p. 57-68.
52. Solan, J.L. and P.D. Lampe, Connexin phosphorylation as a regulatory event linked to gap junction channel assembly. Biochim Biophys Acta, 2005. 1711(2): p. 154-63.
53. Leithe, E. and E. Rivedal, Ubiquitination of gap junction proteins. J Membr Biol, 2007. 217(1-3): p. 43-51.
54. Su, V. and A.F. Lau, Ubiquitination, intracellular trafficking, and degradation of connexins. Arch Biochem Biophys, 2012. 524(1): p. 16-22.
55. Kjenseth, A., et al., The gap junction channel protein connexin 43 is covalently modified and regulated by SUMOylation. J Biol Chem, 2012. 287(19): p. 15851-61.
56. Juszczak, G.R. and A.H. Swiergiel, Properties of gap junction blockers and their behavioural, cognitive and electrophysiological effects: animal and human studies. Prog Neuropsychopharmacol Biol Psychiatry, 2009. 33(2): p. 181-98.
57. Kim, S.K., et al., Natural killer activity and antibody-dependent cellular cytotoxicity in patients with primary lung cancer. Yonsei Med J, 1992. 33(1): p. 41-7.

58. Panchin, Y., et al., A ubiquitous family of putative gap junction molecules. Curr Biol, 2000. 10(13): p. R473-4.
59. Baranova, A., et al., The mammalian pannexin family is homologous to the invertebrate innexin gap junction proteins. Genomics, 2004. 83(4): p. 706-16.
60. Panchin, Y.V., Evolution of gap junction proteins--the pannexin alternative. J Exp Biol, 2005. 208(Pt 8): p. 1415-9.
61. Bruzzone, R., et al., Pharmacological properties of homomeric and heteromeric pannexin hemichannels expressed in Xenopus oocytes. J Neurochem, 2005. 92(5): p. 1033-43.
62. Ambrosi, C., et al., Pannexin1 and Pannexin2 channels show quaternary similarities to connexons and different oligomerization numbers from each other. J Biol Chem, 2010. 285(32): p. 24420-31.
63. Locovei, S., J. Wang, and G. Dahl, Activation of pannexin 1 channels by ATP through P2Y receptors and by cytoplasmic calcium. FEBS Lett, 2006. 580(1): p. 239-44.
64. Charles, A.C., et al., Intercellular calcium signaling via gap junctions in glioma cells. J Cell Biol, 1992. 118(1): p. 195-201.
65. Boitano, S., E.R. Dirksen, and M.J. Sanderson, Intercellular propagation of calcium waves mediated by inositol trisphosphate. Science, 1992. 258(5080): p. 292-5.
66. Dietrich, H.H., et al., Red blood cell regulation of microvascular tone through adenosine triphosphate. Am J Physiol Heart Circ Physiol, 2000. 278(4): p. H1294-8.

67. Harrington, L.S. and J.A. Mitchell, Novel role for P2X receptor activation in endothelium-dependent vasodilation. Br J Pharmacol, 2004. 143(5): p. 611-7.
68. Locovei, S., L. Bao, and G. Dahl, Pannexin 1 in erythrocytes: function without a gap. Proc Natl Acad Sci U S A, 2006. 103(20): p. 7655-9.
69. Takeuchi, H., et al., Tumor necrosis factor-alpha induces neurotoxicity via glutamate release from hemichannels of activated microglia in an autocrine manner. J Biol Chem, 2006. 281(30): p. 21362-8.
70. Orellana, J.A., et al., Modulation of brain hemichannels and gap junction channels by pro-inflammatory agents and their possible role in neurodegeneration. Antioxid Redox Signal, 2009. 11(2): p. 369-99.
71. Ray, A., et al., Site-specific and developmental expression of pannexin1 in the mouse nervous system. Eur J Neurosci, 2005. 21(12): p. 3277-90.
72. Vogt, A., S.G. Hormuzdi, and H. Monyer, Pannexin1 and Pannexin2 expression in the developing and mature rat brain. Brain Res Mol Brain Res, 2005. 141(1): p. 113-20.
73. Bruzzone, R., et al., Pannexins, a family of gap junction proteins expressed in brain. Proc Natl Acad Sci U S A, 2003. 100(23): p. 13644-9.

74. Huang, Y., et al., Pannexin1 is expressed by neurons and glia but does not form functional gap junctions. Glia, 2007. 55(1): p. 46-56.
75. Zappala, A., et al., Expression of pannexin1 in the CNS of adult mouse: cellular localization and effect of 4-aminopyridine-induced seizures. Neuroscience, 2006. 141(1): p. 167-78.
76. Zoidl, G., et al., Localization of the pannexin1 protein at postsynaptic sites in the cerebral cortex and hippocampus. Neuroscience, 2007. 146(1): p. 9-16.
77. Zappala, A., et al., Expression of pannexin2 protein in healthy and ischemized brain of adult rats. Neuroscience, 2007. 148(3): p. 653-67.
78. 216. Pakhotin, P. and A. Verkhratsky, Electrical synapses between Bergmann glial cells and Purkinje neurones in rat cerebellar slices. Mol Cell Neurosci, 2005. 28(1): p. 79-84.
79. Boassa, D., et al., Trafficking dynamics of glycosylated pannexin 1 proteins. Cell Commun Adhes, 2008. 15(1): p. 119-32.
80. Barbe, M.T., H. Monyer, and R. Bruzzone, Cell-cell communication beyond connexins: the pannexin channels. Physiology (Bethesda), 2006. 21: p. 103-14.
81. Bunse, S., et al., The potassium channel subunit Kvbeta3 interacts with pannexin 1 and attenuates its sensitivity to changes in redox potentials. FEBS J, 2009. 276(21): p. 6258-70.
82. C.P. Taylor, F.E. Dudek, A physiological test for electrotonic cou- pling between CA1 pyramidal cells in rat hippocampal slices, Brain Res. 235 (1982) 351 – 357.
83. M.J.Christie, J.T. Williams, R.A. North, Electrical coupling synchronizes subthreshold activity in locus coeruleus neurons in vitro from neonatal rats, J. Neurosci. 9 (1989) 3584 – 3589
84. Y. Bouskila, F.E. Dudek, Neuronal synchronization without calcium- dependent synaptic transmission in the hypothalamus, Proc. Natl. Acad.Sci.U. S.A.90 (1993) 3207 – 3210.
85. R.O.L. Wong, A. Chernjavsky, S.J. Smith, C.J. Shatz, Early func- tional neural networks in the developing retina, Nature 374 (1995) 716 – 718.
86. B.W. Connors, L.S. Benardo, D.A. Prince, Coupling between neu- rons of the developing rat neocortex, J. Neurosci. 3 (1983) 773 – 782.
87. J.J. Lo Turco, A.R. Kriegstein, Clusters of coupled neuroblasts in embryonic neocortex, Science 252 (1991) 563 – 566.
88. R. Yuste, A. Peinado, L.C. Katz, Neuronal domains in developing neocortex, Science 257 (1992) 665 – 669.
89. A. Peinado, R. Yuste, L.C. Katz, Extensive dye coupling between rat neocortical neurons during the period of circuit formation, Neuron10(1993)103 – 114.

90. K.S. Bittman, J.J. Lo Turco, Differential regulation of connexin 26 and 43 in murine neocortical precursors, Cereb. Cortex 9 (1999) 188 – 195.
91. K. Bittman, D.F. Owens, A.R. Kriegstein, J.J. Lo Turco, Cell coupling and uncoupling in the ventricular zone of developing neocortex, J.Neurosci.17(1997) 7037 – 7044.
92. A. Peinado, R. Yuste, L.C. Katz, Gap junctional communication and the development of local circuits in neocortex, Cereb. Cortex 3 (1993)488 – 498.
93. S. Fushiki, C. Kinoshita, in: Y. Kanno, K. Kataoka, Y. Shiba, Y. Shimazu, T. Shimazu (Eds.), Prog. Cell Res. 4: Intercellular Com- munication Through Gap Junctions, Elsevier, Amsterdam, 1995, pp.239 – 243.
94. J.E. Rash, T. Yasumura, K.G. Davidson, C.S. Furman, F.E. Dudek, J.I. Nagy, Identification of cells expressing Cx43, Cx30, Cx26, Cx32 and Cx36 in gap junctions of rat brain and spinal cord, Cell Com- mun.Adhes.8(2001)315 – 320.
95. J.E. Rash, T. Yasumura, F.E. Dudek, J.I. Nagy, Cell-specific expres- sion of connexins and evidence of restricted gap junctional coupling between glial cells and between neurons, J. Neurosci. 21 (2001) 1983 – 2000.
96. B. Nadarajah, A.M. Jones, W.H. Evans, J.G. Parnavelas, Differential expression of connexins during neocortical development and neuro- nal circuit formation,J.Neurosci. 17 (1997) 3096 – 3111.
97. G. Sohl, J. Degen, B. Teubner, K. Willecke, The murine gap junction gene connexin36 is highly expressed in mouse retina and regulated during brain development, FEBSLett. 428(1998)27 – 31.
98. N. Belluardo, G. Mudo, A. Trovato-Salinaro, S. Le Gurun, A. Charollais, V. Serre-Beinier, G. Amato, J.A. Haefliger, P. Meda, D.F. Condorelli, Expression of connexin36 in the adult and developing rat brain, Brain Res.865 (2000) 121 – 138.
99. B. Teubner, B. Odermatt, M. Guldenagel, G. Sohl, J. Degen, F. Bukauskas, J. Kronengold, V.K. Verselis, Y.T. Jung, C.A. Kozak, K. Schilling, K. Willecke, Functional expression of the new gap junction gene connexin47 transcribed in mouse brain and spinal cord neurons, J. Neurosci. 21 (2001) 1117–1126.
100. Q. Chang, M. Gonzalez, M.J. Pinter, R.J. Balice-Gordon, Gap junctional coupling and patterns of connexin expression among neonatal rat lumbar spinal motor neurons, J. Neurosci. 19 (1999) 10813 – 10828.
101. S. Maxeiner, O. Kruger, K. Schilling, O. Traub, S. Urschel, K. Willecke, Spatiotemporal transcription of connexin45 during brain development results in neuronal expression in adult mice, Neurosci- ence 119 (2003) 689–700.

102. M.R. Deans, J.R. Gibson, C. Sellitto, B.W. Connors, D.L. Paul, Synchronous activity of inhibitory networks in neocortex requires electrical synapses containing connexin36, Neuron 31 (2001) 477 – 485.

103. S.G. Hormuzdi, I. Pais, F.E. LeBeau, S.K. Towers, A. Rozov, E.H. Buhl, M.A. Whittington, H. Monyer, Impaired electrical signaling disrupts gamma frequency oscillations in connexin 36-deficient mice, Neuron 31 (2001) 487 – 495.

104. C. Zhang, D. Restrepo, Expression of connexin 45 in the olfactory system, Brain Res. 929 (2002) 37 – 47.

105. A. Feigenspan, B. Teubner, K. Willecke, R. Weiler, Expression of neuronal connexin36 in AII amacrine cells of the mammalian retina, J. Neurosci. 21 (2001) 230 – 239.

106. J.I. Nagy, X.B. Li, J. Rempel, G. Stelmack, D. Patel, W.A. Staines, T. Yasumura, J.E. Rash, Connexin26 in adult rodent central nervous system: demonstration at astrocytic gap junctions and colocalization with connexin30 and connexin43, J. Comp. Neurol. 441 (2001) 302 – 323.

107. J.I. Nagy, A.V. Ionescu, B.D. Lynn, J.E. Rash, Coupling of astrocyte connexins Cx26, Cx30, Cx43 to oligodendrocyte Cx29, Cx32, Cx47: implications from normal and connexin32 knockout mice, Glia 44 (2003) 205 – 218.

108. A. Hofer, R. Dermietzel, Visualization and functional blocking of gap junction hemichannels (connexons) with antibodies against external loop domains in astrocytes, Glia 24 (1998) 141 – 154.

109. R.A. Meyer, D.W. Laird, J.P. Revel, R.G. Johnson, Inhibition of gap junction and adherens junction assembly by connexin and A-CAM antibodies, J.Cell Biol. 119 (1992) 179 – 189.

110. C.C. Naus, M. Bani-Yaghoub, Gap junctional communication in the developing central nervous system, Cell Biol. Int. 22 (1998) 751 – 763.

111. A.G. Reaume, P.A. de Sousa, S. Kulkarni, B.L. Langille, D. Zhu, T.C. Davies, S.C. Juneja, G.M. Kidder, J. Rossant, Cardiac malformation in neonatal mice lacking connexin43, Science 267 (1995) 1831 – 1834.

112. C.W. Lo, K.L. Waldo, M.L. Kirby, Gap junction communication and the modulation of cardiac neural crest cells, Trends Cardiovasc. Med. 9 (1999) 63 – 69.

113. X. Xu, W.E. Li, G.Y. Huang, R. Meyer, T. Chen, Y. Luo, M.P. Thomas, G.L. Radice, C.W. Lo, Modulation of mouse neural crest cell motility by N-cadherin and connexin 43 gap junctions, J. Cell Biol. 154 (2001) 217 – 230.

114. S. Fushiki, J.L. Perez Velazquez, L. Zhang, J.F. Bechberger, P.L. Carlen, C.C. Naus, Changes in neuronal migration in neocortex of connexin43 null mutant mice, J. Neuropathol. Exp. Neurol. 62 (2003) 304 – 314.

115. P. Anzini, D.H. Neuberg, M. Schachner, E. Nelles, K. Willecke, J. Zielasek, K.V. Toyka, U. Suter, R. Martini, Structural abnormalities and deficient maintenance of peripheral nerve myelin in mice lack- ing the gap junction protein connexin 32, J. Neurosci. 17 (1997) 4545 – 4551.

116. S.S. Scherer, Y.T. Xu, E. Nelles, K. Fischbeck, K. Willecke, L.J. Bone, Connexin32-null mice develop demyelinating peripheral neu- ropathy, Glia 24 (1998) 8 – 20.

117. B. Sutor, C. Schmolke, B. Teubner, C. Schirmer, K. Willecke, Mye- lination defects and neuronal hyperexcitability in the neocortex of connexin 32-deficient mice, Cereb. Cortex 10(2000)684 – 697.

118. L. Melanson-Drapeau, S. Beyko, S. Dave, A.L. Hebb, D.J. Franks, C. Sellitto, D.L. Paul, S.A. Bennett, Oligodendrocyte progenitor enrichment in the connexin32 null-mutant mouse, J. Neurosci. 23 (2003) 1759 – 1768.

119. M. Guldenagel, J. Ammermuller, A. Feigenspan, B. Teubner, J. Degen, G. Sohl, K. Willecke, R. Weiler, Visual transmission deficits in mice with targeted disruption of the gap junction gene connexin36, J. Neurosci. 21 (2001) 6036 – 6044.

120. D.L. Buhl, K.D. Harris, S.G. Hormuzdi, H. Monyer, G. Buzsaki, Selective impairment of hippocampal gamma oscillations in con- nexin-36 knock-out mouse in vivo, J. Neurosci. 23 (2003) 1013 – 1018.

121. H.D. Gabriel, D. Jung, C. Butzler, A. Temme, O. Traub, E. Win- terhager, K. Willecke, Transplacental uptake of glucose is decreased in embryonic lethal connexin26-deficient mice, J. Cell Biol. 140 (1998) 1453 – 1461.

122. M. Cohen-Salmon, T. Ott, V. Michel, J.P. Hardelin, I. Perfettini, M. Eybalin, T. Wu, D.C. Marcus, P. Wangemann, K. Willecke, C. Petit, Targeted ablation of connexin26 in the inner ear epithelial gap junc- tion network causes hearing impairment and cell death, Curr. Biol. 12 (2002) 1106 – 1111.

123. O. Kruger, A. Plum, J.S. Kim, E. Winterhager, S. Maxeiner, G. Hallas, S. Kirchhoff, O. Traub, W.H. Lamers, K. Willecke, Defective vascular development in connexin 45-deficient mice, Development 127 (2000) 4179 – 4193.

124. M. Bani-Yaghoub, J.F. Bechberger, C.C.G. Naus, Reduction of con- nexin43 expression and dye-coupling during neuronal differentia- tion of human NTera2/Clone D1 cells, J. Neurosci. Res. 49 (1997) 19–31.

125. M. Bani-Yaghoub, J.F. Bechberger, T.M. Underhill, C.C. Naus, The effects of gap junction blockage on neuronal differentiation of hu- man NTera2/clone D1 cells, Exp. Neurol. 156 (1999) 16 – 32.

126. M. Bani-Yaghoub, T.M. Underhill, C.C. Naus, Gap junction block- age interferes with neuronal and astroglial differentiation of mouse P19 embryonal carcinoma cells, Dev. Genet. 24 (1999) 69 – 81.

127. S. Boucher, S.A. Bennett, Differential connexin expression, gapjunction intercellular coupling, and hemichannel formation in NT2/ D1 human neural progenitors and terminally differentiated hNT neurons, J. Neurosci. Res.72 (2003) 393 – 404.

128. A.M. Jensen, S. Chiu, Astrocyte networks, in: S. Murphy (Ed.), Astrocytes: Pharmacology and Function, Academic Press, New York, 1993, pp. 309 – 329.

129. A. Warner, Gap junctions in development—a perspective, Semin. Cell Biol. 3 (1992) 81 – 91.

130. R. Dermietzel, E.L. Hertberg, J.A. Kessler, D.C. Spray, Gap junctions between cultured astrocytes: immunocytochemical, molecular, and electrophysiological analysis, J. Neurosci.11(1991)1421 – 1432.

131. C. Giaume, C. Fromaget, A. el Aoumari, J. Cordier, J. Glowinski, D. Gros, Gap junctions in cultured astrocytes: single-channel currents and characterization of channel-forming protein, Neuron 6 (1991) 133 – 143

132. J.I. Nagy, J.E. Rash, Connexins and gap junctions of astrocytes and oligodendrocytes in the CNS, Brain Res. Brain Res. Rev. 32 (2000) 29–44.

133. J.I. Nagy, D. Patel, P.A. Ochalski, G.L. Stelmack, Connexin30 in rodent, cat and human brain: selective expression in gray matter astrocytes, colocalization with connexin43 at gap junctions and late developmental appearance, Neuroscience 88 (1999) 447 – 468.

134. E. Mugnaini, Cell junctions of astrocytes, ependyma, and related cells in the mammalian central nervous system, with emphasis on the hypothesis of a generalized functional syncytium of supporting cells, in: S. Federoff, A. Vernadakis (Eds.), Development, Morphol- ogy, and Regional Specialization of Astrocytes, vol. I, Academic Press, Orlando, FL, 1986, pp. 329 – 371.

135. R. Dermietzel, Y. Gao, E. Scemes, D. Vieira, M. Urban, M. Kremer, M.V. Bennett, D.C. Spray, Connexin43 null mice reveal that astro- cytes express multiple connexins, Brain Res. Rev. 32 (2000) 45 – 56.

136. T. Yamamoto, A. Ochalski, E.L. Hertzberg, J.I. Nagy, On the orga- nization of astrocytic gap junctions in rat brain as suggested by LM and EM immunohistochemistry of connexin43 expression, J. Comp. Neurol. 302 (1990) 853 – 883.

137. J.I. Nagy, T. Yamamoto, M.A. Sawchuk, D.M. Nance, E.L. Hertzberg, Quantitative immunohistochemical and biochemical correlates of connexin43 localization in rat brain, Glia 5 (1992) 1 – 9.

138. W. Walz, L. Hertz, Functional interactions between neurons and astrocytes: II. Potassium homeostasis at the cellular level, Prog. Neurobiol. 20 (1983) 133 – 183.

139. J.G.R. Jefferys, Nonsynaptic modulation of neuronal activity in the brain: electric currents and extracellular ions, Physiol. Rev. 75 (1995) 689 – 723.

140. A. Charles, Intercellular calcium waves in glia, Glia 24 (1998) 39–49.

141. A.C. Charles, C.C. Naus, D. Zhu, G.M. Kidder, E.R. Dirksen, M.J. Sanderson, Intercellular calcium signaling via gap junctions in glioma cells, J. Cell Biol. 118 (1992)195 – 201.

142. A.H. Cornell-Bell, S.M. Finkbeiner, M.S. Cooper, S.J. Smith, Glutamate induces calcium waves in cultured astrocytes: long-range glial signaling, Science 247 (1990) 470 – 473.

143. L. Venance, N. Stella, J. Glowinski, C. Giaume, Mechanism in- volved in initiation and propagation of receptor-induced intercellular calcium signaling in cultured rat astrocytes, J. Neurosci. 17 (1997) 1981 – 1992.

144. D.A. Goodenough, D.L. Paul, Beyond the gap: functions of unpaired connexon channels, Nat. Rev., Mol. Cell Biol. 4 (2003) 285 – 294.

145. C.E. Stout, J.L. Costantin, C.C.G. Naus, A.C. Charles, Intercellular calcium signaling in astrocytes via ATP release through connexin hemichannels, J. Biol. Chem. 277 (2002) 10482 – 10488.

146. J.E. Contreras, H.A. Sanchez, E.A. Eugenin, D. Speidel, M. Theis, K. Willecke, F.F. Bukauskas, M.V. Bennett, J.C. Saez, Metabolic inhibition induces opening of unapposed connexin 43 gap junction hemichannels and reduces gap junctional communication in cortical astrocytes in culture, Proc. Natl. Acad. Sci. U. S. A. 99 2002, pp. 495 – 500.

147. C.C. Naus, J.F. Bechberger, Y. Zhang, L. Venance, H. Yamasaki, S.C. Juneja, G.M. Kidder, C. Giaume, Altered gap junctional com- munication, intercellular signaling, and growth in cultured astrocytes deficient in connexin43, J. Neurosci. Res.49 (1997) 528 – 540.

148. E. Scemes, R. Dermietzel, D.C. Spray, Calcium waves between astrocytes from Cx43 knockout mice, Glia 24 (1998)65 – 73.

149. R. Siushansian, J.F. Bechberger, D.F. Cechetto, V.C. Hachinski, C.C. Naus, Connexin43 null mutation increases infarct size after stroke, J.Comp. Neurol. 440 (2001) 387 – 394.

150. M. Theis, R. Jauch, L. Zhuo, D. Speidel, A. Wallraff, B. Doring, C. Frisch, G. Sohl, B. Teubner, C. Euwens, J. Huston, C. Stein- hauser, A. Messing, U. Heinemann, K. Willecke, Accelerated hip- pocampal spreading depression and enhanced locomotory activity in mice with astrocyte-directed inactivation of connexin43, J. Neu- rosci. 23 (2003) 766 – 776.

151. B. Teubner, V. Michel, J. Pesch, J. Lautermann, M. Cohen-Salmon, G. Sohl, K. Jahnke, E. Winterhager, C. Herberhold, J.P. Hardelin, C. Petit, K. Willecke, Connexin30 (Gjb6)-deficiency causes severe hearing impairment and lack of endocochlear potential, Hum. Mol. Genet. 12 (2003) 13 – 21.

152. W.J. Streit, S.A. Walter, N.A. Pennell, Reactive microgliosis, Prog. Neurobiol. 57 (1999) 563 – 581.

153. A.D. Martinez, E.A. Eugenin, M.C. Branes, M.V. Bennett, J.C. Saez, Identification of second messengers that induce expression of func- tional gap junctions in microglia cultured from newborn rats, Brain Res. 943 (2002) 191 – 201.

154. R. Parenti, A. Campisi, A. Vanella, F. Cicirata, Immunocytochemical and RT-PCR analysis of connexin 36 in cultures of mammalian glial cells, Arch. Ital. Biol. 140 (2002) 101 – 108.

155. N. Rouach, C.F. Calvo, J. Glowinski, C. Giaume, Brain macrophages inhibit gap junctional communication and downregulate con- nexin 43 expression in cultured astrocytes, Eur. J. Neurosci. 15 (2002) 403 – 407.

156. P.M. Faustmann, C.G. Haase, S. Romberg, D. Hinkerohe, D. Szlachta, D. Smikalla, D. Krause, R. Dermietzel, Micro- glia activation influences dye coupling and Cx43 expression of the astrocytic network, Glia 42 (2003)101 – 108.

157. R. Dermietzel, O. Traub, T.K. Hwang, E. Beyer, M.V. Bennett, D.C. Spray, K. Willecke, Differential expression of three gap junction proteins in developing and mature brain tissues, Proc. Natl. Acad. Sci. U.S.A. 86(1989)10148 – 10152.

158. P.E. Micevych, L. Abelson, Distribution of mRNAs coding for liver and heart gap junction proteins in the rat central nervous system, J.Comp.Neurol.305 (1991) 96 – 118.

159. D.J. Belliveau, C.C.G. Naus, Differential localization of gap junc- tion mRNAs in developing rat brain, Dev. Neurosci. 17 (1995) 81–96.

160. D.C. Spray, R. Dermietzel, X-linked dominant Charcot – Marie – Tooth disease and other potential gap-junction diseases of the ner- vous system,Trends Neurosci.18(1995) 256 – 262.

161. D.J. Belliveau, C.C. Naus, Cortical type 2 astrocytes are not dye coupled nor do they express the major gap junction genes found in the central nervous system, Glia 12 (1994) 24 – 34.

162. C. Giaume, L. Venance, Gap junctions in brain glial cells and de- velopment, Perspect. Dev. Neurobiol. 2 (1995) 335 – 345.

163. B.M. Altevogt, K.A. Kleopa, F.R. Postma, S.S. Scherer, D.L. Paul, Connexin29 is uniquely distributed within myelinating glial cells of the central and peripheral nervous systems, J. Neurosci. 22 (2002) 6458 – 6470.

164. B. Odermatt, K. Wellershaus, A. Wallraff, G. Seifert, J. Degen, C. Euwens, B. Fuss, H. Bussow, K. Schilling, C. Steinhauser, K. Wil- lecke, Connexin 47 (Cx47)-deficient mice with enhanced green fluo- rescent protein reporter gene reveal predominant oligodendrocytic expression of Cx47 and display vacuolized myelin in the CNS, J. Neurosci. 23 (2003) 4549 – 4559.

165. D.J. Belliveau, G.M. Kidder, C.C.G. Naus, Expression of gap junc- tion genes during postnatal neural development, Dev. Genet. 12 (1991) 308 – 317.

166. U. Suter, G.J. Snipes, Biology and genetics of hereditary motor and sensory neuropathies, Annu. Rev. Neurosci. 1845 – 75 (1995)75.

167. D.L. Paul, New functions for gap junctions, Curr. Opin. Cell Biol. 7 (1995)665 – 672.

168. J. Bergoffen, S.S. Scherer, S. Wang, M. Oronzi Scott, L.J. Bone, D.L. Paul, K. Chen, M.W. Lensch, P.F. Chance, K.H. Fishbeck,

169. Connexin mutations in X-linked Charcot – Marie – Tooth disease, Science 262 (1993) 2039–2042.

170. N. Fairweather, C. Bell, S. Cochrane, J. Chelly, S. Wang, M.L. Mostacciuolo, A.P. Monaco, N.E. Haites, Mutations in the con- nexin32 gene in X-linked dominant Charcot – Marie – Tooth disease (CMTX1), Hum. Mol. Genet. 3 (1994) 29 – 34.

171. R. Bruzzone, T.W. White, S.S. Scherer, K.H. Fischbeck, D.L. Paul, Null mutations of connexin32 in patients with X-linked Charcot– Marie–Tooth disease, Neuron 13 (1994) 1253–1260.

172. V. Ionasescu, C. Searby, R. Ionasescu, W. Meschino, New point mutations and deletions of the connexin 32 gene in X-linked Charcot – Marie – Tooth neuropathy, Neuromuscul. Dis. 5 (1995) 297 – 299.

173. B. Sutor, C. Schmolke, B. Teubner, C. Schirmer, K. Willecke, Mye- lination defects and neuronal hyperexcitability in the neocortex of connexin 32-deficient mice, Cereb. Cortex 10 (2000) 684 – 697.

174. P. Anzini, D.H. Neuberg, M. Schachner, E. Nelles, K. Willecke, J. Zielasek, K.V. Toyka, U. Suter, R. Martini, Structural abnormalities and deficient maintenance of peripheral nerve myelin in mice lack- ing the gap junction protein connexin 32, J. Neurosci. 17 (1997) 4545 – 4551.

175. S.S. Scherer, Y.T. Xu, E. Nelles, K. Fischbeck, K. Willecke, L.J. Bone, Connexin32-null mice develop demyelinating peripheral neu- ropathy, Glia 24 (1998) 8 – 20.

176. L.J. Bone, N. Dahl, M.W. Lensch, P.F. Chance, T. Kelly, E. Leguern, S. Magi, G. Parry, H. Shapiro, S. Wang, K.H. Fischbeck, New con- nexin32 mutations associated with X-linked Charcot – Marie – Tooth disease, Neurology 45 (1995) 1863–1866.

177. S.S. Scherer, S.M. Deschenes, Y.T. Xu, J.B. Grinspan, K.H. Fischbeck, D.L. Paul, Connexin32 is a myelin-related pro- tein in the PNS and CNS, J. Neurosci. 15 (1995) 8281–8294.

178. Gibson, J.R., M. Beierlein, and B.W. Connors, Functional properties of electrical synapses between inhibitory interneurons of neocortical layer 4. J Neurophysiol, 2005. 93(1): p. 467-80.

179. Kandler, K. and L.C. Katz, Neuronal coupling and uncoupling in the developing nervous system. Curr Opin Neurobiol, 1995. 5(1): p. 98-105.

180. Balice-Gordon, R.J., L.J. Bone, and S.S. Scherer, Functional gap junctions in the schwann cell myelin sheath. J Cell Biol, 1998. 142(4): p. 1095-104.

181. Kleopa, K.A., J. Orthmann-Murphy, and I. Sargiannidou, Gap junction disorders of myelinating cells. Rev Neurosci, 2010. 21(5): p. 397-419.

182. American Stroke Association, About stroke > Impact of stroke, 2003, http://www.strokeassociation.org/.

183. Heart and Stroke Foundation of Canada, Stroke>General Info>S- troke Statistics, 2003, http://ww2.heartandstroke.ca.

184. M.A. Ozog, R. Siushansian, C.C. Naus, Blocked gap junctional coupling increases glutamate-induced neurotoxicity in neuron-astro- cyte co-cultures, J. Neuropathol. Exp. Neurol. 61 (2002) 132 – 141.

185. E.M. Blanc, A.J. Bruce-Keller, M.P. Mattson, Astrocytic gap junctional communication decreases neuronal vulnerability to ox- idative stress-induced disruption of Ca2 + homeostasis and cell death, J. Neurochem. 70 (1998) 958 – 970.

186. T. Nakase, S. Fushiki, C.C. Naus, Astrocytic gap junctions com- posed of connexin43 reduce apoptotic neuronal damage in cerebral ischemia, Stroke 34 (2003) 1987–1993. M.V.

187. Frantseva, L. Kokarovtseva, J. Perez Velazquez, Ischemia- induced brain damage depends on specific gap-junctional coupling, J. Cereb. Blood Flow Metab. 22 (2002) 453–462.

188. A. Rawanduzy, A. Hansen, T.W. Hansen, M. Nedergaard, Effective reduction of infarct volume by gap junction blockade in a rodent model of stroke, J. Neurosurg. 87 (1997) 916–920.

189. M.L. Cotrina, J. Kang, J.H. Lin, E. Bueno, T.W. Hansen, L. He, Y. Liu, M. Nedergaard, Astrocytic gap junctions remain open during ischemic conditions, J. Neurosci. 18 (1998) 2520–2537.

190. T. Nakase, S. Fushiki, G. Sohl, M. Theis, K. Willecke, C.C.G. Naus, Neuroprotective role of astrocytic gap junctions in ischemic stroke, Cell Commun. Adhes. 10 (2003) 413–417.

191. Z.C. Ye, M.S. Wyeth, S. Baltan-Tekkok, B.R. Ransom, Functional hemichannels in astrocytes: a novel mechanism of glutamate release, J. Neurosci. 23 (2003) 3588–3596.

192. L.I. Plotkin, S.C. Manolagas, T. Bellido, Transduction of cell sur- vival signals by connexin-43 hemichannels, J. Biol. Chem. 277 (2002) 8648–8657.

193. K. Oguro, T. Jover, H. Tanaka, Y. Lin, T. Kojima, N. Oguro, S.Y. Grooms, M.V. Bennett, R.S. Zukin, Global ischemia-induced increases in the gap junctional proteins connexin 32 (Cx32) and Cx36 in hippocampus and enhanced vulnerability of Cx32 knock-out mice, J. Neurosci. 21 (2001) 7534–7542.

194. Epilepsy Canada, Facts: Types of seisures, 2003, http://www. epilepsy.ca.

195. D.A. McCormick, D. Contreras, On the cellular and network bases of epileptic seizures, Annu. Rev. Physiol. 63 (2001) 815 – 846.

196. J.L. Perez Velazquez, P.L. Carlen, Gap junctions, synchrony and seizures, Trends Neurosci. 23 (2000) 68–74.

197. K. Fujita, K. Nakanishi, K. Sobue, T. Ueki, K. Asai, T. Kato, Astrocytic gap junction blockage and neuronal Ca2 + oscillation in neuron-astrocyte cocultures in vitro, Neurochem. Int. 33 (1998) 41–49.

198. J. Li, H. Shen, C.C. Naus, L. Zhang, P.L. Carlen, Upregulation of gap junction connexin 32 with epileptiform activity in the isolated mouse hippocampus, Neuroscience 105 (2001) 589 – 598.

199. G. Sohl, M. Guldenagel, H. Beck, B. Teubner, O. Traub, R. Gutier- rez, U. Heinemann, K. Willecke, Expression of connexin genes in hippocampus of kainate-treated and kindled rats under conditions of experimental epilepsy, Brain Res. Mol. Brain Res. 83 (2000) 44 – 51.

200. R.D. Traub, M.A. Whittington, E.H. Buhl, F.E. LeBeau, A. Bibbig, S. Boyd, H. Cross, T. Baldeweg, A possible role for gap junctions in generation of very fast EEG oscillations preceding the onset of, and perhaps initiating, seizures, Epilepsia 42 (2001) 153–170.

201. C.C. Naus, J.F. Bechberger, D.L. Paul, Gap junction gene expression in human seizure disorder, Exp. Neurol. 111 (1991) 198 – 203.

202. Ahn, M., Lee, J., Gustafsson, A., Enriquez, A., Lancaster, E., Sul, J.Y., Haydon, P.G., Paul, D.L., Huang, Y., Abrams, C.K., Scherer, S.S., 2008. Cx29 and Cx32, two connexins expressed in myelinating glia, do not interact and are functionally distinct. J. Neurosci. Res. 86, 992–1006.

203. Kamasawa, N., Sik, A., Morita, M., Yasumura, T., Davidson, K.G.V., Nagy, J.I., Rash, J.E., 2005. Connexin-47 and Connexin-32 in gap junctions of oligodendrocyte somata, myelin sheaths, para- nodal loops and Schmidt–Lanterman incisures: implications for ionic homeostasis and potassium siphoning. Neuroscience 136, 65–86.

204. Cotrina, M.L., Lin, J.H.C., Nedergaard, M., 2008. Adhesive proper- ties of connexin hemichannels. Glia 56, 1791–1798.

205. R.L. Nussbaum, C.E. Ellis, Alzheimer's disease and Parkinson's disease, N. Engl. J. Med. 348 (2003) 1356 – 1364.

206. K. Duff, C. Eckman, C. Zehr, X. Yu, C.M. Prada, J. Perez-tur, M. Hutton, L. Buee, Y. Harigaya, D. Yager, D. Morgan, M.N. Gordon, L. Holcomb, L. Refolo, B. Zenk, J.

Hardy, S. Younkin, Increased amyloid-beta42(43) in brains of mice expressing mutant presenilin 1, Nature 383 (1996) 710 – 713.

207. K. Pak, S.L. Chan, M.P. Mattson, Presenilin-1 mutation sensitizes oligodendrocytes to glutamate and amyloid toxicities, and exacer- bates white matter damage and memory impairment in mice, Neuro- molecular Med. 3 (2003) 53 – 64.

208. M. Buttini, G.Q. Yu, K. Shockley, Y. Huang, B. Jones, E. Masliah, M. Mallory, T. Yeo, F.M. Longo, L. Mucke, Modulation of Alz- heimer-like synaptic and cholinergic deficits in transgenic mice by human apolipoprotein E depends on isoform, aging, and overexpres- sion of amyloid beta peptides but not on plaque formation, J. Neuro- sci. 22 (2002) 10539 – 10548.

209. G.A. Higgins, C.H. Large, H.T. Rupniak, J.C. Barnes, Apolipopro- tein E and Alzheimer's disease: a review of recent studies, Pharma- col. Biochem. Behav. 56 (1997) 675 – 685.

210. G. Ophir, S. Meilin, M. Efrati, J. Chapman, D. Karussis, A. Roses, D.M. Michaelson, Human apoE3 but not apoE4 rescues impaired astrocyte activation in apoE null mice, Neurobiol. Dis. 12 (2003) 56–64

211. M. Rufer, S.B. Wirth, A. Hofer, R. Dermietzel, A. Pastor, H. Kettenmann, K. Unsicker, Regulation of connexin-43, GFAP, and FGF- 2 is not accompanied by changes in astroglial coupling in MPTP- lesioned, FGF-2-treated parkinsonian mice, J. Neurosci. Res. 46 (1996) 606–617.

212. R.J. Elble, Central mechanisms of tremor, J. Clin. Neurophysiol. 13 (1996)133 – 144. Y.

213. Y. Loewenstein, A possible role of olivary gap-junctions in the generation of physiological and pathological tremors, Mol. Psychi- atry 7 (2002) 129–131.

214. I. Lampl, Y. Yarom, Subthreshold oscillations and resonant behavior: two manifestations of the same mechanism, Neuroscience 78 (1997) 325 – 341.

215. M.A. Long, M.R. Deans, D.L. Paul, B.W. Connors, Rhythmicity without synchrony in the electrically uncoupled inferior olive, J. Neurosci. 22 (2002) 10898 – 10905.

216. H.L. Weiner, D.J. Selkoe, Inflammation and therapeutic vaccination in CNS diseases, Nature 420 (2002) 879 – 884.

217. P.S. Aisen, Anti-inflammatory agents in Alzheimer's disease, Curr. Neurol. Neurosci. Rep. 2 (2002) 405 – 409.

218. E.G. McGeer, P.L. McGeer, Brain inflammation in Alzheimer dis- ease and the therapeutic implications, Curr. Pharm. Des. 5 (1999) 821 – 836.

219. Cappuccio I, Calderone A, Busceti CL, Biagioni F, Pontarelli F, Bruno V, et al. (2005). Induction of Dickkopf-1, a negative modulator of the Wnt pathway, is required for the development of ischemic neuronal death. J Neurosci 25:2647–2657.

220. Busceti CL, Biagioni F, Aronica E, Riozzi B, Storto M, Battaglia G, et al. (2007). Induction of the Wnt inhibitor, Dickkopf-1 is associated with neurodegenera- tion related to temporal lobe epilepsy. Epilepsia 48:694–705.

221. Dill J, Wang H, Zhou F, Li S (2008). Inactivation of glycogen synthase kinase 3 promotes axonal growth and recovery in the CNS. J Neurosci 28:8914–8928

222. Sarkar S, Krishna G, Imarisio S, Saiki S, O'Kane CJ, Rubinsztein DC (2008). A rational mechanism for combination treatment of Huntington's disease using lithium and rapamycin. Hum Mol Genet 17:170–178.

223. Youdim MB, Arraf Z (2004). Prevention of MPTP (N-methyl-4-phenyl-1,2,3,6-tetrahydropyridine) dopaminergic neurotoxicity in mice by chronic lithium: involvements of Bcl-2 and Bax. Neuropharmacol 46:1130–1140.

224. Heiseke A, Aguib Y, Riemer C, Baier M, Scha □tzl HM (2009). Lithium induces clearance of protease resistant prion protein in prion-infected cells by induction of autophagy. J Neurochem 109:25–34.

225. Fornai F, Longone P, Cafaro L, Kastsiuchenka O, Ferrucci M, Manca ML, et al. (2008a). Lithium delays progression of amyotrophic lateral sclerosis. Proc Natl Acad Sci USA 105:2052–2057.

226. Watase K, Gatchel JR, Sun Y, Emamian E, Atkinson R, Richman R, et al. (2007). Lithium therapy improves neurological function and hippocampal dendritic arborization in a spinocerebellar ataxia type 1 mouse model. PLoS Med 4:e182.

227. Askanas V, Engel WK (2008). Inclusion-body myositis: muscle-fiber molecular pathology and possible pathogenic significance of its similarity to Alzheimer's and Parkinson's disease brains. Acta Neuropathol 116:583–595.

228. Zhong J, Lee WH (2007). Lithium: a novel treatment for Alzheimer's disease? Expert Opin Drug Saf 6:375–383.

229. Engel T, Gon˜i-Oliver P, Lucas JJ, Avila J, Herna´ndez F (2006). Chronic lithium administration to FTDP-17 tau and GSK-3beta overexpressing mice prevents tau hyperphosphorylation and neurofibrillary tangle formation, but pre-formed neurofibrillary tangles do not revert. J Neurochem 99:1445–1455.

230. Ghosal K, Vogt DL, Liang M, Shen Y, Lamb BT, Pimplikar SW (2009). Alzheimer's disease-like pathological features in transgenic mice expressing the APP intracellular domain. Proc Natl Acad Sci U S A 106:18367–18372

231. Nonaka S, Hough CJ, Chuang DM (1998). Chronic lithium treatment robustly protects neurons in the central nervous system against excitotoxicity by inhibiting N-methyl-D-aspartate receptor-mediated calcium influx. Proc Natl Acad Sci U S A 95:2642–2647.

232. Hashimoto R, Takei N, Shimazu K, Christ L, Lu B, Chuang DM (2002b). Lithium induces brain-derived neurotrophic factor and activates TrkB in rodent cortical neurons: an essential step for neuroprotection against glutamate excitotoxicity. Neuropharmacology 43:1173–1179.

233. Chen RW, Chuang DM (1999). Long-term lithium treatment suppresses p53 and Bax expression but increases Bcl-2 expression. J Biol Chem 274: 6039–6042.

234. Miyashita T, Krajewski S, Krajewska M, Wang HG, Lin HK, Liebermann DA, et al. (1994). Tumor suppressor p53 is a regulator of bcl-2 and bax gene expression in vitro and in vivo. Oncogene 9:1799–1805

235. Ozaki N, Chuang DM (1997). Lithium increases transcriptio factor binding to AP-1 and cyclic AMP-responsive element in cultured neurons and rat brain. J Neurochem 69:2336–2344

236. Grimes CA, Jope RS (2001). The multifaceted roles of glycogen synthase kinase 3, in cellular signalin. Prog Neurobiol 65:391–426.

237. Yuan PX, Chen G, Huang LD, Manji HK (1998). Lithium stimulates gene expression through the AP-1 transcription factor pathway. Brain Res Mol Brain Res 58:225–230.

238. Intracellular pathways underlying the effects of lithium. Pasquali L, Busceti CL, Fulceri F, Paparelli A, Fornai F. Behav Pharmacol. 2010 Sep;21(5-6):473-92.

239. Mason JL, Suzuki K, Chaplin DD, Matsushima GK. 2001. Interleukin- 1beta promotes repair of the CNS. J Neurosci 21:7046–7052.

240. Matsushima GK, Morell P. 2001. The neurotoxicant, cuprizone, as a model to study demyelination and remyelination in the central nerv- ous system. Brain Pathol 11:107–116.

241. Andrade-Rozental, A.F., Rozental, R., Hopperstad, M.G., Wu, J.K., Vrionis, F.D., Spray, D.C., 2000. Gap junctions: the "kiss of death" and the "kiss of life". Brain Res. Brain Res. Rev. 32, 308-315.